Master's thesis

NTNU
Norwegian University of Science and Technology
Faculty of Natural Sciences
Department of Materials Science and Engineering

Nishan Simkhada

Continued study to aluminothermic reduction process for silicon production

Master's thesis in Material Science and Engineering
Supervisor: Gabriella Tranell
Co-supervisor: Harald Philipson
July 2022

NTNU
Kunnskap for en bedre verden

Nishan Simkhada

Continued study to aluminothermic reduction process for silicon production

Master's thesis in Material Science and Engineering
Supervisor: Gabriella Tranell
Co-supervisor: Harald Philipson
July 2022

Norwegian University of Science and Technology
Faculty of Natural Sciences
Department of Materials Science and Engineering

NTNU
Norwegian University of
Science and Technology

NTNU | Department of Materials Science and Engineering

TMT4920 - Master Thesis

Continued study to aluminothermic reduction process for silicon production

Nishan Simkhada

Trondheim, July 3, 2022

Supervisor: Gabriella Tranell, IMA

Co-supervisor: Harald Philipson, IMA

Norwegian University of Science and Technology

Preface

This thesis titled; "Continued study to aluminothermic reduction process for silicon production" was written as a part of the Master Thesis TMT4920. The entire work was conducted at the Department of Materials Science and Engineering at the Faculty of Natural Sciences at Norwegian University of Science and Technology (NTNU) during the semester, spring 2022. The work is part of the SisAl Pilot project, funded by the EU H2020 under Grant Agreement N°869268.

I would like to start by thanking my supervisor, professor Gabriella Tranell for all the opportunities, guidance, feedback, and continuous support throughout the semester.

A large thanks goes to my co-supervisor Harald Philipson for providing all the required resources training and supervision necessary during the project work. I would also like to thank Dmitry Slizovskiy for providing guidance related with lab training and equipment. Also, I want to give huge thanks to Kristian Grøtta Skorpen from SINTEF for helping me in conducting experiment in Meltspinner. Finally, I would also like to thank Morten Peder Raanes for performing the EPMA analysis, and Yingda Yu for assisting me with SEM analysis as well as Degerfors Laboratorium AB in Bruksparken, Sweden for conducting XRF analysis of my slag and metal samples.

Abstract

The main aim of this thesis work was to investigate the effect of under-stoichiometric reductant addition in silica based slag during aluminothermic reduction process. Production of Si with less Ca content has been one of the issue in Sisal process, for which study of under-stoichiometric aluminium addition is supplementary. Experiment has also been conducted with stoichiometric aluminium with silca based slag containing small amount of CaF_2 as CaF_2 is taken as viable options for fluxing agent in this process. Beside these, this thesis study has also covered some investigation over micro-structure and phases of Al-Si alloy formed after rapid solidification process.

Two different slags were tested in this study with three different under stoichiometric amount of pure aluminium. Slags were either acidic or neutral. Neutral slag comes from Elkem often regarded as pre-fused slag in this study, having $CaO:SiO_2$ ratio of 1.01. For acidic slag, same pre-fused slag was mixed with measured amount of quartz for making it acidic. Target acidity of slag was 0.6, but acidic slag we used during study had $CaO:SiO_2$ ratio of 0.56. Three different aluminium stoichiometry i.e 0.3*Al, 0.4*Al and 0.5*Al were used, which were 0.3, o.4 and 0.5 times the stoichiometric aluminium needed for complete reduction. These three different under-stoichiometries had been tested with both acidic and neutral slag and results has been analysed based upon it's product composition, mass balances, product structure, temperature observation and BSE images from EPMA. These results were also compared with the values obtained from Factsage simulation. For Al-Si alloys, alloy having 80% Al and 20% Si was made in muffle furnace which was further taken into melt spinner for rapid solidification. Ribbon shaped Al-Si alloys were prepared which were analysed for micro structure observation.

The results from acidic and neutral slag experiments where under-stoichiometric aluminium was used produced quite comparative trend in contrast with every three trials. Though the trend was similar to

Factsage, the values obtained for product composition were quite deviated from simulated Factsage value. To confirm these deviation, reconfirmation experiment was done where only 0.3*Al stoichiometry was tested with both acidic slag and neutral slag. Experiment using CaF_2 was also done in the same parallel.

Results analysis from first three trials and final reconfirmation trial show that with decreasing amount of reductant, Si content in metal increases, while Al and Ca content in metal decreases. Similarly, in the case of slag, with decreasing amount of reductant, SiO_2 and CaO content in slag increases, while Al_2O_3 content in slag decreases. With increasing CaO:SiO_2 ratio, less pure silicon is obtained, which refered acidic slag to produce highly pure Silicon but our previous trial showed opposite trend. Neutral slag produced pure silicon higher than expected while acidic slag experiments gave less purity of Si in alloy. But, the case was opposite during reconfirmation trial, where acidic slag experiment had almost 98% pure Silicon, tallying closer to Factsage value. Results from reconfirmation trial has also been supported by its product morphology and phase observation.
Results from CaF_2 in terms of chemical composition of metal obtained validates that Si content in metal can be raised with the use of CaF_2. Results from experiment using CaF_2 was compared with previous experiments where CaF_2 was not used and positive outcomes were noticed.

Contents

List of Figures

List of Tables

1 Introduction

1.1 Background and Motivation

Humankind has found silicon to be one of the most consumable elements. Silicon is used in a variety of applications, including the manufacture of high-quality alloys, electronic components, and photovoltaic devices. Silicon has also shown to be useful in the health-care and nano-industry sectors. Despite the fact that Si demand has increased dramatically, silicon output remains unchanged from fifty years ago. For silicon manufacture, enterprises are currently using a carbothermic reduction process, which is not environmentally friendly and consumes a lot of energy. As a result, finding a viable replacement to the present silicon manufacturing method has been a big challenge.

The EU-funded SisAl Pilot Project is based on the aluminothermic reduction process and attempts to establish the process and its many outputs on a pre-industrial scale. For silicon manufacturing, the aluminothermic reduction process might be a viable alternative to the present carbothermic reduction technique. The significant volume of carbon dioxide emitted as well as the high energy demand in the carbothermic reduction process has prompted researchers to investigate this method for silicon manufacture.

1.2 Objectives

The primary goal of this research is to see if the SisAl method can produce silicon with a low calcium component. High amount of calcium in silicon has been a major concern when employing the aluminothermic reduction process, thus a research of under stoichiometric aluminium addition with silica based slags has been conducted.

It is well known fact that CaF_2 acts as a fluxing agent in aluminium industry. So, CaF_2 has evolved as a promising agent in Sisal process in obtaining highly qualitative results. To investigate the effect of CaF_2 in aluminothermic

reduction process, small study has been conducted in this thesis work.

Another goal of this research is to learn more about the phases and characteristics of Al-Si alloy, which is made by alloying aluminium with silicon. Aluminium-silicon alloys are mostly used in casting, although they may also be used in quick solidification techniques and powder metallurgy. Silumin has a strong corrosion resistance, making it ideal for usage in humid situations. The produced alloy is used to examine phase and characteristics at various solidification rates.

2 Theory and Literature Survey

The carbothermic reduction technique is still the most common way to make silicon. This process is negative in terms of the environment and energy consumption due to drawbacks such as high carbon emissions and high energy demand. Mitigating these issues is a key concern these days, and several options have been investigated thus far. This paper delivers into the theory of silicon characteristics, the benefits and downsides of the carbothermic reduction process, as well as prospective alternatives. In light of these circumstances, the Sisal Pilot Project was formed, which is based on the aluminothermic reduction process and intends to demonstrate the process and its many outputs on a pre-industrial scale. In this investigation, understoichiometric aluminium was employed as a reductant, together with SiO_2-CaO slag for silicon synthesis. Also investigated was the rapid solidification of the Al-Si system at various solidification rates. As a result, this literature review includes a description of slag kinds, important slag properties, understoichiometric studies, and quick solidification.

2.1 Silicon uses and properties

Only oxygen outnumbers silicon as the second most prevalent element in the earth's crust. It is typically found in sand, clays, soils, and rocks, either in a combined condition with oxygen as silica ace SiO_2 or in the form of silicates with other elements. This oxidized form, known as silicon dioxide or silicates, may be found in the environment, bodily fluids, water resources, and bones. Silicon has a melting temperature of 1414 °C and a boiling point of 3265°C.

Silicon is one of the most precious elements in the world. Because today's technology are so reliant on silicon, the use of silicon has skyrocketed in the last few generations. Silicon is used to make computer chips, solar panels, high-power lasers, and other electronic components. Furthermore, silicon is frequently employed in the building and manufacture of various alloys, ceramics, and glasses. Silicon, as a non-toxic element, has a wide range of uses in medicine and cosmetics.

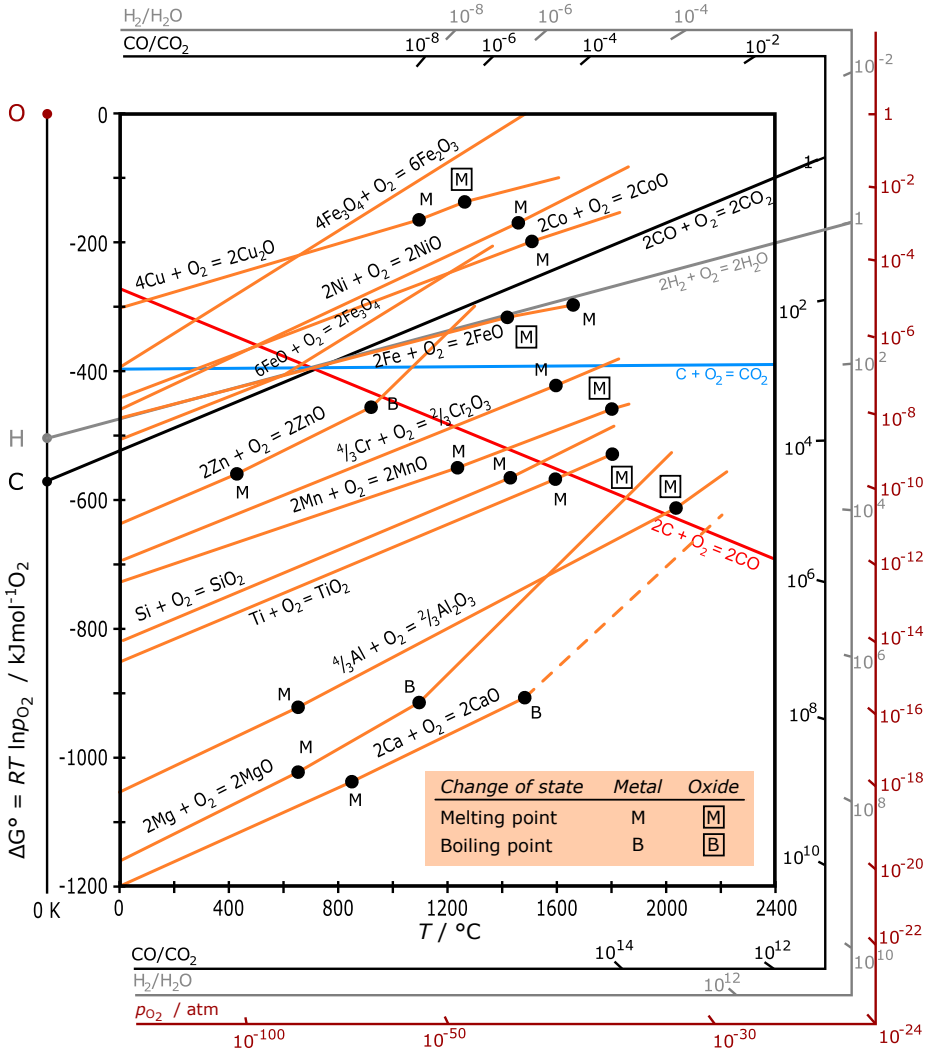

Figure 1: Ellingham diagram showing the free energy of formation for various metal oxides [1].

Metallic oxides of elements such as Ca, Mg, Ti, and Al have lower Gibb's energy than silica, indicating that they are extremely stable, according to Ellingham's figure in Figure 1. This means that these metals can convert silica to pure silicon and so play an important part in the silicon manufacturing process.

2.2 Silicon Production

2.2.1 Carbothermic reduction process

The current industrial practice for silicon production is carbothermic reduction process. In this process, submerged arc furnace is used where quartz (SiO_2) and carbon materials like coke, coal, charcoal and woodchips are heated with supply of electrical energy to produce elemental Silicon. This is very energy intensive process and consumes abut 11-13 kWh of electrical energy per kilogram of silicon produced [2]. The schematic illustration of carbothermic reduction process for silicon production has been shown in Figure 2:

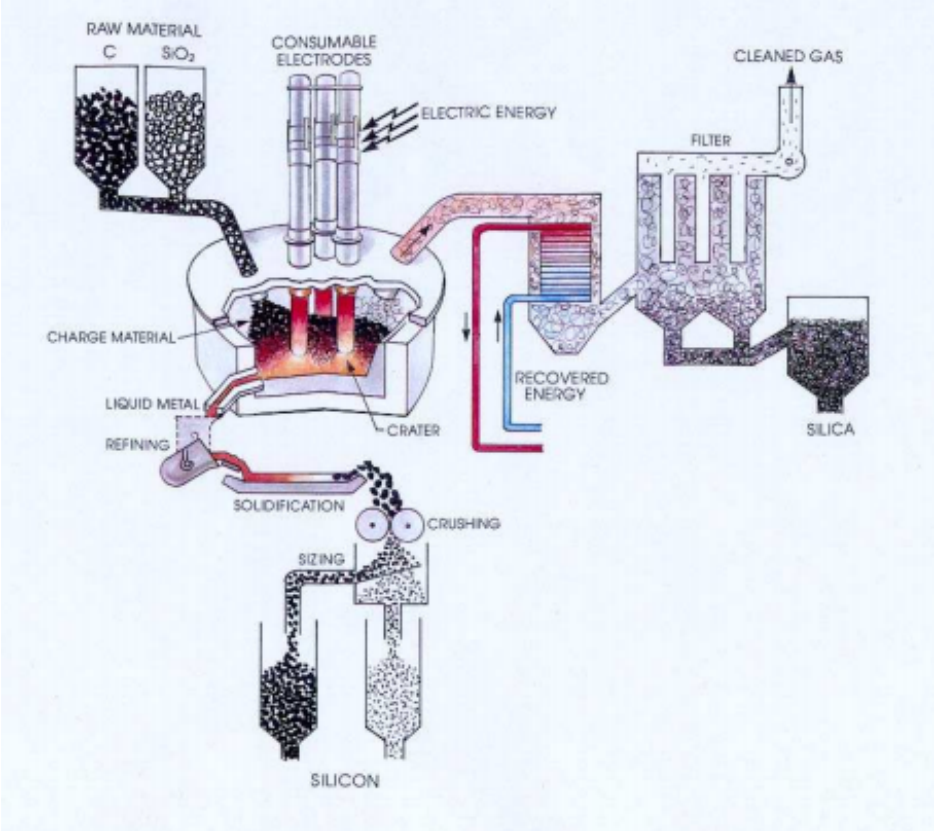

Figure 2: A standard silicon plant following carbithermic reduction process[3].

This process involves arc furnace which contains three electrodes which are submerged into the charge and supply a three phase current which heat up the furnace. In the hottest zone, the temperature reaches up to 2000°C, reducing silicon dioxide to molten silicon. The produced silicon is tapped from taphole at bottom and taken for refining purpose. [4]

General reaction for carbothermic reduction process is described by Equation 1.

$$\mathrm{SiO_2} + 2\,\mathrm{C} = \mathrm{Si} + 2\,\mathrm{CO} \tag{1}$$

Equation 1 represents the ideal case without considering any loss from the system. However, during practical operation, a lot of SiO gas is lost. It is because considerable amount of SiO gets burned with CO in excess air above the charge. Hence, the correct description for this process is more complex and given by Equation 2 and Equation 3 :

$$(1+x)\mathrm{SiO_2} + (2+x)\mathrm{C} = \mathrm{Si} + x\mathrm{SiO} + (2+x)\mathrm{CO} \tag{2}$$

$$(1+x)\mathrm{SiO_2}+(2+x)\mathrm{C}+(1+x)\mathrm{O_2} = \mathrm{Si}+x\mathrm{SiO_2}(silicafume)+(2+x)\mathrm{CO_2}+heat \tag{3}$$

2.2.2 Challenges of Carbothermic Reduction Process

The main challenges of this plant is high energy demand and high rate of emission of toxic substances. From Equation 2 and Equation 3 , we can see that there is formation of CO and CO_2 during the reduction process but there are several more emissions beside them. NOX, SO_2, Dioxin, PAH, Heavy metals and Mechanically and Thermally generated PM are other emissions which should be counted seriously. [5] Some emissions are also evident during postproduction processes such as refining ad transportation. Silica is obtained from quartz so it needs to be mined and processed prior to use in Submerged Arc Furnace. These steps can also contribute to emissions.

2.3 Alternative to Carbothermic Reduction Process

Several new routes for silicon production has been proposed which are more or less likely to mitigate the challenges of carbothermic reduction process. Some of them has been discussed in this section.

2.3.1 Reduction Using Hydrogen

This method could have been one of viable alternative for silicon production since carbon emission would not be found with the use of hydrogen as reductant. Experiments were conducted and the result revealed that high pressure is essential for Si production with high silicon recovery and excessive hydrogen consumption is seen. Such high pressure seems to be impractical for cheap industrial process which demotivated the production of Si by using Hydrogen as reductant.[4]

2.3.2 Electrolysis

Electrolysis method for aluminium production has been common. Silicon is more noble than aluminium due to which expectation of producing silicon through same principle had been made. This study was made by Elwell and Rao in 1988. Study were made with the electrolysis of SiO2 and electrolysis of hydrofluorosilicic acid H_2SiF_6, but the result showed that a lot of development is required for its commercialization. Cost evaluation could not be performed currently but it seems to have low reaction rate and high cost when compared with carbothermic route of silicon production. However, high purity silicon can be extracted with this way. [6]

2.3.3 Metallothermic reduction

Metallothermic reduction reaction are displacement reactions involving the use of reactive metals for production of another metal, alloys nonmetal elementary substances, and composites. These reactive metal acts as reducing agents for reduction of oxides and halides. [7] [8] General equation is given

by Equation 4:

$$AX + B = A + BX \tag{4}$$

Where, X can be either oxygen, chlorine or fluorine. B is the reactive metal which reduces AX into metal A.

Aluminum, calcium, ferrosilicon, magnesium, and sodium are the most commonly used reducing metals. The reducing metals must have certain characteristics to be able to perform metallothermic reduction reaction, such as strong affinity for a compound to be reduced, high boiling point, low vapour pressure, ability to produce a slag which can be easily leached or melted. Similarly, it must be cheap as well as easy to handle. [8]

Different study has been made for suitability of silicon production using this technique. In 1854, Sainte Claire Deville prepared Silicon in its more common crystalline form by electrolyzing impure sodium-aluminum chloride containing around 10% silicon. [8]

2.3.4 Magnesiothermic reduction

Magnesium can also be used to reduce silicon dioxide to silicon, but the process is complicated because of development of several transitional compounds. [9] Magnesiothermic reduction of silicon can be described by Equation 5:

$$2\,\mathrm{Mg} + \mathrm{SiO_2} = 2\,\mathrm{MgO} + \mathrm{Si} \tag{5}$$

Mg_2Si is formed as intermediate compound in initial phase which acts as reducing agent later to reduce silica to silicon. [10] This has been described in equation Equation 6 and Equation 7.

$$\mathrm{SiO_2} + 4\,\mathrm{Mg} = 2\,\mathrm{MgO} + \mathrm{Mg_2Si} \tag{6}$$

$$\mathrm{Mg_2Si} + \mathrm{SiO_2} = 2\,\mathrm{MgO} + 2\,\mathrm{Si} \tag{7}$$

The formation of Mg2Si is enhanced with excess magnesium as Mg consumes Si produced over time, as described by Equation 8 . [10]

$$2\,\mathrm{Mg} + \mathrm{Si} = \mathrm{Mg_2Si} \tag{8}$$

2.3.5 Aluminothermic reduction

Aluminium, having strong affinity for silica can be used as reducing agent for silicon production and it can be taken as suitable alternative to carbothermic reduction process. The reaction using aluminium as reductant is more efficient in terms of energy consumption and carbon emission. General reaction is described by the Equation 9 :

$$3\,\mathrm{SiO_2} + 4\,\mathrm{Al} = 2\,\mathrm{Al_2O_3} + 3\,\mathrm{Si} \tag{9}$$

For overcoming the low productivity of Siemen's process in SoG-grade silicon production, new process based on metallothermic reduction of silicon halides by metal reductants such as zinc and aluminium has been studied.[11] This is described by Equation 10:

$$3\,\mathrm{SiCl_4\,(g)} + 4\,\mathrm{Al\,(s,l)} = 3\,\mathrm{Si\,(s)} + 4\,\mathrm{AlCl_3\,(g)} \tag{10}$$

Aluminum trichloride (AlCl3) is formed as the reaction by-product and it is removed as a vapor. The study showed that the productivity can be greatly increased as compared to that of Siemen's process and thus showing great potential in aluminothermic reduction process. [11]

2.4 SisAl Process

The SisAl Pilot process- Innovative pilot for Silicon Production, funded by the European Commission under the H2020 Funding Programme, targets to replace carbothermic reduction process, with the use of aluminium and silicon raw materials, emphasizing to decrease environmental impact. This

process is based on aluminothermic reduction process where, quartz in the slag is reduced by secondary raw materials such as aluminium scrap and dross. These aluminium by-products act as alternative for carbon reductant which are being used today.[12] General working principle for SisAl process has been shown in Figure 3

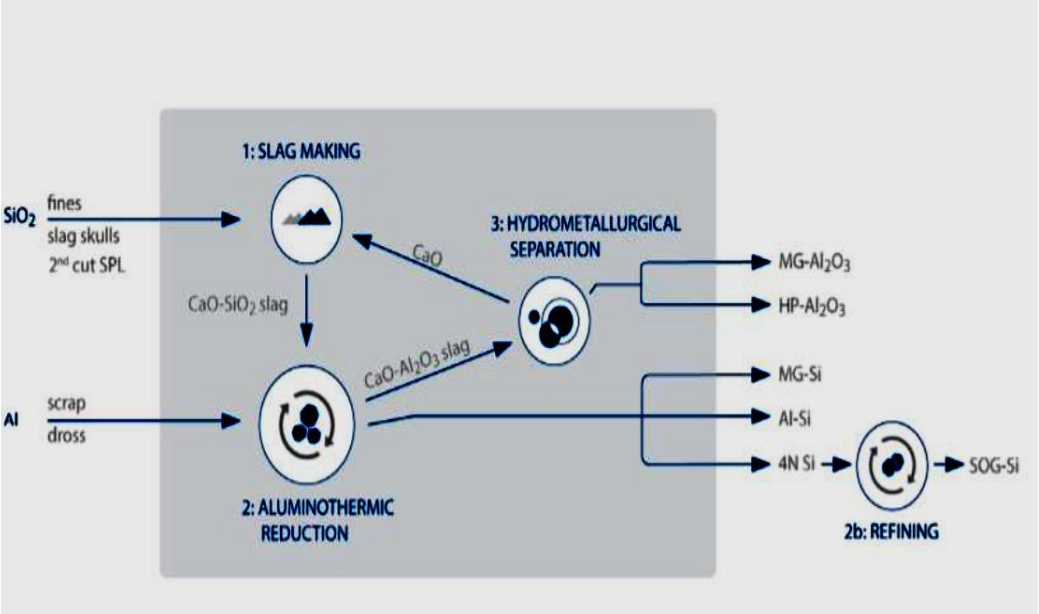

Figure 3: *Schematic representation of SisAl process[12]*

The process requires pre-fused slag containing SiO_2 and CaO which is reduced by aluminium by-products. So, to maintain the ratio of CaO:SiO_2=1.1, pre-fused slag is prepared at temperature between 1600-1700°C. Aluminium by-products are then heated with pre-fused slag at a temperature of 1650-1700°C to reduce SiO_2, thereby forming silicon alloy with slag based on Al_2O_3-CaO. This has been described by Equation 11 :

$$\mathrm{SiO_2\,(in\,CaO{-}SiO_2\,slag)}+\frac{4}{3}\,\mathrm{Al\,(l)}=\mathrm{Si\,(l)}+\frac{2}{3}\,\mathrm{Al_2O_3\,(in\,Al_2O_3{-}SiO_2{-}CaO\,slag\,)} \tag{11}$$

Thus formed Al_2O_3-CaO based slag undergoes hydrometallurgical processing to produce Al_2O_3. CaO can be recycled back into aluminothermic reduction process where as Al_2O_3 can be used for aluminium production plant as raw material. The slag generated from this reduction process can also be used in refining industries.[13]

2.5 Si-Al-Ca Phase Diagram

Ternary phase diagram representing Si-Al-Ca system has been shown in Figure 7. Different phases which can exist under different temperature and concentration has been visible.

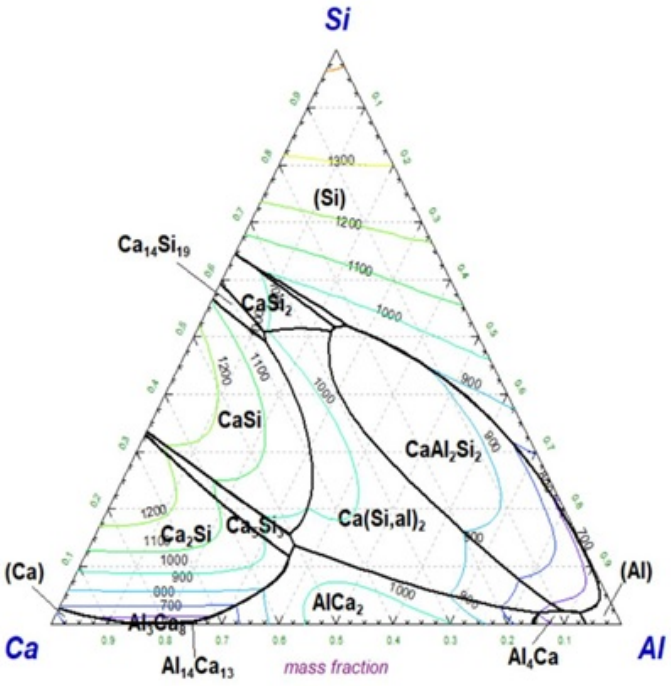

Figure 4: *Si-Al-Ca Phase diagram[14]*

2.6 Slag properties

The $SiO_2 - Al_2O_3 - CaO$ slag system must be completely comprehended because the majority of the slag produced in the Sisal process are based upon it. Investigating the outcomes based on the slag characteristics requires a clear understanding of the slag system in the Sisal process. For defining the engagement among metal and slag in our output, some significant slag properties to be discussed include viscosity, interfacial properties, and slag basicity.

2.6.1 Viscocity

Viscosity is a fluid's (liquid or gas) resistance to shape change or motion of adjacent parts with respect to one another. Because of the high internal friction caused by its molecular structure, a fluid with a high viscosity resists motion. Low viscosity fluids flow easily because their molecular structure causes little to no friction when they are in motion.

In a study, L. Rehakova [15] determined viscosity of molten $SiO_2 - Al_2O_3 - CaO$ system experimentally and assessed the effect of the CaO/SiO_2 ratio on the viscosity and structure of this system. All of the investigated oxide systems' viscosity decreased exponentially as temperature rised. The chemical make-up of the oxide system had a significant impact on dynamic viscosity. Ratio CaO/SiO_2, had a big impact on viscosity. Viscosity initially drops as basicity rises, reaching its lowest point at a CaO/SiO_2 ratio of 1,19 (1,723 K); 1,14. (1 843 K). When the CaO/SiO_2 ratio was higher, viscosity values once more raised. At lower temperatures, the effect of basicity on the viscosity value of slags was much more pronounced.

2.6.2 Basicity

Basicity in metallurgy refers to the proportion of basic and acidic oxides (percent by weight) in slag. The metallurgical characteristics and chemical make-up of such materials are determined by their basicity. The ratio of CaO to SiO_2 or the sum of CaO and MgO to that of SiO_2 and Al_2O_3 is the

simplest way to define basicity.[16]

While basic oxides are known as "network breakers," acid oxides are referred to as "network formers." Richardson [17] provided additional support for this by demonstrating how acid oxides behave as network formers in slags and how they form from oxide species where covalent bonding predominates over ionic bonding (i.e. the elements bonding with oxygen have a high Pauling electronegativity). Basic oxides are formed from oxide species where ionic bonding predominates over covalent bonding and act as network breakers in slags (i.e. the elements bonding with oxygen have a low Pauling electronegativity). Due to the breakdown of the network structure, acid oxides tend to form highly viscous oxide melts, and the addition of basic oxides tends to reduce the viscosity of an acid melt, as schematically depicted in Figure 40.

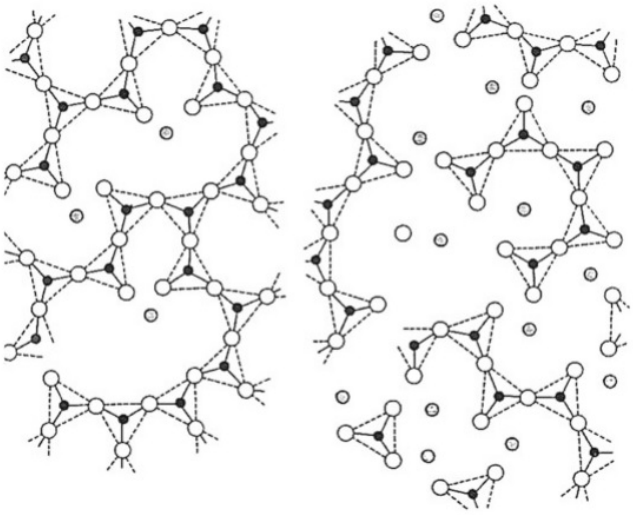

Figure 5: *Schematic representation of the change in a slag structure when the concentration of network breakers (basic oxides species) is added to a silica-rich melt and the network structure is broken down*

2.6.3 Interfacial properties

During the metal production phase, numerous reactions take place. Understanding the kinetics and mechanisms of such reactions is essential, and

interfacial properties play a significant role in this. The work necessary to expand the interface by one unit is referred to as the interfacial energy between two interacting materials . As shown in Equation 12, there is typically a linear relationship between temperature and surface energy (in the gas and liquid phases).[4]

$$\sigma = \sigma o + (d\sigma/dT) \cdot T \tag{12}$$

where,

T = absolute temperature

d(Sigma)/dT = change in surface energy per unit change in temperature. These are constant and are obtained experimentally.

Park et al. [18] conducted a study on the interfacial tension of the CaO-Al_2O_3-SiO_2-MgO-FeO slags with liquid iron at 1550°C. They discovered that for both the CaO-SiO_2-MgO and $CaO - SiO_2 - Al_2O_3 - MgO$ slag systems, the interfacial tensions of molten slag with liquid iron increased continuously with increasing CaO/SiO_2 ratio.

2.7 Aluminium-Silicon alloys

Having numerous uses in the automotive and aerospace industries, aluminum silicon (Al-Si) alloys are among the promising alternatives in the field of casting alloys. Eutectic, hypoeutectic, and hypereutectic alloys from silicon and aluminum can be created depending on the composition of the two elements. Majority of alloys used contain 5 to 25 percent silicon, with trace amounts of magnesium, nickel, and copper. [19]

Silicon is a very inexpensive raw material that increases the melt's fluidity, lowers the melting temperature, and reduces the contraction brought on by solidification. Due to silicon's low density, the overall weight of the alloy that is cast also tends to be lower. It precipitates as virtually pure silicon, increasing the hardness and abrasion resistance, despite having very little solubility in aluminum.[20]

Among all casting alloys, an alloy made of silicon and aluminum has the most important properties. Some of the fundamental characteristics of Al-Si alloys include high corrosion resistance, high wear resistance, and an excellent combination of castability and mechanical properties. It is particularly suitable for making engine blocks due to mechanical properties like good thermal conductivity and a high strength to weight ratio. [21]

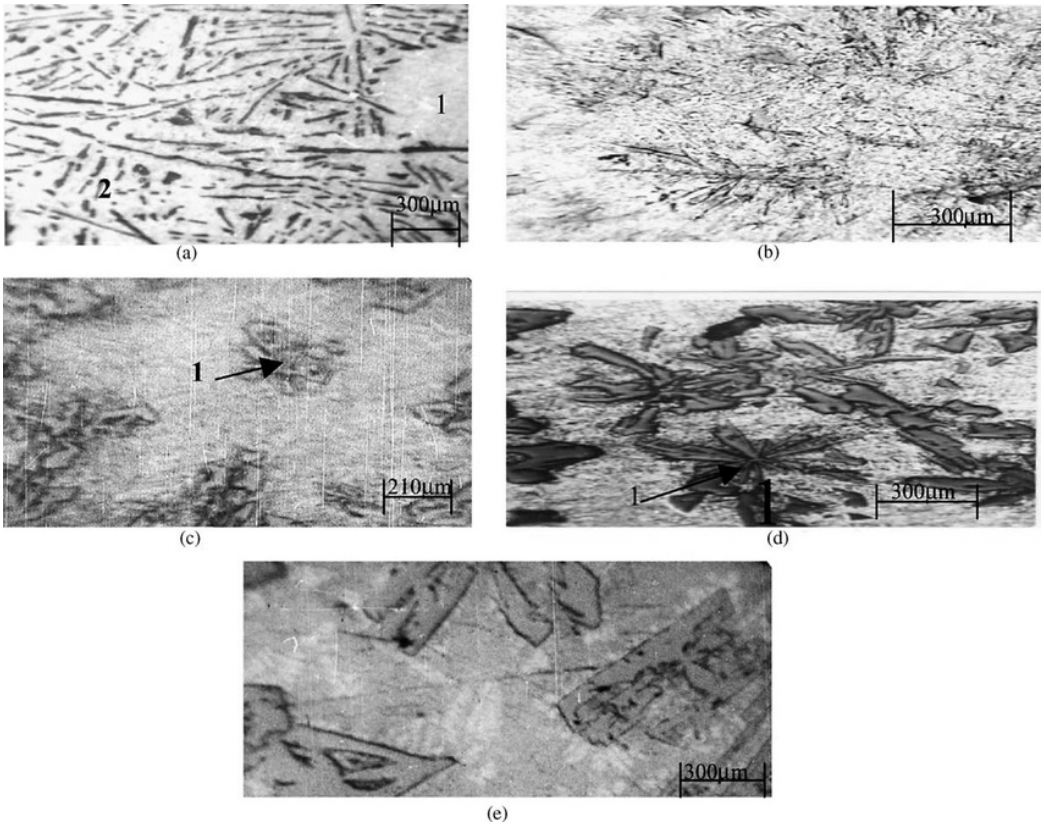

Figure 6: *Microstructure of Al–Si alloys vs. Si content: (a) 11.5 wt.% Si, 1 is the primary crystal of ⌴solid solution, 2 is the eutectic structure with needle like Si component of black colour. (b) 20wt.% Si. (c) 25wt.% Si, 1 is star like primary Si crystal. (d) 30 wt.% Si, 1 is star like Si primary crystal. (e) 35wt.% Si [22]*

Nikanorov et al. [22] conducted research over structural and mechanical properties of Al-Si alloys obtained by fast cooling of a levitated melt. Alloys

with varied silicon composition ranging from 11.5 to 35 wt% were used for rapid cooling, whose research gave in depth sight of linear concentration dependence of density and Young's Modulus. Figure below represents the microstructure of Al-Si alloys with varied Si content. The eutectic structure of the hypoeutectic alloy (Fig. 1a) contains primary crystals of Si solid solution in Al. The alloy with 20 weight percent Si (Fig. 1b) has an unusual finest-grain eutectic structure. The 25-wt% Si composition has primary Si crystals in the shape of stars against a eutectic structure (Fig. 1c). With increasing Si content (30 and 35 wt%), primary Si crystal concentration and size increase.

2.8 Rapid solidification

Rapid solidification is the quick removal of thermal energy, including latent heat and super heat, when a liquid material at a high temperature is transformed into a solid at a lower temperature. Prior to the introduction of solidification, under coolings of up to 100 or more may be caused by the rapid extraction of heat. Only few degrees are attained in the case of conventional casting at a rate of about 1or less per second, which makes rapid solidification effective. [23]

Some rapid solidification technologies also enable high casting speeds, inline winding of the thin ribbon, and automatic reel change during winding without process interruption. Cooling rates in these technologies can be as high as 106 K/s (i.e., from approximately 1400 C to less than 40 in one millisecond). [24]

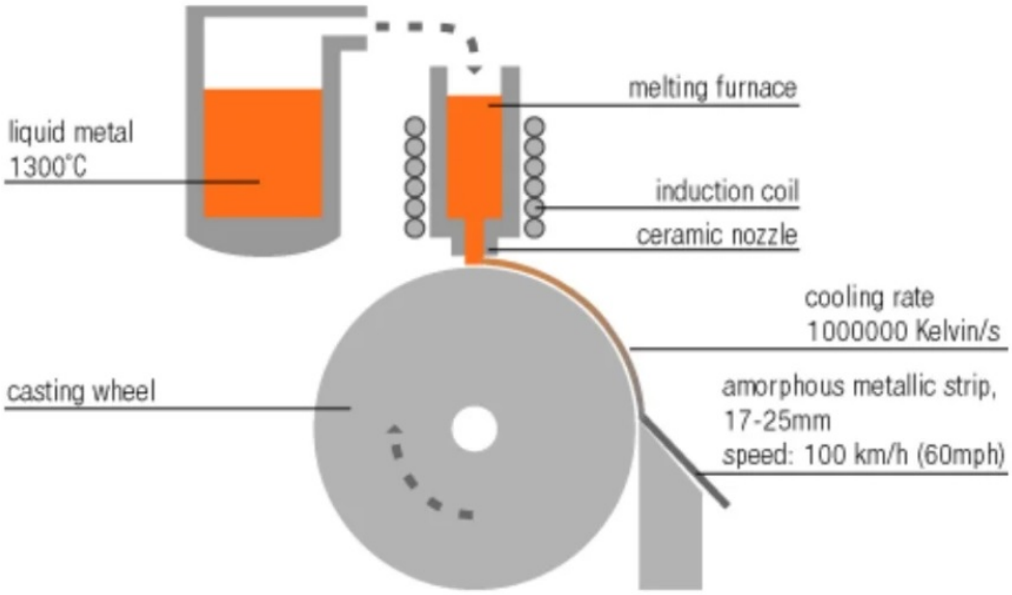

Figure 7: *General working principle of Melt spinner [24]*

The schematic representation of the meltspinner which follows rapid solidification principle is shown in the above figure. The melting furnace in the figure has liquid metal in it, but solid alloys could also be used since there is an induction coil to melt them. The nozzle through which the melted alloy solution drops is typically very small and the solution is forced to drop through by supply of argon gas from the top.

3 Experimental procedure

3.1 Overview of experimental procedure

The purpose of this thesis work is to examine the effect of under-stoichiometric aluminium in aluminothermic reduction process used in SisAl. Experiments based upon study of CaF_2 on aluminothermic reduction process has also been done. In addition, Al-Si alloy with two different composition, slightly above eutectic point has been prepared for the observation of its micro-structure. The experiment conducted for study of under-stoichiometric aluminium in $CaO-SiO_2$ based slag has been presented at first. Experiment for study of effect of CaF_2 in $CaO-SiO_2$ slag and preparation of Al-Si alloy using direct solidification technique has been presented afterwards. Different analysis techniques were utilised for sample characterization which are also introduced at the end of this section.

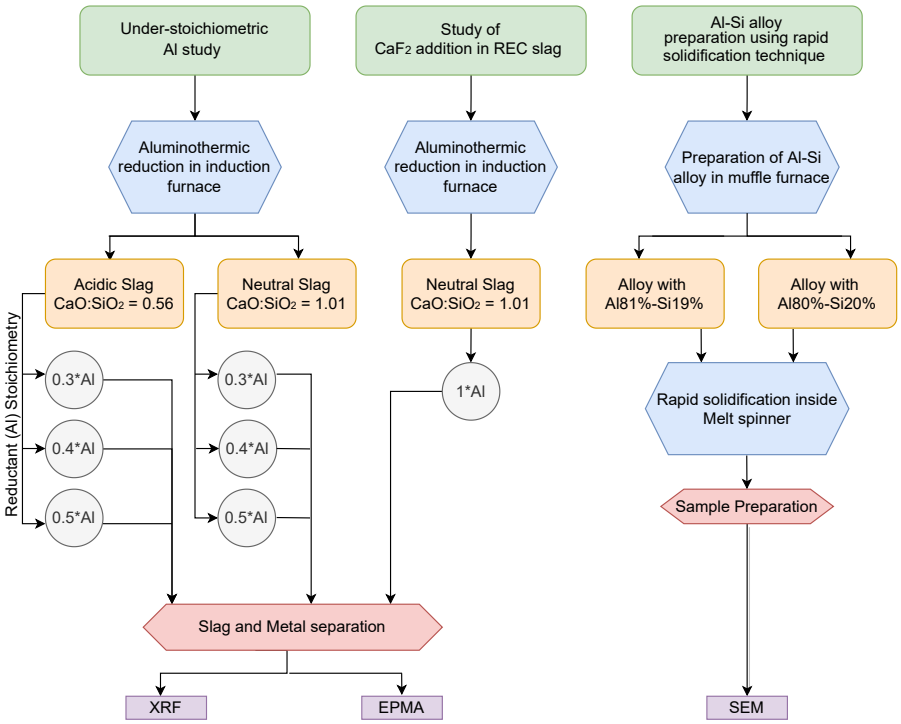

Figure 8: Flowchart representing Overview of experimental procedure

3.2 Aluminothermic Reduction Reaction

3.2.1 Apparatus

The aluminothermic reduction tests in this work were carried out in an Induction Furnace (75kW, 3000Hz), as seen in the picture. Three small sized resina crucibles were used for each set of tests and were put within a single large crucible that was entered inside the furnace, as illustrated in Figure 9. Throughout the experiment, argon gas was continuously purged to maintain an inert environment inside the system. A C-type thermocouple was used to measure the temperature. Thermocouple was kept inside alumina tube which was further kept inside small graphite tube for support during experiment.

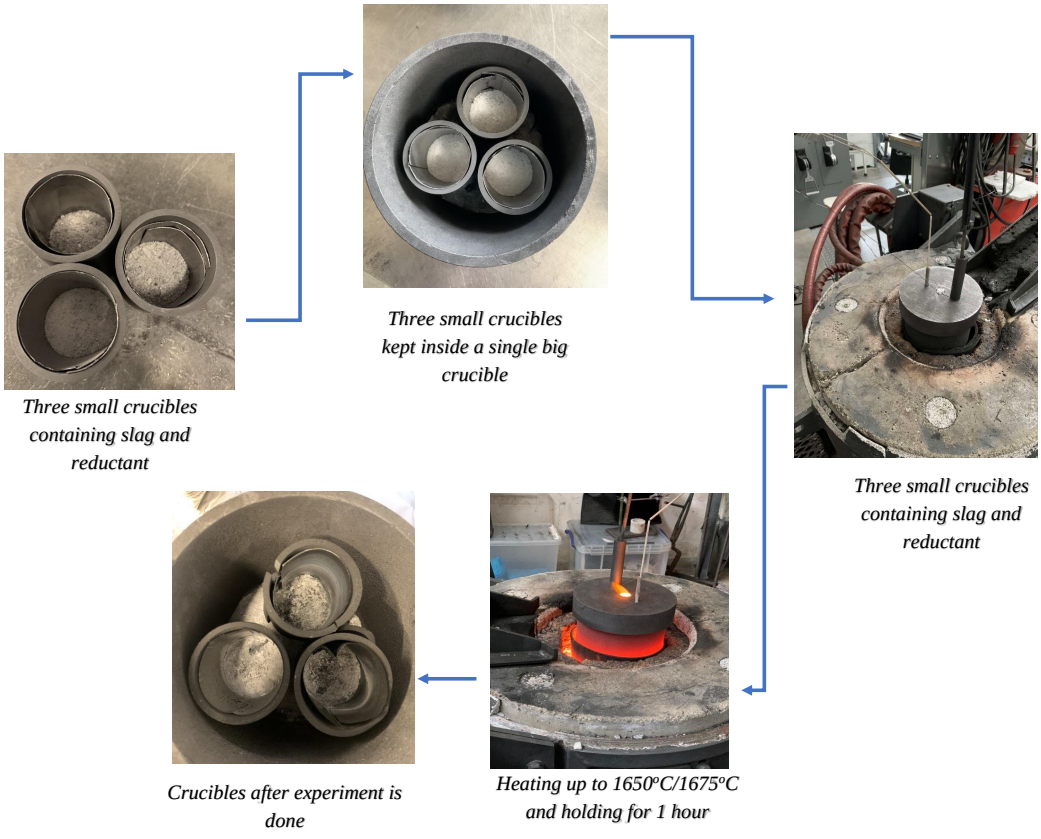

Figure 9: Crucible setup and Experimental setup in Induction furnace

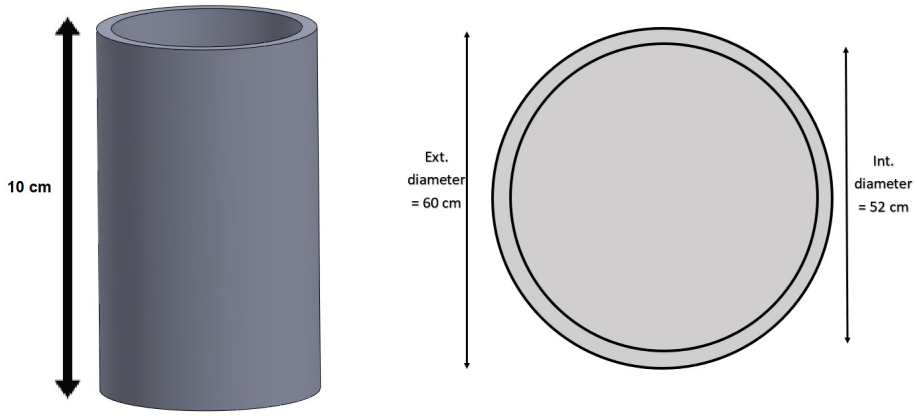

Figure 10: Left image represents front view of crucible used in our experiments, Right image represents it's top view

3.2.2 Reduction of Acidic and Neutral Slag

The primary purpose of this thesis study is to explore the influence of understoichiometric aluminium in the Sisal process end product. Two forms of slag, acidic and neutral, were investigated with three different aluminum stoichiometry. For neutral slag, pre-fused slag from Elkem was utilized, which had a CaO:SiO_2 ratio of 1.01. For acidic slag, pre-fused slag was treated with a determined amount of SiO2 to reduce the CaO:SiO_2 ratio to 0.56. SiO_2 was initially in crystal from which was milled and changed into powder form. In a plastic bag, pre-fused slag was mixed with milled SiO_2 and thoroughly shaken to provide a homogeneous composition.

Three distinct aluminium stoichiometry (0.3*Al, 0.4*Al, and 0.5*Al) were examined in a single experimental setup using either neutral or acidic slag. Three attempts of the same experiment were carried out with both acidic and neutral slag. This investigation made use of a graphite crucible, the specification of which are shown in Figure 10. The inner sides and base of the graphite crucible were wrapped with graphite paper to prevent input from interacting with the graphite and to aid in the easy separation of product from the crucible. Graphite paper used in these experiments were obtained

from "Groupe Carbone Lorraine" which was of quality "N" and had thickness of 0.2mm.

While inserting materials into the crucible, a little quantity of slag was kept at first, then pieces of aluminum were added, and the remaining slag was added afterwards, so that the aluminum was completely covered. In order words, aluminum was held in the midst of the slag employed inside the crucible. In the case of acidic slag, crucibles were heated up to 1650 °C while they were heated up to 1675 °C when neutral slag was used. Amount of reductant, pre-fused slag and SiO_2 used in our acidic slag experiment and neutral slag experiment has been represented on Table 1 and Table 2 respectively.

Table 1: *Amount of slag and reductant used in Aluminothermic reduction reaction using acidic slag and pure aluminium*

	Trial	Crucible	Reductant Stoichiometry	*Slag (g)* Pre-fused	SiO_2	Al (g)
Acidic Slag Experiment (CaO:SiO2=0.56)	1	A	0.3*Al	71.59	28.4	11.46
		B	0.4*Al	71.59	28.5	15.29
		C	0.5*Al	71.59	28.5	19.09
	2	A	0.3*Al	71.6	28.39	11.4
		B	0.4*Al	71.59	28.42	15.29
		C	0.5*Al	71.58	28.41	19.09
	3	A	0.3*Al	71.6	28.4	11.47
		B	0.4*Al	71.59	28.41	15.25
		C	0.5*Al	71.6	28.38	19.09

Table 2: *Amount of slag and reductant used in Aluminothermic reduction reaction using neutral slag and pure aluminium*

	Trial	Crucible	Reductant Stoichiometry	Slag (g) Pre-fused slag	Al (g)
Neutral Slag Experiment (CaO:SiO2=1.01)	1	A	0.3*Al	100	7.77
		B	0.4*Al	100	10.41
		C	0.5*Al	100	12.99
	2	A	0.3*Al	100	7.77
		B	0.4*Al	100	10.38
		C	0.5*Al	100	13.01
	3	A	0.3*Al	100	7.79
		B	0.4*Al	100	10.42
		C	0.5*Al	100	13.01

3.2.3 Reconfirmation Experiment

To validate the findings obtained from under-stoichiometric aluminium addition to acidic and neutral slags, a further trial was performed using just 0.3*Al stoichiometry with both acidic and neutral slag. The experimental equipment and materials utilized were identical to earlier tests, with the main variation being how the aluminum was stored inside the crucible. In the previous setup, the aluminum was maintained in the center of the slag and was completely covered by it, however in this setup, the entire slag was kept inside the crucible initially the aluminum was kept on top.

Table 3: *Amount of slag and reductant used in reconfirmation experiment*

Crucible	Slag Type	Reductant stoichiometry	Slag (g)		Reductant (g)
			Pre-fused	SiO_2	
A	Acidic	0.3*Al	71.59	28.4	11.51
B	Neutral	0.3*Al	100	$\sim$	7.77

3.2.4 Effect of CaF_2 in aluminothermic reduction

A single trial of experiment was carried out using stoichiometric Al and neutral slag (Pre-fused slag from Elkem) containing 10% CaF_2. This experiment was carried out in an induction furnace in exactly similar setup as before. A calculated amount of CaF_2 powder was mixed with pre-fused slag and thoroughly shaken for uniform dispersion. This experiment was conducted in conjunction with a reconfirmation experiment in which only two crucibles was used for under-stoichiometric investigation, and had a space for another crucible to fit.

Table 4: *Amount of slag and reductant used in aluminothermic reduction experiment using CaF_2*

Crucible	Slag Type	Reductant stoichiometry	Slag (g)		Reductant (g)
			Pre-fused	CaF_2	
C	Neutral	1*Al	90	10	28.4

3.3 Preparation of Al-Si Alloy

Another goal of this thesis study is to explore the micro-structure of Al-Si alloy formed by alloying Aluminium and Silicon slightly above its eutectic point. Two distinct Al-Si alloys with varying compositions were produced for this purpose. Since the eutectic point of Al-Si is 577 $\pm$1 °C, the alloy was created at temperatures ranging from 800-850 °C. The resulting Al-Si alloy was then treated in a melt spinner for rapid solidification to generate ribbon-shaped Al-Si which was observed in SEM. Brief description about the experimental procedure for Al-Si alloy has been illustrated in Figure 11.

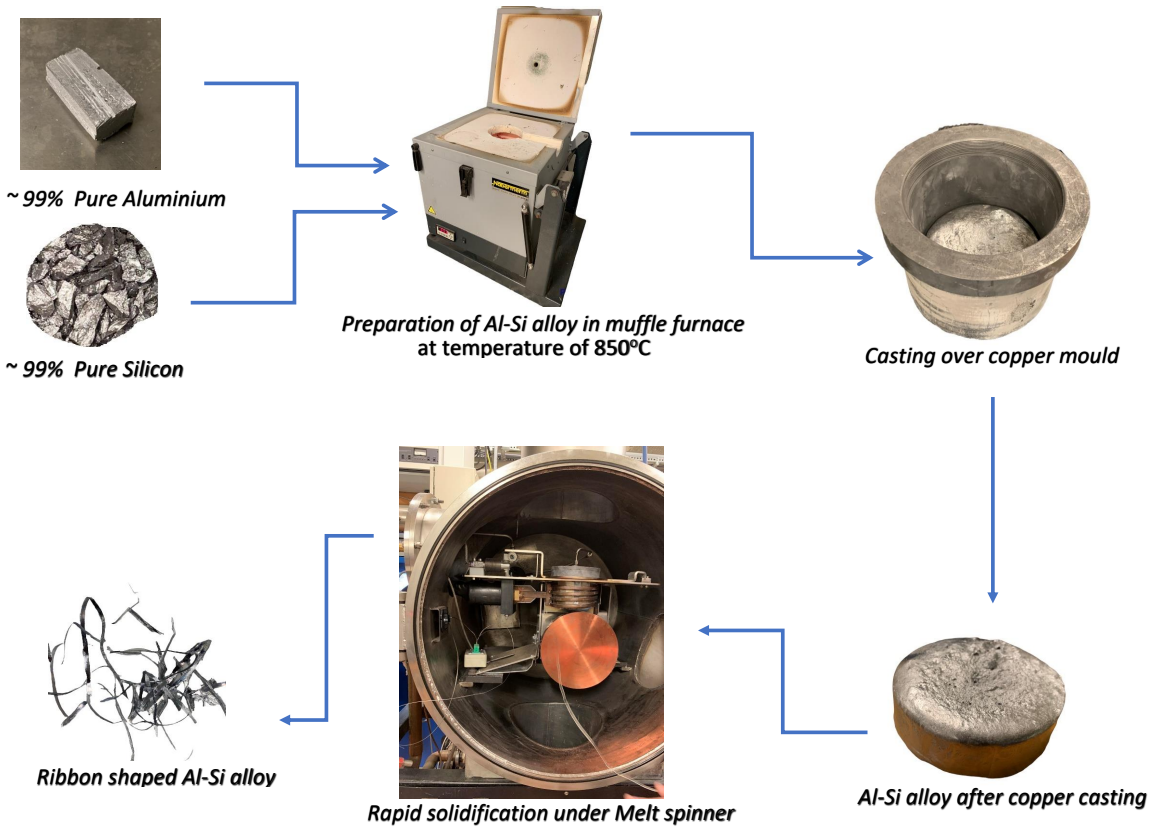

Figure 11: Experimental procedure for Al-Si alloy preparation

3.3.1 Alloy preparation in muffle furnace

The Al-Si alloy was made on a muffle furnace by heating a calculated amount of Silicon and Aluminium at 850 degrees Celsius. The materials utilized were 99 percent pure aluminium from Hydro and 99 percent pure silicon from Elkem. The amount of silicon and aluminum utilized for two different compositions are shown in the Table 5. Aluminium was first kept inside a SiC crucible that was coated with Boron Nitride in the inner walls so that the generated alloy would not be stuck to the crucible. Inside the muffle furnace, this crucible was heated until the aluminum was totally melted. The silicon was then added to the melted aluminum and stirred occasionally so that the silicon would melt and dissolve in the melted aluminum. The entire melting

process took around three hours, and the heated solution was subsequently poured into a copper plate for casting.

Table 5: *Amount of Al and Si used in alloy formation*

Alloy	Pure Al (g)	Pure Si (g)	Al wt %	Si wt %
1	64.8	16.2	80	20
2	470	110	81	19

3.3.2 Rapid solidification in Melt spinner

The alloy generated in the muffle furnace was then sent to the melt spinner for rapid solidification. The fundamental reason for accelerated solidification of this alloy was to achieve finer grain structure and chemical homogenization. Rapid solidification was accomplished using the "Advanced melt spinner" available in NTNU which was made by Marko Materials, Inc, North Billerica, MA. Initially, the alloy produced from the muffle furnace was placed within a specific crucible developed for the melt spinner and heated using the induction furnace installed inside the melt spinner equipment. Due to lack of availability of crucible and time only Alloy 2 made from muffle furnace (81%Al-19%Si) was tested over melt spinner. After heating this alloy up to 710 degrees for 1.5 hours, argon gas was purged through the top of the crucible, forcing the melted Al-Si solution to drop through a tiny hole at the bottom of the crucible. Melted Al-Si from the crucible's base came into touch with a spinning copper wheel spinning at 513 rpm. When melted Al-Si came into contact with a spinning copper wheel, it solidified quickly, resulting in the production of a ribbon-shaped Al-Si alloy.

3.4 Characterisation

3.4.1 Sample Preparation

Following the experimental process, slag and metal samples from each crucible of each experiment were prepared for characterisation. The crucibles

were removed and the slag alloy separation process began. Hammering had been used done to remove the product from the crucible, followed by sand-blasting to remove the attached graphite papers from the product's outer surface. The product was hammered once more to separate the silicon metal from the slag. Small pieces of metal and slag were cast in epoxy and polished using the following methods and grinding surfaces:

Table 6: Steps in polishing epoxy samples

Step	Surface	Lubricant	Speed[rpm]	Force[N]	Time[min]
1	MD-Piano 200	Water	300	35	1
2	MD-Piano 1200	Water	150	35	2
3	MD-Largo	DiaPro Allegro	150	35	8
4	MD-Dac	DiaPro Dac	150	35	8
5	MD-Nap	DiaPro Dac	150	35	1

Alloy and Slag samples were aimed to have XRF characterization, so every slag obtained from experiments were milled upto 70 microns, where as alloy pieces were not milled for XRF analysis. The crushing of samples were done in disc mill with speed of 900rpm for 3 minutes.

3.4.2 EPMA

Every metal sample was investigated using Electron Probe Microanalysis (EPMA). Senior Engineer Morten Peder Raanes performed the analysis on the JXA-8500F Field Emission Electron Probe Microanalyzer at NTNU, Trondheim (NTNU). We used backscattered electrons for sample imaging and obtained visual representations of the various phases present in our metal. EPMA's focus was on determining the elemental distribution and composition of silicon metal produced. As a result, an energy dispersive X-ray spectrometer (EDS) was employed. EDS was performed over a specific area, taking six random points to determine an estimate of the element distribution of the various main elements. EPMA was also used for performing EDS analysis and mapping analysis of Al-Si alloy prepared from melt spinner,

3.4.3 XRF

Alloy and slag samples from our experiment were analyzed using the X-Ray Fluorescence (XRF) technique at Degerfors Laboratorium AB in Bruksparken, Sweden. Thermo Fischer Scientific's ARL 9900 Series XRF device was used to analyze slag and alloy samples. recognizing the composition of Si, Al, and Ca was primary goal, but other impurities in significant amount such as Fe, B, C and P were also studied focused.

3.4.4 SEM

To investigate the morphology of the reaction product, SEM imaging was performed on samples obtained from alloy produced by muffle furnace and melt spinner. SEM analysis was done on Zeiss Supra 55VP FEG SEM, present in EM-lab at NTNU. The SEM was set to 10 kV electron beam with a working distance of around 10 mm. Secondary electron and backscattered electron images were used in SEM to confirm phase distribution in the samples.

4 Results

The results and observations from the experiments and analysis described in the experimental section have been presented in this section. Prior to the experiments, an XRF analysis of the pure aluminum and rec Slag used in the aluminothermic reduction experiments was performed, and the results have been first illustrated.

Second, the results of an aluminothermic reduction process using neutral and acidic slag have been presented. Temperature observations during the experimental process, physical structure of the product formed, alloy and slag yield in different trials, chemical composition of alloy and slag obtained from XRF and EPMA (EDS) analysis have all been used to illustrate the results. Similarly, mass balances of vital elements for each trial, as well as BSE images of metal and slag, combined with phase identification from WDS analysis, have been used to express results from aluminothermic reduction experiments. Simulated equilibrium composition obtained from Factsage 7.3 done by PhD candidate Harald Philipson has also been presented.

Following are the results of an aluminothermic reduction experiment in which CaF_2 was used, as well as observations of its physical structure, metal and slag yield, and chemical composition of the alloy and slag formed. A comparison was also made between an aluminothermic reduction experiment using CaF_2 in slag and an experiment that did not use CaF_2.

Finally, the results of an Al-Si alloy preparation experiment have been demonstrated, where images obtained from SEM are used to assess the alloy prepared from melt spinner and compare it to the one obtained from copper quenched Al-Si alloy coming from muffle furnace.

4.1 XRF analysis of rec slag and Pure Al

XRF analysis technique was done from D-lab for determining the composition of rec slag and pure aluminium. Acidic slag was prepared by mixing rec slag with pure quartz, but XRF analysis of quartz used was not done assuming

used quartz to be 100% pure. Three different samples of rec slag and pure aluminium were tested, and average of those values has been illustrated in the table. CaO/SiO_2 mass ratio for the rec slag was found to be 1.014 rather than the intended 1.1, but XRF analysis revealed that the purity of aluminium used in our experiment was around 99% which is similar to what we had proposed.

Table 7: XRF result for three samples of rec used in experiments

	CaO	MgO	SiO_2	Al_2O_3	Fe_2O_3	K_2O	SO_3
rec Sample 1	50.1	0.45	48.6	0.54	0.18	0.02	0.03
rec Sample 2	49.7	0.4	49.3	0.36	0.13	0.03	0.04
rec Sample 3	49.9	0.42	49.1	0.38	0.15	0.04	0.03

Table 8: XRF result for Pure Aluminium used in experiments

	Al	Si	Fe	Cu	Mg	Ni	Ti	Ga
Pure Al	99.816	0.04	0.11	0.001	0.004	0.004	0.004	0.01

4.2 Results from Aluminothermic Reduction Experiment

Three different trials of aluminothermic reduction experiments were done for both acidic slag and neutral slag whose results has been revealed in this section. Results from different trials were similar in some parameters whereas unique variations were also seen with some trails where exact same parameters were used. To validate the results obtained from these sets of experiments, reconfirmation experiments were done whose results has also been shown parallelly.

4.2.1 Temperature observation

C-type thermocouple was used for entire experiment during which thermocouple was kept in centre of crucible touching its base for temperature measurement. For most of the experiments, the time taken to reach the holding temperature was about 1 hour but some of trials of neutral slag experiment took less time than it. The picture representing the rise in temperature along time and change in temperature along time has been illustrated in **??**.

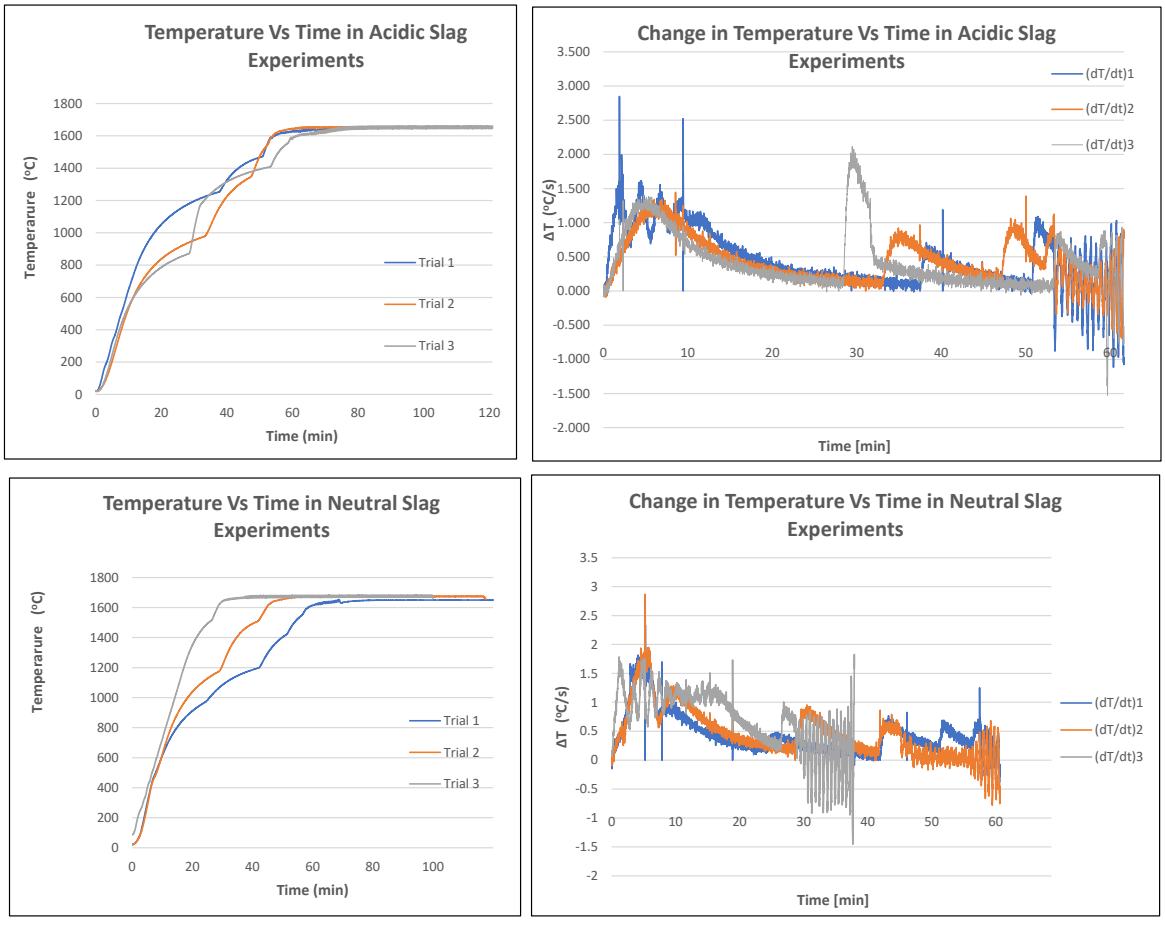

Figure 12: Temperature and change in temperature plot against time for i. Acidic Slag experiment (Top) ii. Neutral Slag experiments (Bottom)

In the case of experiments using acidic slag, the time taken to reach target temperature was around 60 minutes for all three trials. The graph in top left section illustrated in **??** reveals several small temperature drop around 30 to 40 minutes. The temperature plot for neutral slag experiments show different trend. Time taken to reach target temperature is quite less. For trial 1, it took the least time as 1650 °C temperature was maintained within 30 min while it took 50 min and 60 min for trial 2 and 3 respectively. Fluctuations in temperature were observed more during 30 to 40 minutes comparatively similar to acidic slag experiments.

4.2.2 Physical Structure

This section depicts the physical structure of the product obtained from aluminothermic reduction experiments using acidic slag and neutral slag. The product structure from the experiment using CaF_2 in slag as well as the product obtained from the Al-Si alloy preparation have been discussed afterward. Even when identical input parameters were used, the products from different trials were similar in some trials and different in others in terms of morphology. The experiments with acidic slag revealed the most non-uniform product structure.

Crucible breakage following the experiment was observed in most of the trials during aluminothermic reduction tests using acidic slag. Breakage might have happened during heating or when the crucibles were left to cool after being held up to the target temperature for an hour. When metal was produced, it was found to be present in the crucibles in powder form without being firmly attached to the slag. On a few areas of the powdered slag, small metal coalesces were visible. In some acidic slag experiment trials, the products appeared to be firm, but they were actually very soft and easily broke with little hand effort. In contrast to previous aluminothermic reduction studies the author had conducted, the silicon alloy produced in this study was seen to be gathered at one end of the crucibles with several tiny pieces dispersed along different areas. For the acidic slag experiment with 0.3*Al stoichiometry, the product was entirely powder with some hard slag at the base, whereas they

were typically found to have a hard, rigid structure for 0.4*Al and 0.5*Al stoichiometry.

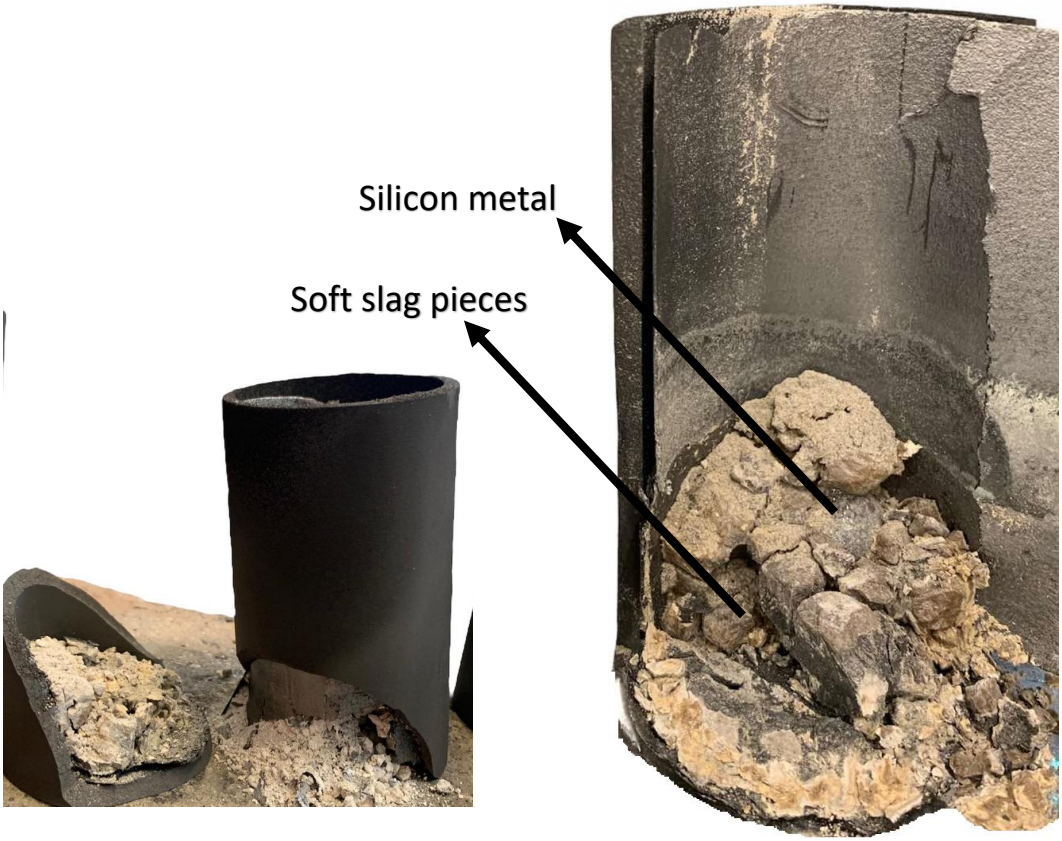

Figure 13: *Picture in left represents the product from acidic slag and 0.3*Al stoichiometry where crucible breakage was observed. Picture in right represents slag and metal setup inside the same crucible*

The product obtained with reconfirmation experiment mentioned in section 3.2.3 had made the use of acidic slag and 0.3*Al stoichiometry. The result from this trial had different physical structure as compared to previous three trials. The product obtained was too hard and slag were found to be more rigid, brittle, and shiny black in colour. Silicon metal was found in the topmost part of the product in oval shape and a brownish coloured layer of

slag was seen at the base of crucible. Slag obtained in this trial was found to be more homogeneous as compared with previous trials.

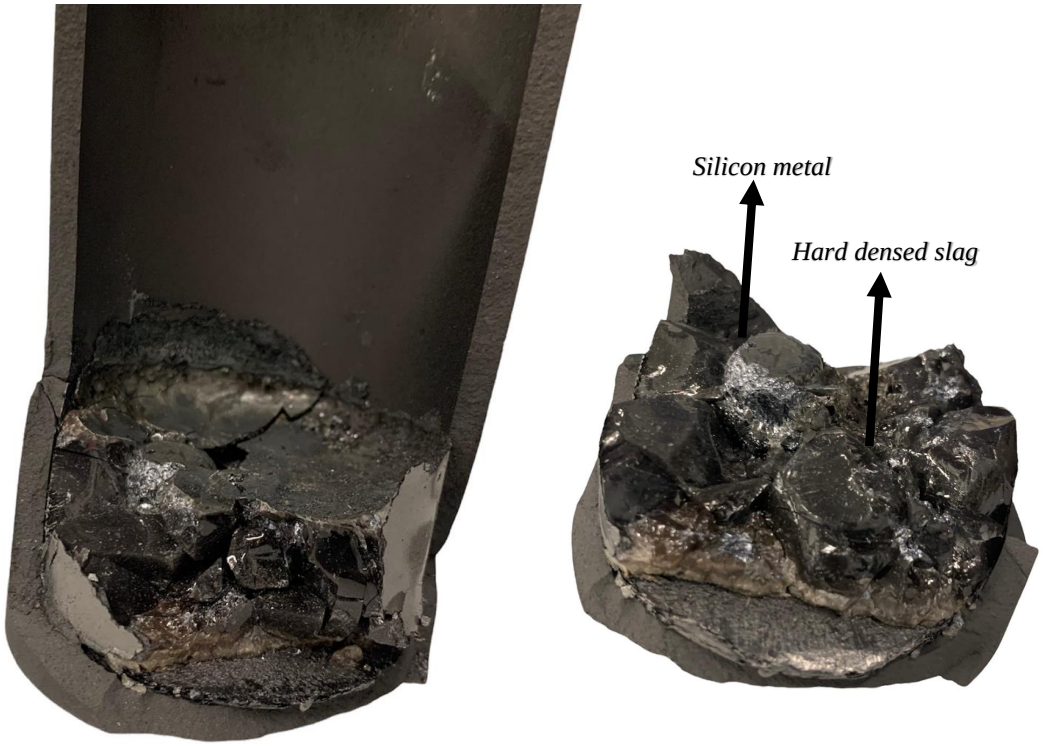

Figure 14: *Figure in the left represents product along with crucible obtained from reconfirmation experiment with use of acidic slag and 0.3*Al stoichiometry Picture in right represents detail structure of the same product*

The product obtained from neutral slag experiments also made product morphology variation in most of the trials. Soft slags with little amount in powder form were observed in some trials of 0.3*Al and 0.4*Al stoichiometry, whereas product were hard with silicon metal and slag being attached strongly in 0.5*Al stoichiometry. Silicon metal was generally present in oval shape without having distinct location. Metal films were observed in few

parts of slag where small silicon pieces were also noticed in some trials with soft slag observation.

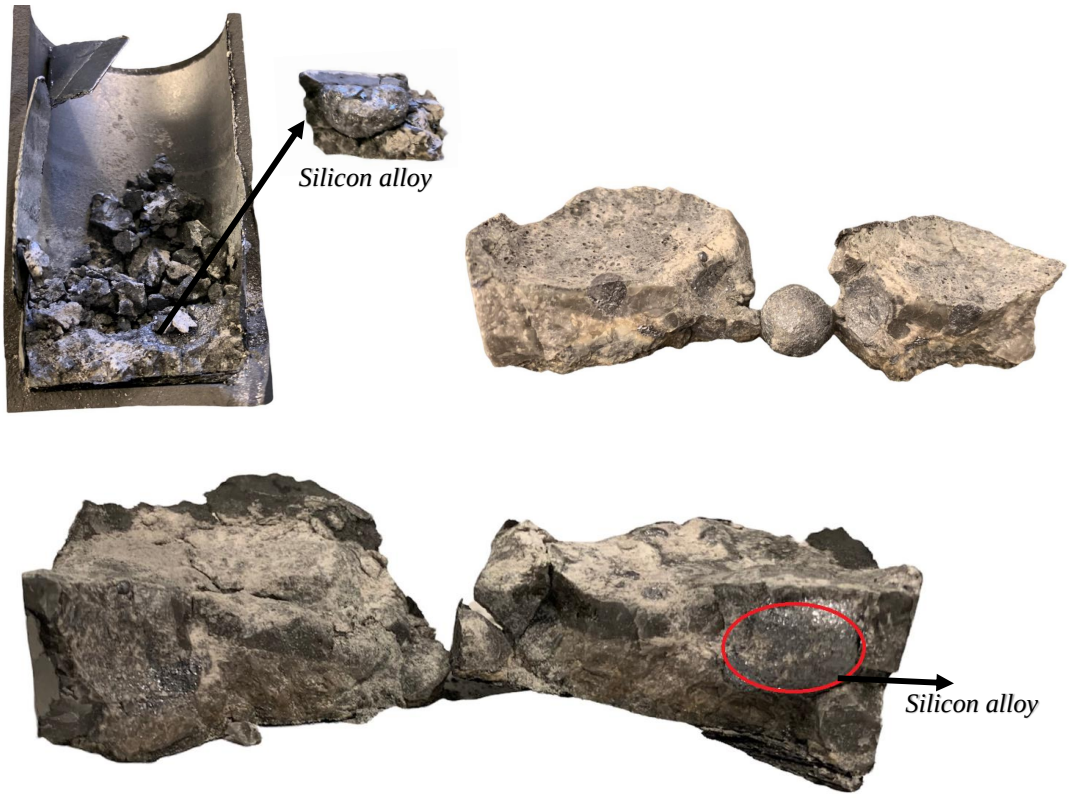

Figure 15: *Top left represents product along with crucible obtained from aluminothermic reduction experiment with use of neutral slag and 0.3*Al stoichiometry (Trial 3). Picture in top right represents product from experiment using 0.4*Al stoichiometry and neutral slag(Trial 3). Picture at bottom represents product from reconfirmation experiment*

In most of the trials using 0.3*Al stoichiometry and neutral slag, the product were not in bulk structure while they were either soft slag pieces or collection of small hard slag pieces with small portion of bulk piece at the base. Small silicon pieces was seen to be dispersed around slag which had not coalesced with big silicon pieces. The case was inverse when reconfirmation experi-

ment was done with exact same parameter i.e with 0.3*Al stoichiometry and neutral slag. In this case, product was bulk structure with silicon and slag firmly attached as shown in bottom of Figure 16.

The case was almost similar in experiments using 0.4*Al stoichiometry and neutral slag. Some trials had given crucibles containing small slag pieces with some in crushed form and oval shaped silicon alloy freely locating within slag. Slag formed were usually yellowish white in colour with little silicon pieces getting noticed within the mass. Few trials gave product with oval shaped silicon and bulky but soft slag. In every trials of 0.5*Al stoichiometry, product were in concentrated form with strongly bound slag and metal. Metal films were noticed in few parts of slag when it was broken in pieces.

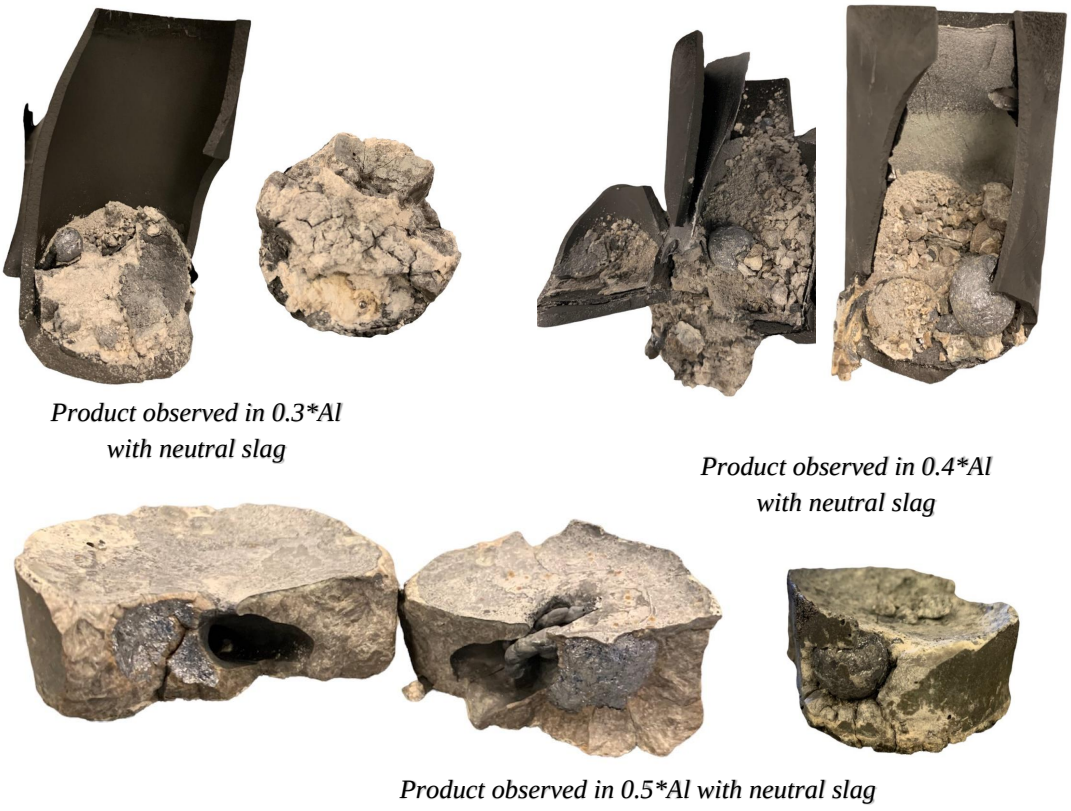

Figure 16: *Different product structure under different stoichiometries of Aluminium in Neutral Slag experiments*

4.2.3 Metal yield

The product obtained after each trial of aluminothermic reduction experiments were taken into slag and metal separation. Hammering was done to separate slag and metal but it was not necessary in the case of trials where powdered form soft slags were observed. The silicon metal produced within the product was collected separately and weighed to know about the silicon yield in our under-stoichiometric study. The metal obtained from our experiments were compared with the simulated Factsage values. Obtained metal were less than expected values from Factsage results. Pieces of silicon were observed in different part of slag in very tiny sizes, inconvenient to collect

which also made the measurement of total metal produced difficult.

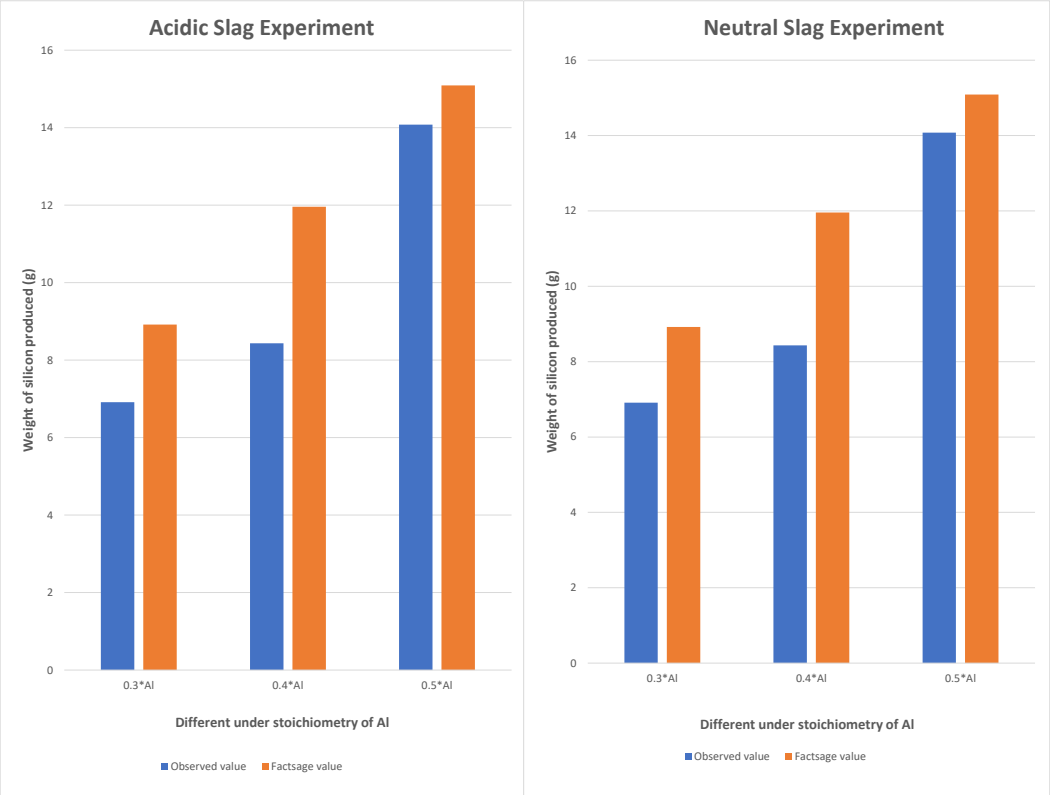

Figure 17: *Silicon produced in product from different stoichiometries of Al. The value of metal produced shown here for each stoichiometry is the average of three trials conducted for similar stoichiometries*

The graph illustrated in Figure 17 shows that yield is more in acidic slag experiments as compared to neutral slag which is also supported as amount of silica in slag and amount of reductant used is also higher in acidic slag experiments. Less deviation has been seen on 0.5*Al stoichiometric trials when compared with Factsage values. Significant difference was noticed on 0.3*Al and 0.4*Al stoichiometries where crushed form slag with small metal pieces were spotted.

4.2.4 Chemical Composition

The chemical composition obtained through XRF ad EPMA analysis of slag and metal has been illustrated in this section. The composition of all three trials for all stoichiometric experiments were done with XRF. For reconfirmation experiments, both EPMA and XRF was done and comparison between both results has been shown.

XRF analysis was done to know the composition of Si, Al and Ca in the metal produced from aluminothermic reduction experiments. The values in Table 9 represents the average of values of Si, Al and Ca composition obtained in three similar trials of both acidic and neutral slag.

Table 9: *Composition of Si, Al and Ca in metal obtained from three different stoichiometries of Al with acidic and neutral slag. Values given represents the average of three trials in each case*

Slag Type	Stoichiometry	Si wt%	Al wt%	Ca wt%
Acidic Slag (CaOCaO=0.56)	0.3*Al	90.06	0.96	8.08
	0.4*Al	85.96	1.81	11.29
	0.5*Al	81.98	2.69	14.56
Neutral Slag (CaOCaO=1.02)	0.3*Al	94.32	0.42	4.44
	0.4*Al	91.18	0.87	7.05
	0.5*Al	88.49	1.26	9.43

The result from metal composition revealed the composition of Si in metal to be increased with decreasing Al stoichiometry. Decreasing trend in Si weight composition in alloy has been seen as we go from 0.3*Al stoichiometry to 0.5*Al stoichiometry. The case is same in both acidic and neutral slag experiment. Weight composition of Al and Ca has opposite trend though. As the stoichiometry of Al increases, the weight composition of Al and Ca has been gradually increased in both acidic slag and neutral slag experiments.

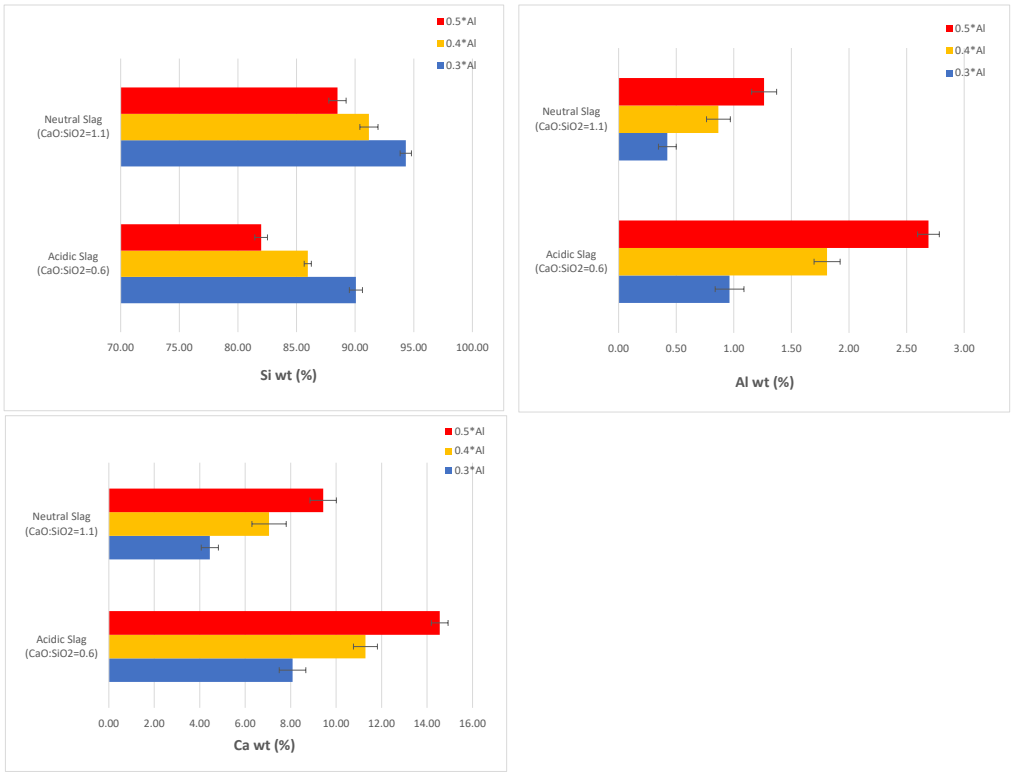

Figure 18: *Average wt% of Si, Al and Ca in metal for the different input slags and reductant amount. Each composition represents average of three trials. Error bar represents the standard deviation from three different trials*

The chemical composition expected in metal and slag were also simulated through Factsage. Table 10 below represents the composition of Si, Al and Ca to be obtained in our three different stoichiometries with corresponding slag treatment.

Table 10: *Composition of Si, Al and Ca in metal expected from three different stoichiometries of Al with acidic and neutral slag. Values given represents the simulated values from Factsage*

Slag Type	Stoichiometry	Si wt%	Al wt%	Ca wt%
Acidic Slag (CaO:SiO2=0.56)	0.3*Al	98.65	0.33	1.02
	0.4*Al	97.55	0.74	1.71
	0.5*Al	95.68	1.43	2.89
Neutral Slag (CaO:SiO2=1.02)	0.3*Al	89.88	1.01	9.09
	0.4*Al	85.70	1.73	12.55
	0.5*Al	82.19	2.49	15.35

The values we expected from Factsage simulation was somehow different from the results we obtained from three trails of every stoichiometries in acidic and neutral slag experiment. The results obtained from XRF analysis by D-lab had higher Si wt% in neutral slag experiments and less in acidic slag experiments, which is opposed by results coming from Factsage simulation. It shows high purity of Si to be obtained from acidic slag experiment which was not in our experimental result.

reconfirmation experiment were done to re-validate our results where two crucibles were tested with acidic slag and neutral slag on each. Both of them were reduced using 0.3*Al stoichiometry and product from both crucibles were analysed with EPMA and XRF. Results from both analysis has been enlisted in Table 11.

Table 11: *Composition of Si, Al and Ca in product obtained from reconfirmation experiment done for 0.3*Al stoichiometry with acidic and neutral slag*

Slag Type	Stoichiometry	Analysis	Si wt%	Al wt%	Ca wt%
Acidic Slag	0.3*Al	XRF	85.80	1.66	4.35
(CaO:SiO2=0.56)		EPMA	98.77	0.33	0.10
Neutral Slag	0.3*Al	XRF	94.2	0.58	4.02
(CaO:SiO2=1.01)		EPMA	93.87	0.35	3.15

The results from reconfirmation experiment showed some differences as compared to previous three trials of each experiment. Results from EPMA were quite similar to expected results from Factsage simulation but the case was different when results from XRF were observed. XRF revealed that the Si purity in acidic slag experiment were less than previous three trials as significant amount of O was noticed in the alloy. The amount of Ca and Al preset in our alloy has been seen significant when analysed by Dlab where as it was very low and around expected Factsage values when analysed by EPMA. Si purity in neutral slag experiments were higher than anticipated Factsage value which was the same case as previous three trials of 0.3*Al and neutral slag. Comparison between the results from previous three trials, reconfirmation experiment and simulated Factsage values in terms of Si, Al and Ca wt% has been illustrated in Figure 19

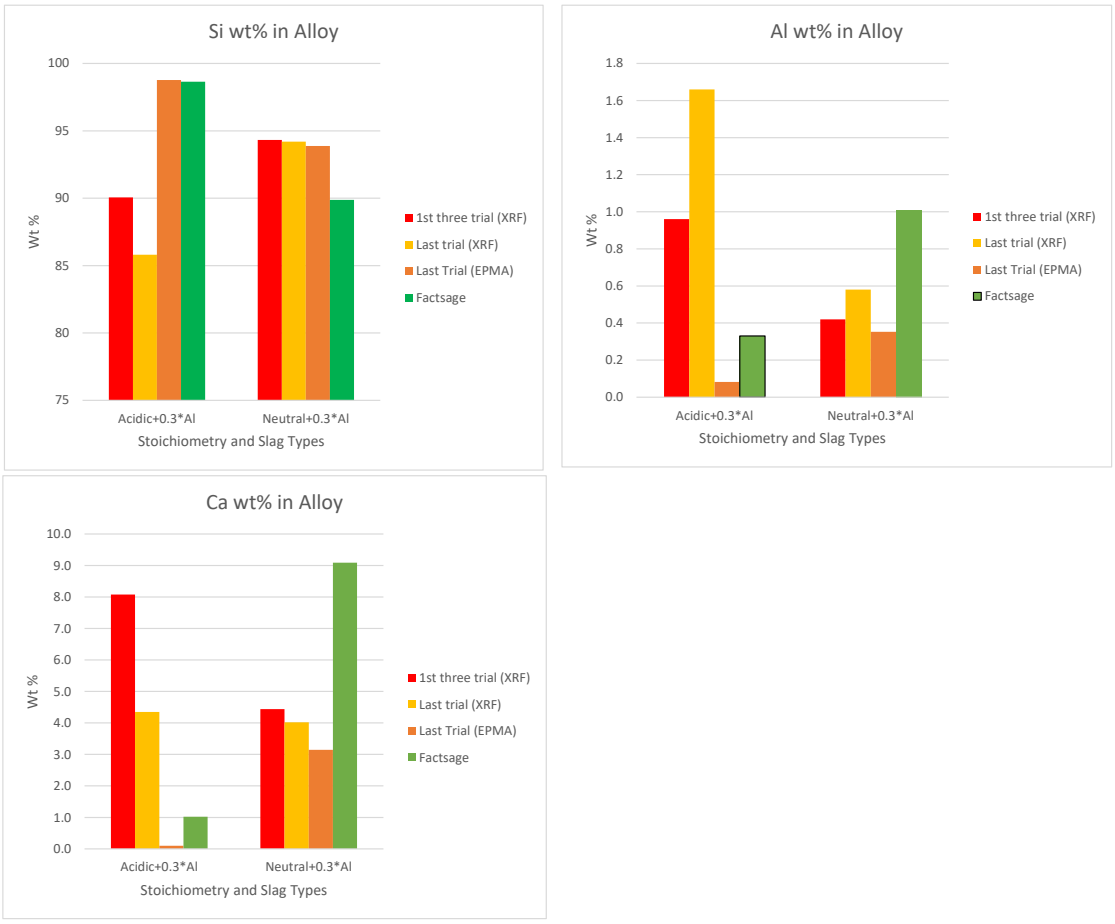

Figure 19: *Comparison between the results from previous three trials, reconfirmation experiment and simulated Factsage values in terms of Si, Al and Ca wt%. Red : average value from first three trials, yellow : reconfirmation experiment results analysed with XRF, orange : reconfirmation experiment results analysed with EPMA and green represents weight composition obtained from Factsage simulation*

Slag analysis was done using XRF to study about it's SiO_2, Al_2O_3 and CaO content. Slag present inside crucible after various trials were different in physical structure. Some trials had slag in the form of mixture of powder and small hard pieces. In such cases, about 10g of powdered slag and 10g of small hard slag pieces were milled together and taken for XRF analysis. In

the case of trials where hard bulky slag pieces were obtained, slag samples were made by milling those hard slag pieces. Table 12 here represents the composition of SiO_2, Al_2O_3, CaO in slag from three different stoichiometries in acidic and neutral slag experiments.

Table 12: *Composition of SiO_2, Al_2O_3 and CaO in metal obtained from three different stoichiometries of Al with acidic and neutral slag. Values given represents the average of three trials in each case*

Slag Type	Stoichiometry	SiO_2 wt%	Al_2O_3 wt%	CaO wt%
Acidic Slag	0.3*Al	35.60	16.80	47.33
(CaO:SiO2=0.56)	0.4*Al	29.10	27.73	42.77
	0.5*Al	24.73	33.57	41.40
Neutral Slag	0.3*Al	38.23	13.50	48.00
(CaO:SiO2=1.01)	0.4*Al	37.33	15.03	47.20
	0.5*Al	29.77	24.63	45.40

Slag analysis from XRF shows both experiments using acidic and neutral slag results in slag formation rich in CaO with significant Al_2O_3 and SiO_2. Slag composition in both acidic and neutral slag experiments were quite comparable. SiO_2 and CaO content in slag was seen high on 0.3*Al stoichiometry and the value started decreasing with increasing stoichiometry. The content of Al_2O_3 meanwhile increased with increasing stoichiometry in both acidic and neutral slag trials.

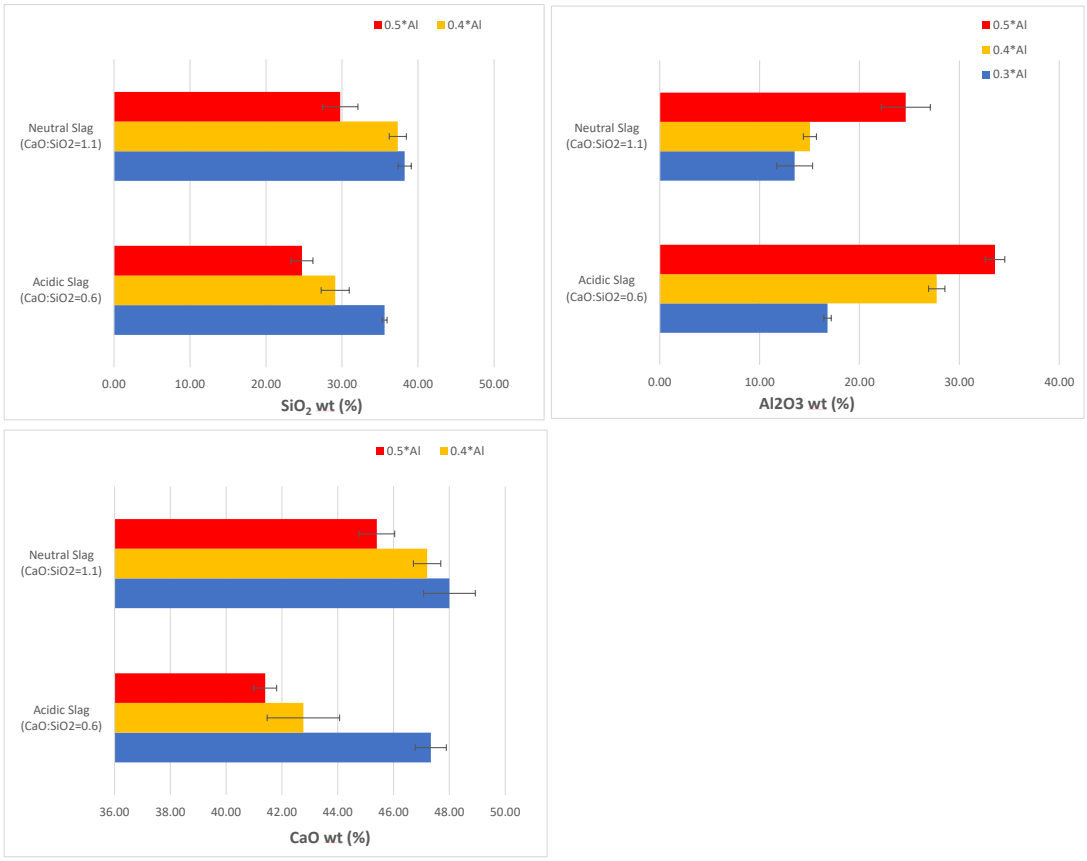

Figure 20: *Composition of SiO_2, Al_2O_3 and CaO wt% in slag obtained from three different stoichiometries of Al with acidic and neutral slag. Values given represents the average of three trials in each case*

Slag composition simulation using similar parameters was carried out in Factsage to compare the outcomes of various trials with various stoichiometries. The results of our XRF experiments also differed slightly from Factsage in the case of neutral slag experiments but more significantly from Factsage in the case of acidic slag experiments. Composition of SiO_2, Al_2O_3 and CaO content in experiments with different Al stoichiometries obtained from Factsage has been shown in Table 13.

Table 13: *Composition of SiO_2, Al_2O_3 and CaO wt% in slag expected from three different stoichiometries of Al with acidic and neutral slag. Values given represents the simulated values from Factsage*

Slag Type	Stoichiometry	SiO_2 wt%	Al_2O_3 wt%	CaO wt%
Acidic Slag	0.3*Al	42.65	20.87	36.49
(CaO:SiO2=0.56)	0.4*Al	36.40	27.53	36.07
	0.5*Al	30.46	34.01	35.54
Neutral Slag	0.3*Al	34.43	14.55	51.02
(CaO:SiO2=1.01)	0.4*Al	30.58	19.24	50.18
	0.5*Al	26.90	23.86	49.24

SiO_2 content in slags from acidic slag experiment were supposed to be higher than neutral slag experiment according to the result of Factsage. But the case was reverse according to our experimental trails where SiO_2 content was high in neutral slag experiments. CaO content in slag from our acidic slag experiment and neutral slag experiments were quite similar while Factsage indicates more CaO observation in neutral slag experiment and less in acidic slag experiment.

Table 14: *Composition of SiO_2, Al_2O_3 and CaO in product obtained from reconfirmation experiment done for 0.3*Al stoichiometry with acidic and neutral slag*

Slag Type	Stoichiometry	Analysis	SiO_2 wt%	Al_2O_3 wt%	CaO wt%
Acidic Slag	0.3*Al	XRF	45	19.9	34.6
(CaO:SiO2=0.56)		EPMA	47.1	16.02	36.41
Neutral Slag	0.3*Al	XRF	38.9	12.8	47.9
(CaO:SiO2=1.01)		EPMA	30.24	24.88	44.05

The results from reconfirmation experiment was analysed with EPMA and

XRF; both results tend to appear closer to results of Factsage. Rigid structured product with highly densed slag was observed in reconfirmation experiment done for both types of slags with 0.3*Al as reductant. This bulky slag was milled and used for XRF while small piece of hard slag pieces was mounted over epoxy of EPMA. SiO_2 and Al_2O_3 content has been observed higher in acidic slag experiment and CaO content has been noticed high in slags from neutral slag experiment, which is in accordance with Factsage results illustrated in Table 13.

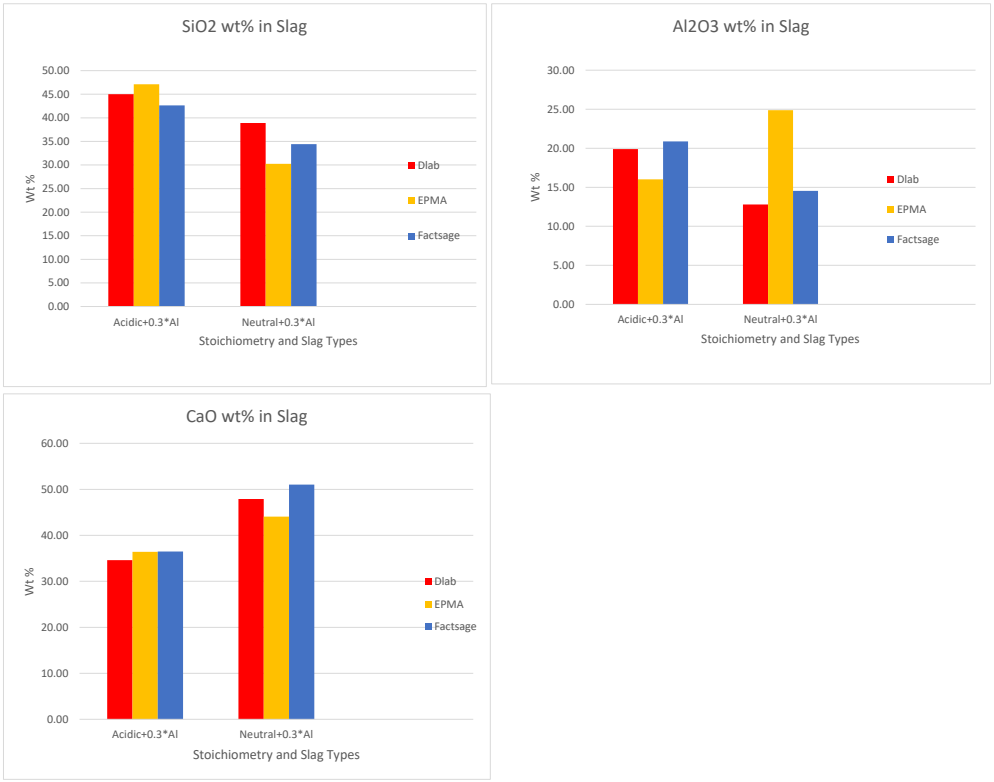

Figure 21: *Composition of SiO_2, Al_2O_3 and CaO wt% in slag obtained from reconfirmation experiment.*

4.2.5 BSE images and WDS analysis

In this section, backscatter images from both slag and metal samples from all input variations will be displayed side by side with the findings from the

WDS analysis (to identify the phases). Acidic master slag will be followed by neutral rec slag in the presentation of the findings. Each slag's samples will be presented with increasing amounts of reductant. Almost all of the metal samples show four distinct phases: a pure Si phase, a Si_2Al_2Ca phase, a Si_2Ca phase, and a Si-Al-Ca phase containing the main impurities, such as Fe, Mn, and Mg. The phases, types of phases, and compositions of the phases in the slags are much more diverse. The backscatter images of metals obtained from three different stoichiometry in acidic slag experiment are shown in the Figure 22.

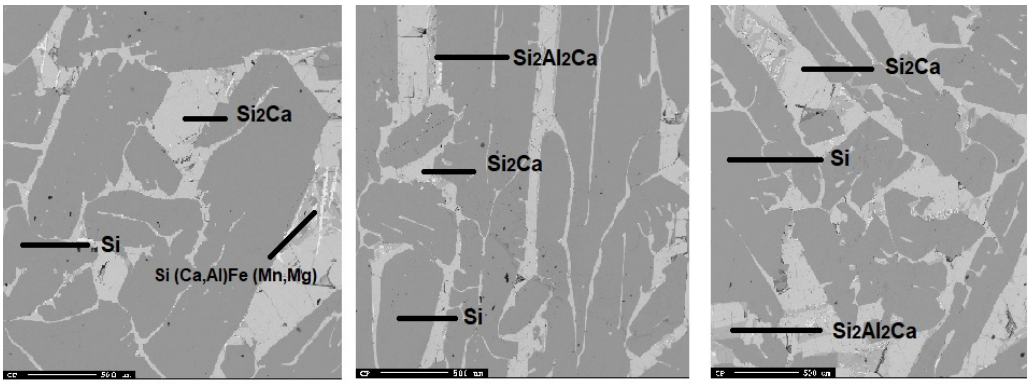

Figure 22: *BSE-images; acidic slag and 0.3*stoichiometric reductant, trial 1 (Left) acidic slag and 0.4*stoichiometric reductant, trial 1 (Middle) and acidic slag and 0.5*stoichiometric reductant, trial 1 (Right)*

Backscattered images of metal from EPMA reveals three distinct phases as discussed earlier in this section. Si phase is the most abundant phase in all three stoichiometries.Si_2Ca phase are represented by the light grey phases and are seen significantly in all three stoichiometric experiments. Si_2Al_2Ca phase is rarely seen in backscattered image of metal from 0.3*Al stoichiometry while they are seen in small traces in 0.4*Al and 0.5*Al stoichiometry.

Experiments with 0.3*Al stoichiometry was tested again to reconfirm the results during which highly pure Silicon metal was obtained in product coming from acidic slag and 0.3*Al as reductant. The phases present in metal from corresponding trial has been illustrated in Figure 23, showing around 98%

Si phase and small traces of Si_2Ca phase. Back-scattered image present in right side of Figure 19 shows phases of metal from neutral slag and 0.3*Al stoichiometry; reveals significant amount of Si_2Ca phase as well as other impurities.

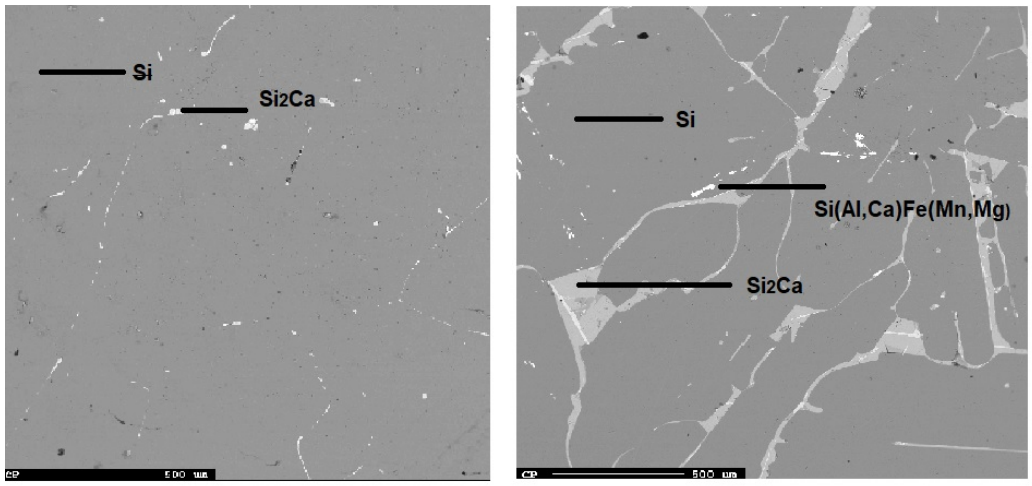

Figure 23: *BSE-images; acidic slag and 0.3*stoichiometric reductant, reconfirmation trial (left); neutral slag and 0.3*stoichiometric reductant, reconfirmation trial (right)*

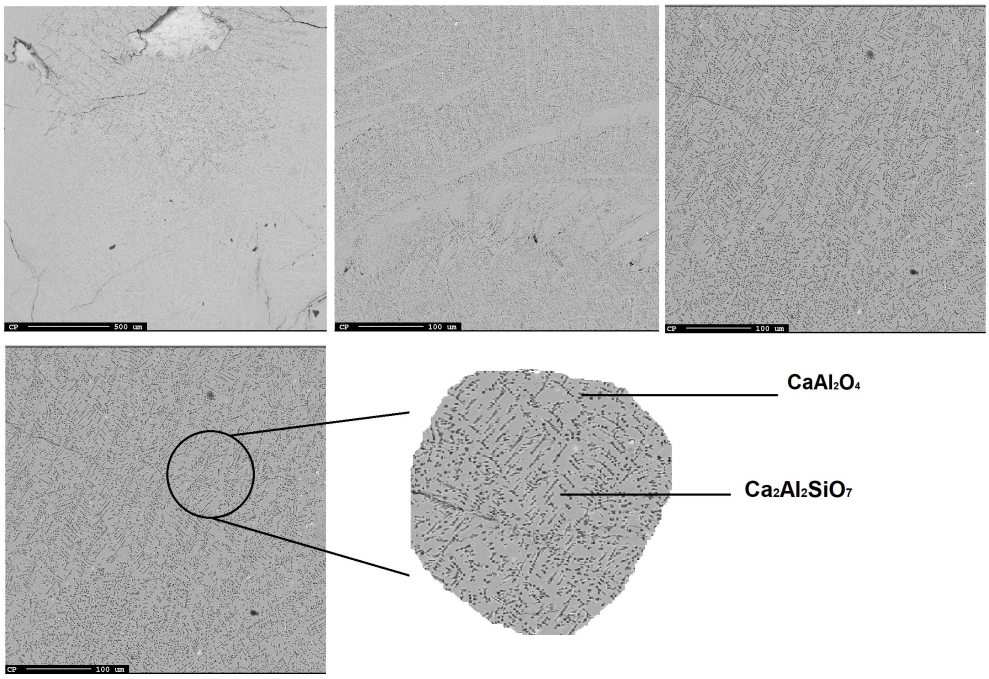

Figure 24: *BSE-images of slag from acidic slag experiments; 0.3*Al, trial 1 (left); 0.4*Al, trial 1 (middle); 0.5*Al, trial 1 (right)*

The phases seen on slag obtained from acidic slag experiments were similar;two phases were dominant in all three stoichiometry; especially $CaAl_2O_4$ and $Ca_2Al_2SiO_7$. Images were taken at 40x magnification due to which clear structure of phases are not seen in the Figure available. $CaAl_2O_4$ phases are seen in little traces in slag from 0.3*Al stoichiometry while it seems to grow with slag 0.4*Al and 0.5*Al stoichiometry.

Slag obtained from neutral slag experiments has similar observation as in acidic slag experiments. Two phases can be seen in all three stoichiometries with some images showing small traces of impurities in it.

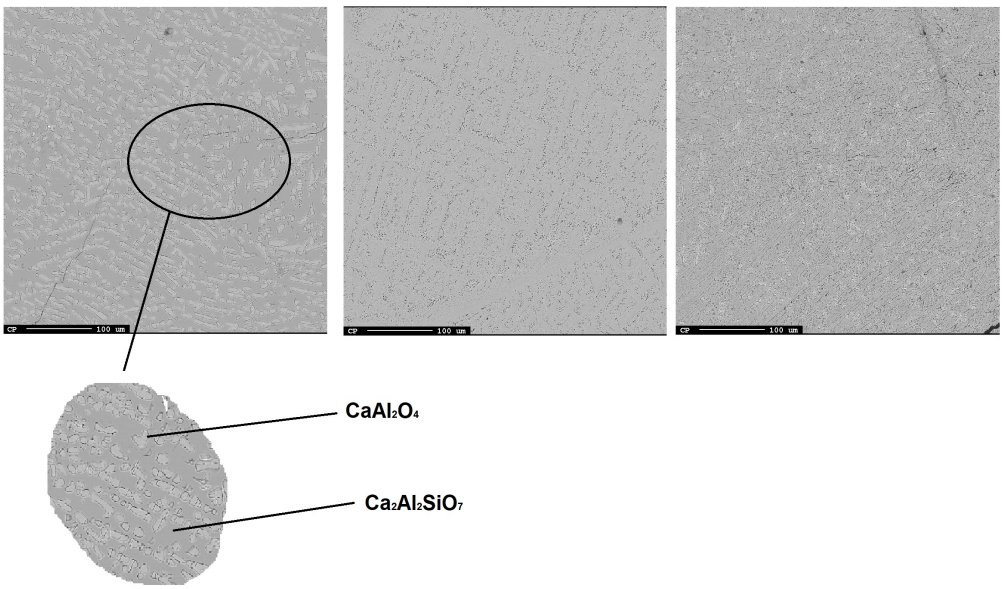

Figure 25: *BSE-images of slag; neutral slag and 0.3*Al, trial 1 (left); neutral slag and 0.4*Al, trial 1 (middle); neutral slag and 0.5*Al, trial 1 (right)*

Powder form slag obtained from neutral slag experiment with 0.4*Al was analysed with EPMA for back scattered images. The images obtained revealed two different abundant phases with some minor phases containing SiC impurities as illustrated in Figure 26.

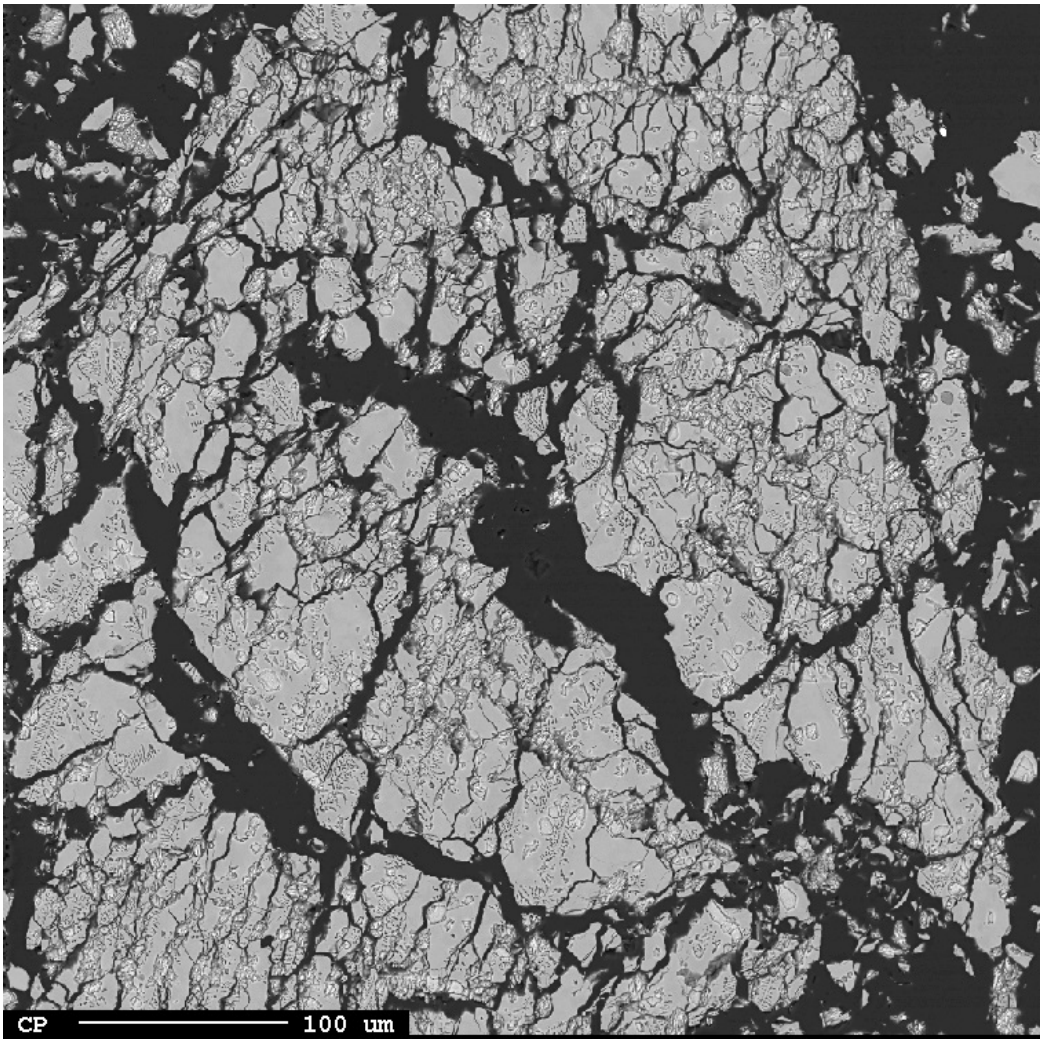

Figure 26: *BSE-images of powder form slag obtained from experiment with rec slag and o.4*Al stoichiometry, trial 1.*

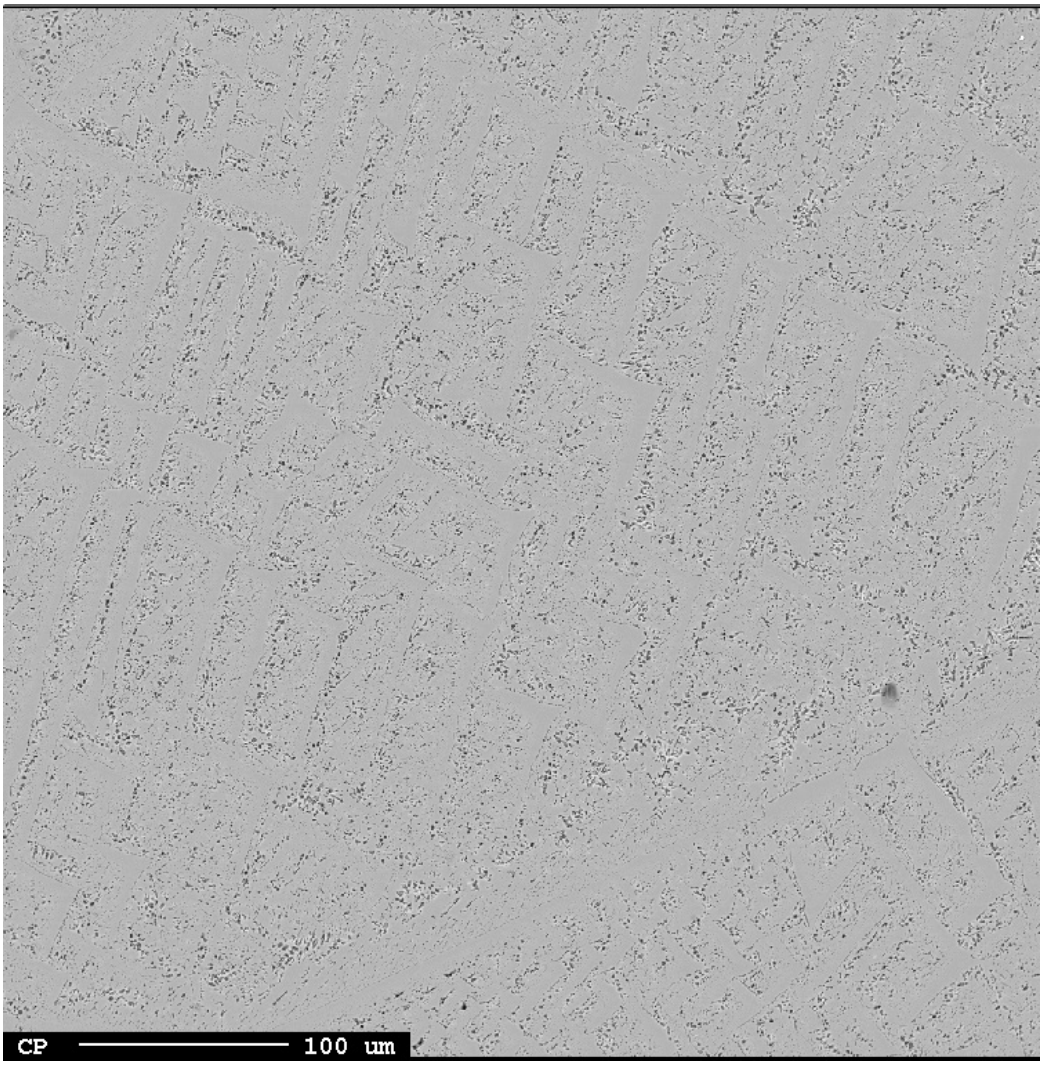

Figure 27: *BSE-images of slag obtained from reconfirmation experiment done with rec slag and o.3*Al stoichiometry*

BSE image of slag shown in Figure 27 reveals phases present in slag from reconfirmation experiment where 0.4*Al stoichiometry was tested with neutral slag. The phase structure looks similar to phases present in slag formed in earlier trials of neutral slag experiment with 0.3*Al stoichiometry as shown in Figure 25.

4.2.6 Mass Balance

Mass Balance was done for estimating how much many parameters (Si, Al, Ca) had been kept in the system and where they ended up after the experiment. This was done by analysing the chemical composition of raw materials and their input amount with total output amount with its composition. Chemical composition of raw materials were obtained from XRF analysis illustrated in Table 7 and Table 8. Amount of input slag and understoichiometric reductant necessary were calculated and has been mentioned in Table 1 and Table 2. The amount of product obtained i.e slag and metal was taken for weight measurement and this was coupled with composition of slags and metal obtained from XRF for comparing the mass balances.

Figure 28: *Illustrate the distribution between extracted metal yield and the presumed slag for all experiments.*

Figure 28 shows the percentage composition of metal and slag in output product coming from all under-stoichiometric experiments. Metal weight% is little high in acidic slag experiments which is obvious because of high amount of reductant addition. Some trials have very small metal yield due to losses through different ways and has resulted in inconsistent observation within same experimental trials.

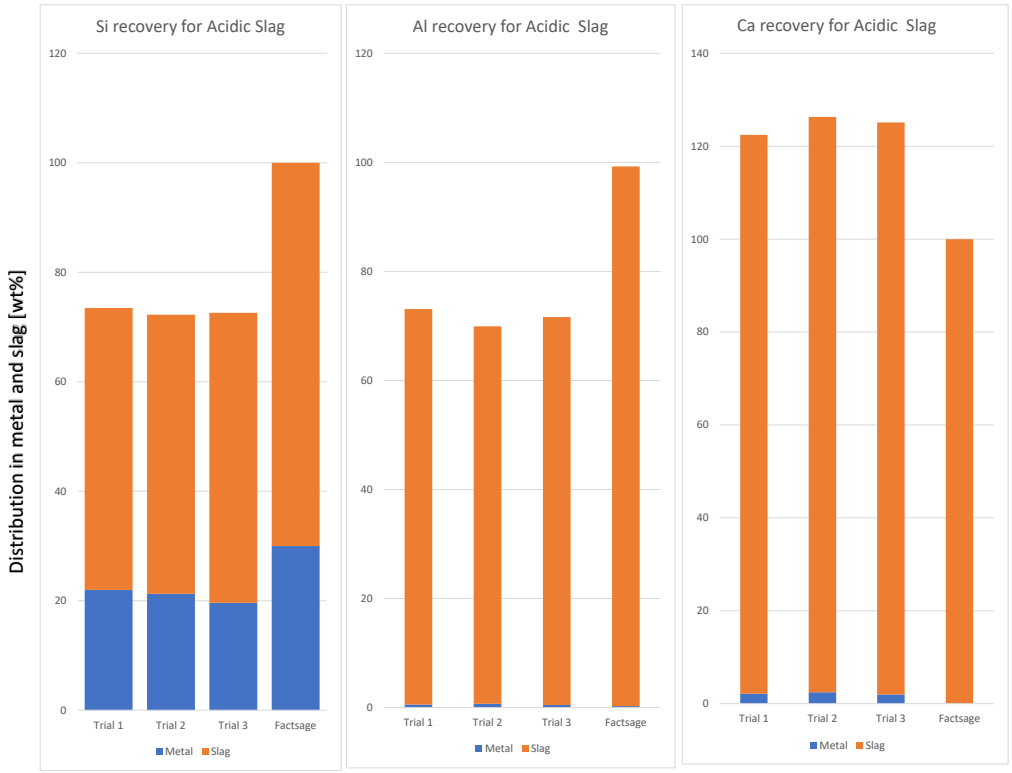

Figure 29: *Illustrate the distribution of Si, Al and Ca in extracted metal and slag from different trials and Factsage simulation for experiment using acidic slag and 0.3*Al stoichiometry.*

The weight percentage of Si that has entered into alloy produced during experiment is slightly less than predicted value from Factsage but it is not significant. Total Si recovery to alloy and slag has been found less than 100 in all three trials which is due to various losses accompanied during the experiment. Ca recovery in metal has been seen significant as compared to

desired transport. Total Ca recovery in all three trials has been noticed to be higher than 100%.

The mass balances graph for 0.4*Al and 0.5*Al stoichiometry with acidic slag as represented in Figure 30 and Figure 31 are similar to 0.3*Al mass balance observation. Si has not been totally recovered into the system while Ca recovery has been observed more than 100%.

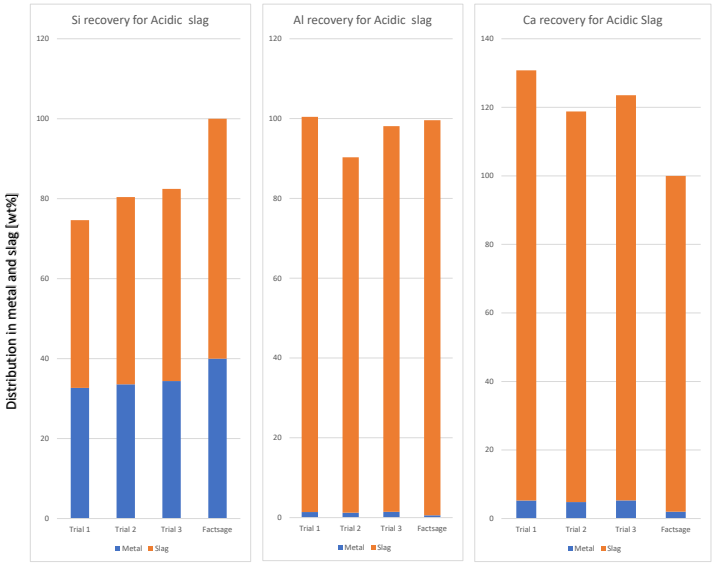

Figure 30: *Illustrate the distribution of Si, Al and Ca in extracted metal and slag from different trials and Factsage simulation for experiment using acidic slag and 0.4*Al stoichiometry.*

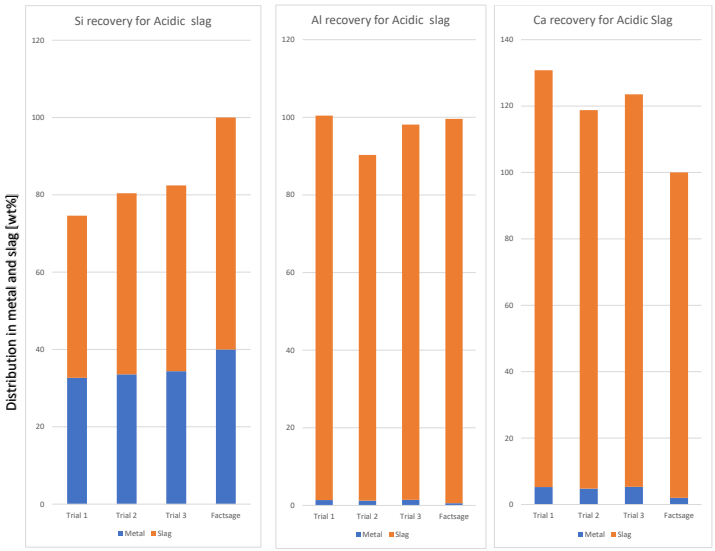

Figure 31: *Illustrate the distribution of Si, Al and Ca in extracted metal and slag from different trials and Factsage simulation for experiment using acidic slag and 0.5*Al stoichiometry.*

recovery of Si, Al and Ca into the output system in experiments using neutral slag and three different stoichiometries has been shown in the Figure 28, Figure 29 and Figure 30. In the case of 0.3*Al stoichiometry, Si recovery to output system is less than 100% because of the losses which was also determinant in acidic slag experiments. Si has been found to be recovered in alloy with a little deviation (slightly less)from Factsage values. Al recovery to metal are however less than the values shown by mass balance obtained from Factsage values. Ca recovery to metal is zero which is in accordance with Factsage with the exception of trial 3. Similar trend has been observed in experiments with 0.4*Al and 0.5*Al stoichiometries. Si recovery higher in slag as compared to recovery in metal, Al recovery in metal less than indicated Factsage mass balance calculation and comparable outcome in Ca recovery are the major results highlights from mass balance study of this aluminothermic reduction experiment.

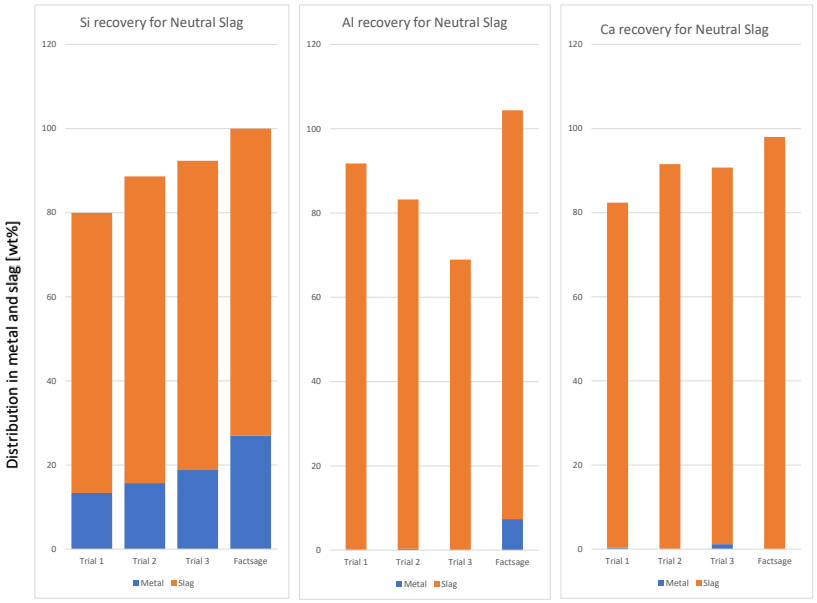

Figure 32: *Illustrate the distribution of Si, Al and Ca in extracted metal and slag from different trials and Factsage simulation for experiment using neutral slag and 0.3*Al stoichiometry.*

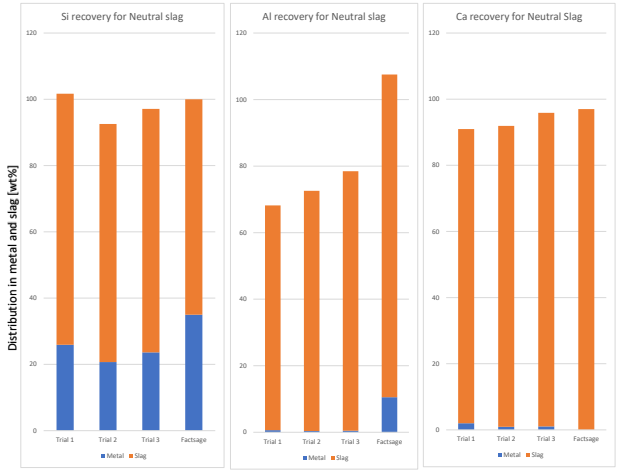

Figure 33: *Illustrate the distribution of Si, Al and Ca in extracted metal and slag from different trials and Factsage simulation for experiment using neutral slag and 0.4*Al stoichiometry.*

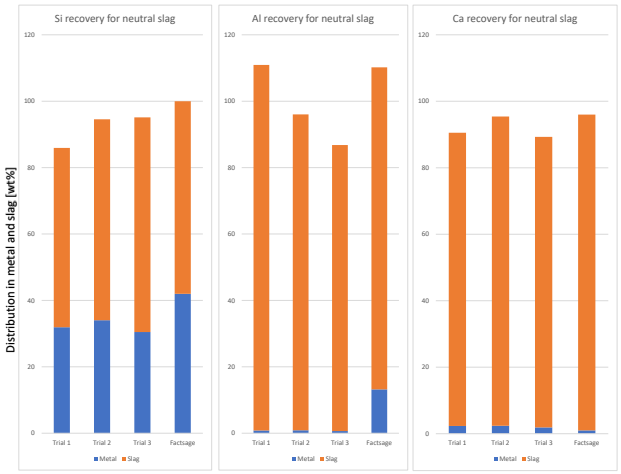

Figure 34: *Illustrate the distribution of Si, Al and Ca in extracted metal and slag from different trials and Factsage simulation for experiment using neutral slag and 0.5*Al stoichiometry.*

4.3 Aluminothermic Reduction Using Pre-fused slag with CaF_2

4.3.1 Product Observation

The product coming from experiment using CaF_2 in pre-fused slag with stoichiometric aluminium as reductant has quite distinct observation as compared to other experiments performed in this study. Rigid structured product containing hemispherical shaped silicon alloy was seen at top and heavily densed slag at the bottom. Slag formed in this experiment was slightly bluish grey and seemed to be more homogeneous as compared to other stoichiometric experiments with pre-fused slag conducted by author.

Figure 35: *Product structure in experiment using CaF_2 in pre-fused slag and stoichiometric Aluminium as Reductant*

4.3.2 Metal yield

The product obtained from experiment was taken into sandblasting for removing attached graphite paper and weighed afterwards. Loss in mass as compared to total input feed was observed. Losses can evolved from the fumes produced during the holding time. Metal was separated from slag by hammering and weighed. Input and output parameters are shown in Table 15.

Table 15: *Input raw material and output slag and metal stoichiometry*

Input				Output			Loss
Al	pre-fused slag	CaF_2	Total	Si	Slag	Total	in weight
25.98	90	10	125.98	21.93	101.79	123.72	2.26

4.3.3 Chemical composition

Slag and metal obtained from this set of experiment was taken for XRF analysis. EPMA was also done for BSE images and EDS analysis. Table 16

below represents the slag and metal composition in terms of Si, Al and Ca obtained from XRF.

Table 16: *Composition of metal and slag in terms of Si, Ca, Al and SiO_2, CaO, Al_2O_3 obtained from XRF and EPMA*

	Metal				Slag			
	Si	Al	Ca	F	SiO_2	Al_2O_3	CaO	F
XRF	74.5	7.98	16.7	<0.5	11	42.8	38.6	6.63
EPMA	76.91	6.04	15.20		11.33	41.31	46.63	

Results from XRF and EPMA are quite similar; indicates that stoichiometric aluminium addition gives high yield but metal with less Si content. But Si content was slightly higher than other stoichiometric experiments conducted by author in previous study where CaF_2 was not used. At the same time, Al and ca content in metal were least than usual experiments. F was seen in slag in significant amount where as only few traces of F was detected in metal produced.

4.3.4 BSE images

Backscattered images obtained from EPMA for both metal and slag samples for this experiment has been shown in Figure 36.

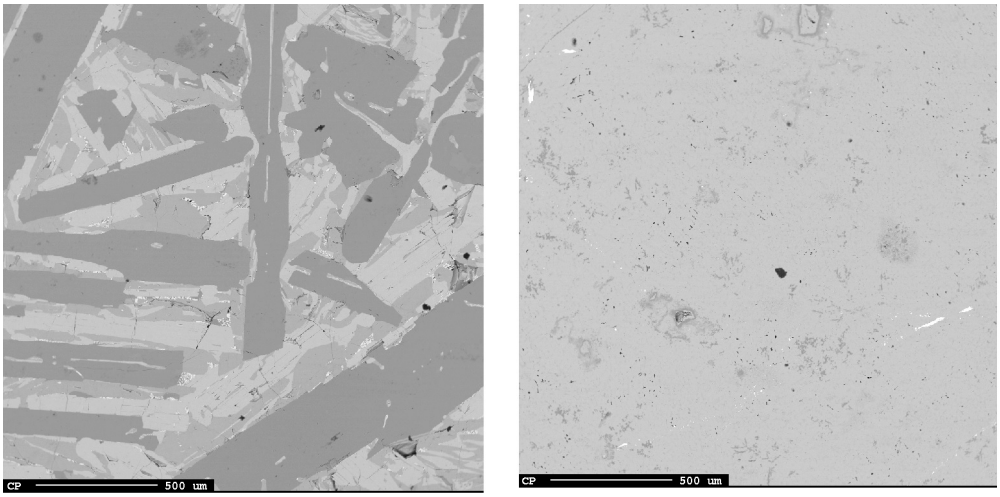

Figure 36: *BSE image of metal obtained from experiment with CaF_2 (image in the left); BSE image of slag from same experiment(image in the right)*

Three dominant phases has been observed in metal similar to previous under-stoichiometric studies but portion of dark Si is significantly less than previous under-stoichiometric study. Si_2Ca and Si_2Al_2Ca phase has been seen abundantly with very few small phases of other impurities like Fe, Mn, Mg.

4.4 Results from Al-Si alloy analysis

Al-Si alloy prepared from muffle furnace and melt spinner were analysed with SEM. Secondary electron was used for imaging our alloy samples. For comparision, SEM observation of pure Al which was used to make alloy in this study was also done. Images were taken in different magnification scales ranging from 50X to 1000X. Observation were made by looking at its morphology, phases determination and grain structure.

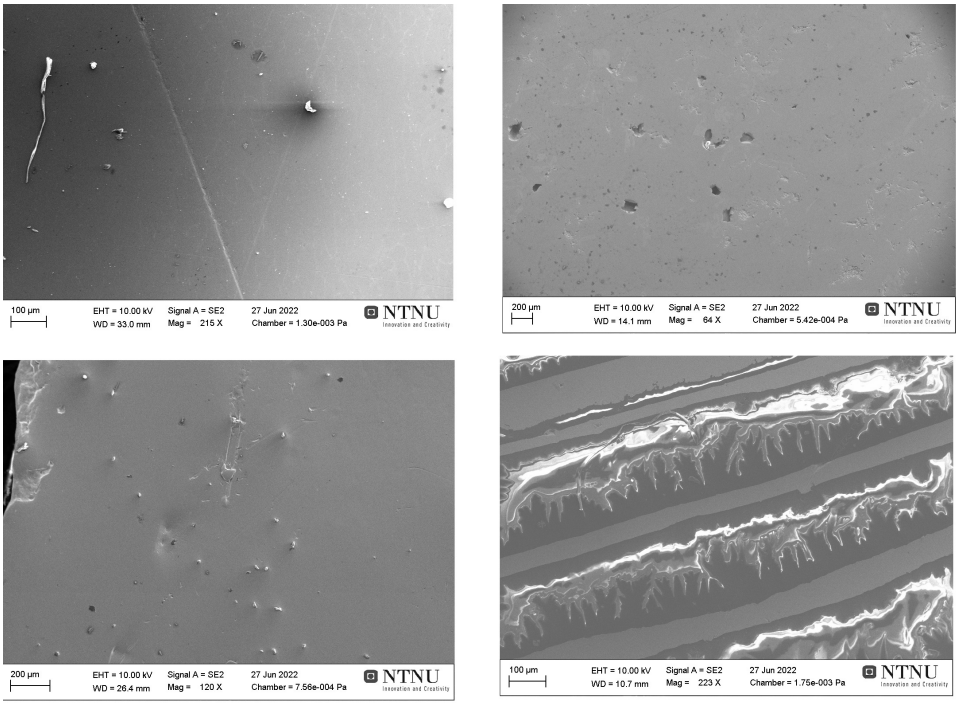

Figure 37: *SE image in magnification (60X-250X) SE image of pure aluminium (top left); SE image of Al-Si alloy from muffle furnace (top right); SE image of Al-Si ribbon from melt spinner in horizontal view (bottom left); SE image of Al-Si ribbon from melt spinner in vertical view (bottom right)*

In low magnification observation of pure aluminium, single phase was observed with very few points and dislocations. In alloy obtained from muffle furnace, small traces of different phase was seen which must have been as a result of Si present in alloy. SE image of Al-Si alloy obtained after rapid solidification under melt spinner has small but several Si phases dispersed along the primary Al phase. SE image present in bottom left of Figure 37 represents alloy from melt spinner kept in vertical position. The images belongs to the part of edges of Al-Si ribbon yielded and several ribbons were stacked together vertically inside the sample to know its micro-structure on the edges.

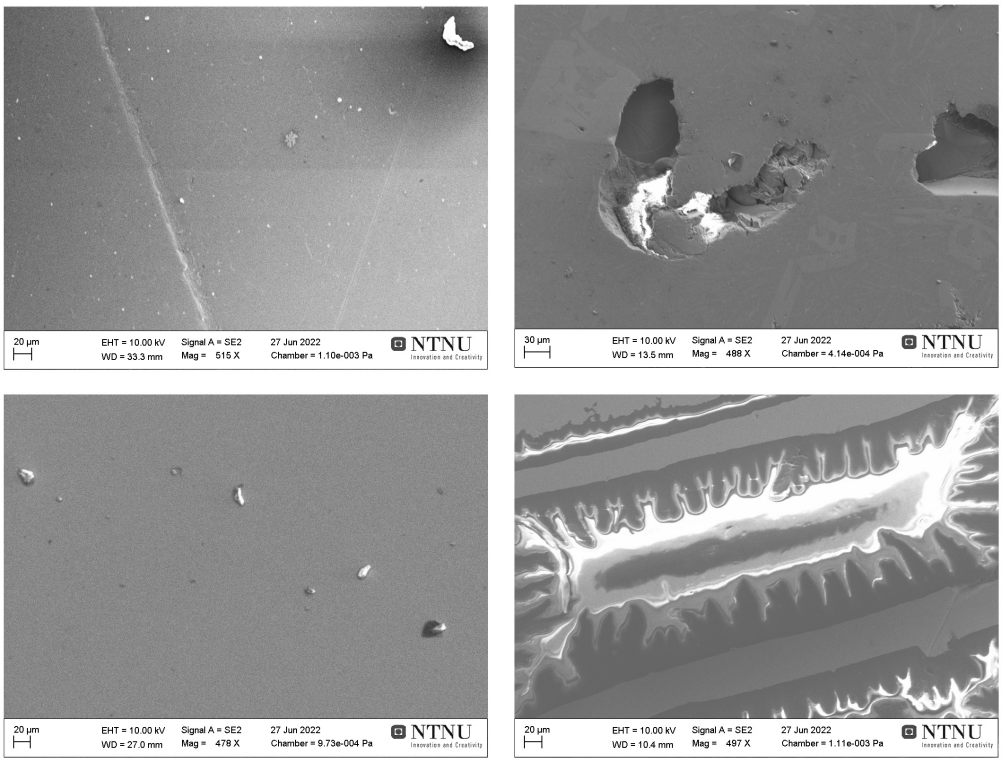

Figure 38: *SE image in magnification (450X-500X); SE image of Al-Si alloy from muffle furnace (top right); SE image of Al-Si ribbon from melt spinner in horizontal view (bottom left); SE image of Al-Si ribbon from melt spinner in vertical view (bottom right)*

Under magnification of 500X, difference were observed in the phase composition between samples with different content. Image in the bottom right of Figure 34 represents the Al-Si alloy kept vertically in epoxy sample. This sample gave clear overview of phases located inside Al-Si alloy in contrast to Al-Si sample which was kept horizontally in epoxy. Three distinct phases has been observed; one phase represented by white, another two by grey and dark grey, as illustrated in bottom right image of Figure 38. Similar phase observation is observed on 1000X magnification of same sample illustrated in right image of Figure 39.

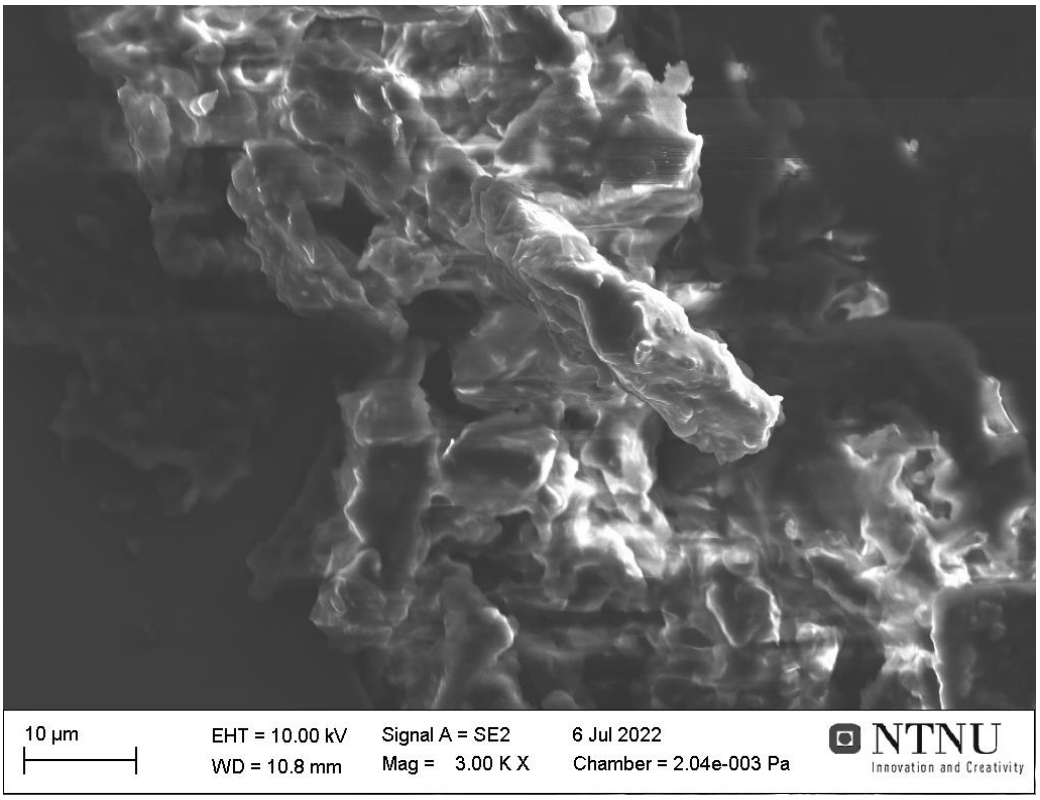

Figure 39: *SE image of Al-Si alloy from meltspinner under 3000X magnification*

4.4.1 EPMA

WDS analysis was done to know about the details of content present in each phase of Al-Si alloy produced. 10 WDS point analysis was done with 20µm. Since, each phase was very small, it was difficult to analyze component in each phase. However, ten random points has been selected and composition of Al and Si with other impurities has been detected as illustrated in **??**.

Table 17: *Weight percentage of Al and Si in ten different points present in Al80-20Si Sample from melt spinner*

No.	1	2	3	4	5	6	7	8	9	10
Al	84.24	78.81	81.01	78.53	80.34	79.41	78.54	81.38	79.83	80.22
Si	15.30	20.79	18.62	21.18	19.33	20.39	21.28	18.30	20.03	19.44
Mg	0.20	0.17	0.15	0.14	0.14	0.11	0.14	0.13	0.07	0.14
Fe	0.26	0.23	0.23	0.15	0.19	0.09	0.04	0.18	0.07	0.21

EPMA analysis was used for mapping analysis, to get a better overview of the element present in the alloy prepared from melt spinner. This has been represented in Figure 40.

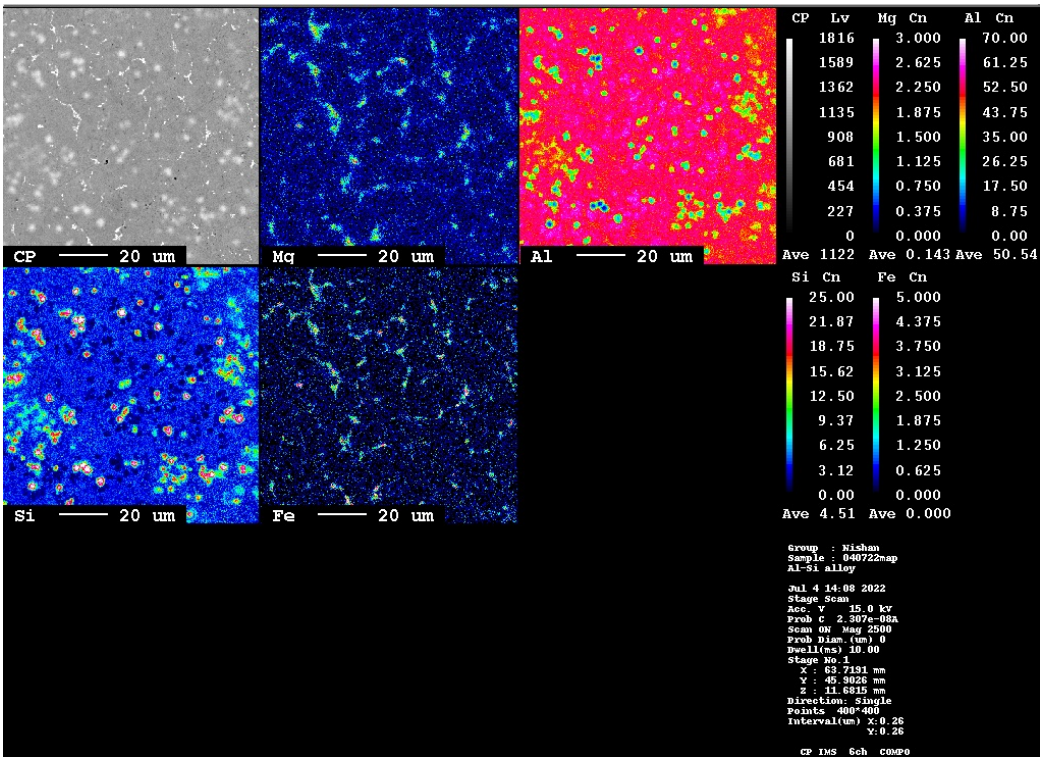

Figure 40: *Mapping image of Al-Si sample from Melt spinner*

The sample obtained from Al-Si alloy coming from melt spinner was not

much homogeneous. Mapping image of Si shown in Figure 36 reveals the distribution of Si in Al to be somehow homogeneous, but from SEM observation under high magnification, it was not as uniform as expected. Si phases can be observed in pink colour getting dispersed around Al phase represented by blue colour in mapping image of Si shown in bottom left of Figure 40. The point where mapping was done Contamination of Mg and Fe was observed on several locations. Content of Fe in the alloy was higher than Mg, but both were present in significant amount.

5 Discussion

5.1 Under stoichiometric studies

5.1.1 Acidic and neutral slag and experiment stoichiometries

The experimental work were previously aimed for conducting trials with acidic slag having $CaO:SiO_2$=0.6 and neutral slag having $CaO:SiO_2$=1.1 and Factsage simulation was done assuming same ratio for CaO to SiO_2. However, from XRF analysis, little variation was found in the composition of rec slag. With the presence of Al_2O_3 and Fe_2O_3 as impurities in significant amount, $CaO:SiO_2$ in the rec slag had decreased to 1.01 and the same had decreased to 0.56 which is not considerable difference but it certainly made some fluctuations with expected experimental results. For the preparation of acidic slag, SiO_2 was inserted into a plastic bag containing rec slag and shake well for uniform mixing. This is not good technique for mixing; melting of two oxides together could have been done for uniform mixing but because of time constraints, they were mixed without melting and used in the experiments. The aluminium used as reductant in this study was 99.8% pure and had no effect in fluctuation in our experimental results.

5.1.2 Composition of metal and slag

The metal and slag yield from every trial done from under-stoichiometric studies had been compared with simulated values obtained from Factsage. Obtained results were less than expected values in most of the trials since losses were obtained in various form during and after the experiment. During the experimental process, while input materials were heated up to 1650 °C and holded for an hour, high amount of fumes was evolved and found to be escaped through central opening of covering lid. This gas must be SiO which had taken significant amount of Si out from the system resulting in major loss. Similarly, during some trials, crucible breakage was observed with powder form slag getting dispersed out of the small crucible in initial three trials of acidic and neutral slag experiments. Although careful gathering

of entire powder slag was done, there might have been some losses of slag because of this reason.

5.1.2.1 Effect of reductant

Factsage simulation for both acidic and neutral slag shows that with increasing amount of reductant, Si content in metal decreases with increasing Al and Ca content. In the case of slag, with increasing reductant, SiO_2 and CaO content in slag decreases with increasing amount of reductant while the case is reverse for Al_2O_3 content. This trend has been supported with our experimental result although the expected Si was fluctuated with simulated values.

Figure 41 shows that the Si concentration in the metal produced from acidic slag experiments is lower than the values predicted. It is true that the expected trend of increasing Si with decreasing reduction amount is present, meaning that the purity of the metal Si in the final product will increase as the reductant addition decreases. This is backed by research conducted by L. Solbakk,[25] where purity in Si metal was seen to be increasing with decreasing reductant amount. As mentioned in section 4.2.2, crucible breakage and the presence of powdered slag were frequently seen during the experiment with acidic slag. This gives the impression that the transport of Si from SiO_2 to silicon metal in the finished product is lacking in the previous three trials with acidic slag experiment.

In the case of slag, it can be observed that it is a co-relation between the simulated and the experimental values with regards to the increasing SiO_2 amount with a decreasing reduction amount. The experimental values are however less than the expected SiO_2 concentration, which can be caused by loss of silicon in the form of fumes as well as insufficient reaction between slag and reductant as discussed earlier in this section. It can be seen that there is a significant relation between the experimental and simulated values for slag in terms of an increase in SiO_2 concentration with decrease in reduction concentration. However, the experimental values fall short of the predicted

SiO_2 concentration, which can be attributed to silicon loss in the form of fumes as well as a lack of sufficient reaction between the reductant and slag, as discussed earlier in this section.

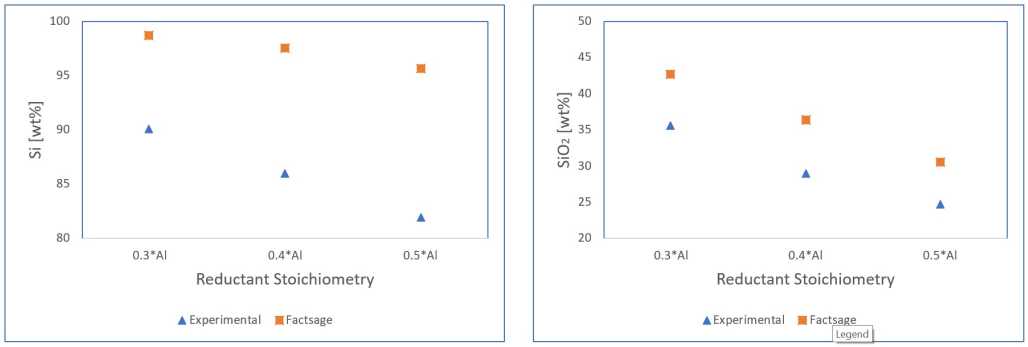

Figure 41: *Simulated and experimental concentration of Si and SiO_2 in metal and slag respectively in acidic slag experiment*

Al concentration in acidic slag experiments has followed the general trend of increasing Al content in metal with increasing reduction stoichiometry. The observed values, however, exceeded the Factsage-generated simulated values. Aside from the 0.3*Al stoichiometry having a lower value than expected where typically powdered form slag was observed, the experimental values in the slag were almost closer to the simulated values.

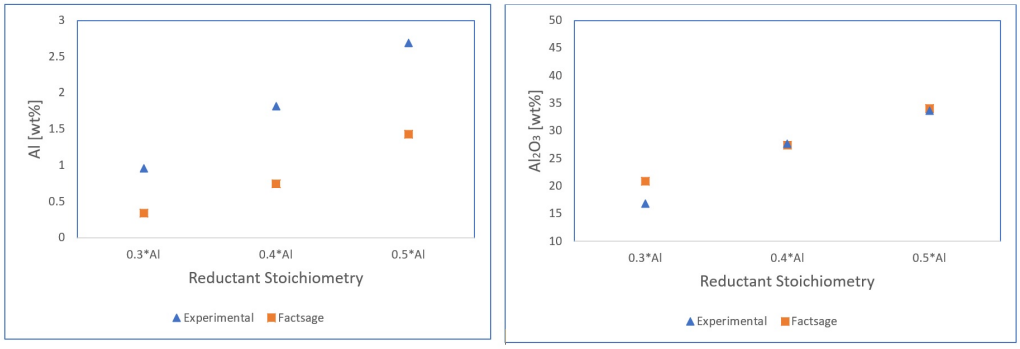

Figure 42: *Simulated and experimental concentration of Al and Al_2O_3 in metal and slag respectively in acidic slag experiment*

The concentration of Ca in metal has followed the same trend as that of Al; an increase in Ca concentration occurs with an increase in Al stoichiometry, and simulated results also support this. However, the Ca concentration values from the acidic slag experiments are higher than anticipated. The trend in slag, where CaO concentration appears to decrease with increasing stoichiometry, is the exact opposite. Higher deviation is seen with trials of 0.3*Al stoichiometry, where experimental CaO content was very higher than expected concentration.

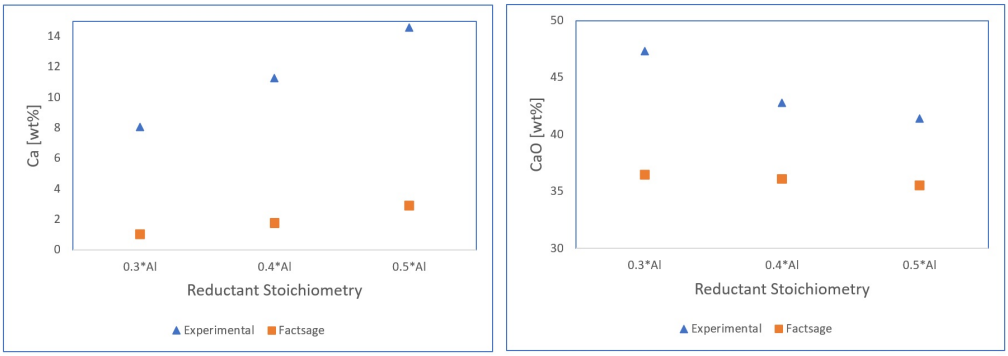

Figure 43: *Simulated and experimental concentration of Ca and CaO in metal and slag respectively in acidic slag experiment*

reconfirmation experiment as mentioned in section 3.2.3 had been done as higher fluctuation were seen in concentration of metal and slag when compared to simulated values, though the trend of concentration variation with change of reductant stoichiometry was in line with simulated one. Observation of hard densed shiny slag was made in reconfirmation experiment with 0.3*Al and acidic slag; totally different with observation from previous three trials. Metal and slag composition analysis from EPMA had closer results when compared with simulated one as tabulated in Figure 44; Si and Al concentration in metal are almost similar to Factsage values where as Ca concentration is less than expected which is a positive aspect. Deviation was still persistent with XRF results.

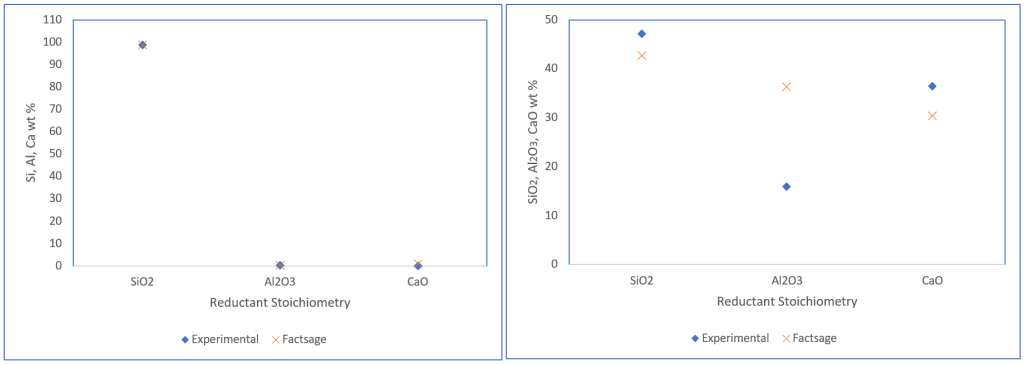

Figure 44: *Simulated and experimental concentration of (Si,Al,Ca) and (SiO2, CaO, Al2O3) in metal and slag respectively from reconfirmation experiment with 0.3*Al and acidic slag*

This implies that experiment done with 0.3*Al and acidic slag in reconfirmation trial had consistent result indicating complete equilibrium condition have been met. This can be justified with chemical composition of slag and metal and physical structure of product obtained from reconfirmation experiment. As mentioned in section 3.2.3, during the previous three trials of acidic slag experiment, aluminium was kept in the middle of acidic slag while inserting feed inside crucible while in reconfirmation experiment, reductant aluminium was kept at top after feeding entire slag inside the crucible. This might have some impact on observation of powdered form slag, crucible breakage and deviation in metal and slag composition from simulated composition. Acidic slag being highly viscous, might have expanded a lot at temperature of 1650°C, when reacted with Aluminium.

Figure 45 reveals the experimental and simulated Si and SiO_2 content present in metal from neutral slag experiments. The trend has followed the similar pattern as in acidic slag experiment, where increase in Si and SiO_2 content in metal and slag was seen with decreasing reductant amount, which is in line with Factsage values. The content of Si in metal and SiO_2 in slag is however higher than expected result, which was opposite in contrast to the result of acidic slag experiments.

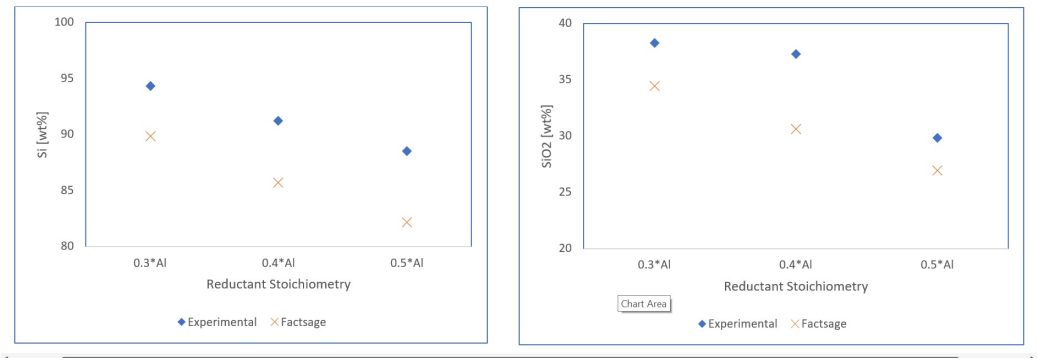

Figure 45: *Simulated and experimental concentration of Si and SiO_2 in metal and slag respectively in neutral slag experiment*

The results were similar to acidic slag experiments in terms of fluctuation in Al concentration with reductant variation. With the increase in reductant amount, Al content in metal and Al_2O_3 content in slag has been raised up. But experimental values are less than Factsage values which was not in the case with acidic slag experiments.

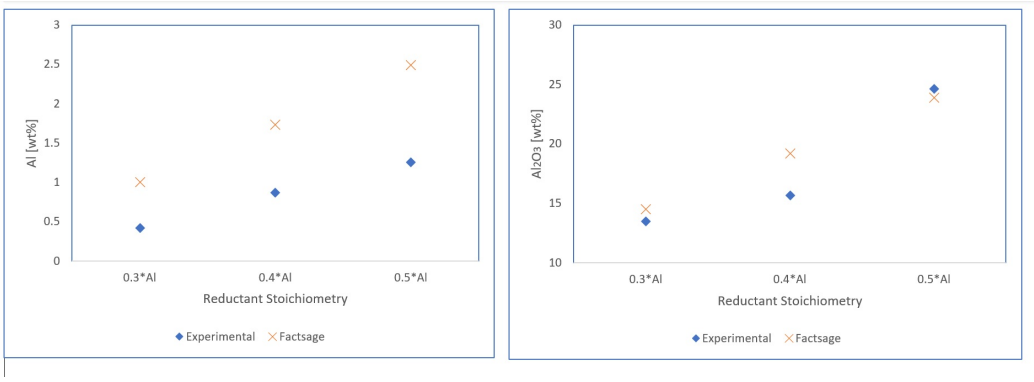

Figure 46: *Simulated and experimental concentration of Al and Al2O3 in metal and slag respectively in neutral slag experiment*

The Ca and CaO concentrations in metal and slag, respectively, from neutral slag experiments are shown in Figure 47. According to Factsage results, Ca in metal appears to increase while CaO in slag appears to decrease with

increasing reductant stoichiometry. However, the experiment's results are higher than anticipated.

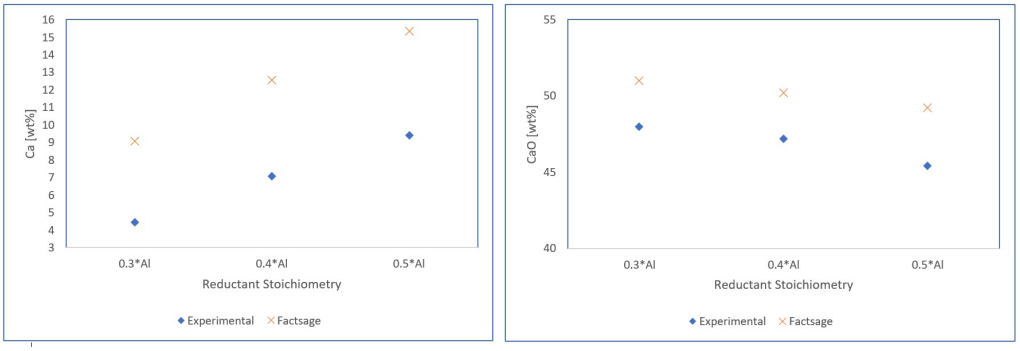

Figure 47: *Simulated and experimental concentration of Ca and CaO in metal and slag respectively in neutral slag experiment*

The concentration of Si, Al, Ca in metal and SiO_2, Al_2O_3, CaO in slag obtained from output of reconfirmation experiment (0.3*Al + neutral slag) has been shown in Figure 48. Similar to previous three trials, Si content in metal has been observed higher than expected Factsage value, but SiO_2 content in slag is less as compared to previous three trials. Similarly, Al and Ca content in metal are lower than Factsage which was same in previous three trials. Al_2O_3 content is lower and CaO content is higher than required when compared with simulated results which is similar to previous three trials. On contrary, there were no appreciable variations on the first three trails of the neutral slag experiment and reconfirmation experiment. The physical structure of product from neutral slag experiments were almost similar and chemical composition obtained from slag and metal has almost similar results when analysed with EPMA and XRF. Despite having the trend similar to Factsage result in regard to Si,Al,Ca variation with different reductant, expected values were seen somehow deviated from experimental values. Si content has been found much more than expectation whose further discussion has been made section later.

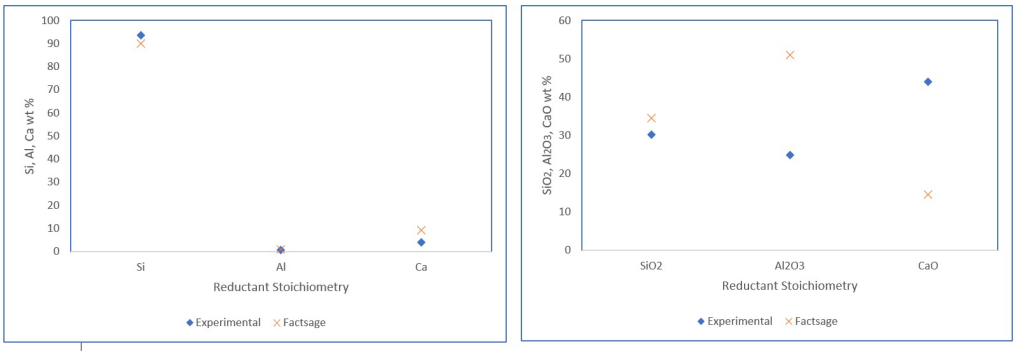

Figure 48: *Simulated and experimental concentration of (Si,Al,Ca) and (SiO_2, CaO, Al_2O_3) in metal and slag respectively from reconfirmation experiment with 0.3*Al and neutral slag*

5.1.2.2 Effect of slag composition

Factsage simulation revealed that with decreasing ratio of CaO:SiO_2 in the input feed will result in higher content of Si and SiO_2 in metal and slag respectively. This was further backed by the study conducted by L.Solbakk. This means higher purity of Si was supposed to be obtained from acidic slag experiments. But from previous three trials of acidic and neutral slag experiment. Si concentration in metal and SiO_2 content in slag has been seen higher in neutral slag experiments (CaO:SiO_2=1.01) rather than in acidic slag experiments (CaO:SiO_2=0.65). Inconsistent result in previous three trials with powder form slag observation and crucible breakage might be cause of less pure silicon from acidic slag experiments. Silicon purity was observed to be higher in reconfirmation experiment, where bulky structured product was obtained. It was around 98%, tentatively similar to Factsage simulation, implying that high Si and SiO_2 can be obtained in metal and slag respectively with less reductant amount in aluminothermic reduction experiments. However, the content of Si and SiO_2 in metal and slag were observed to be higher than expectation in reconfirmation experiment using neutral slag and 0.3*Al stoichiometry. This can be in fact due to alternation in values of rec slag composition while simulation. As discussed earlier in section 5.1.1, the experimental work ere aimed for neutral slag having CaO:SiO_2=1.1, but

analysis of rec showed that it had ratio of $CaO:SiO_2$=1.01. This might not be huge difference in ratio and might not have caused huge fluctuation in result's composition, but still it has made impact in demonstrating large gap between experimental and simulated values.

According to a Factsage simulation, a decreasing $CaO:SiO_2$ ratio in the input feed will lead to a lower Al content in metal and a higher Al_2O_3 content in slag. This implies that metal obtained from acidic slag experiments must have a low aluminum content while having a high Al_2O_3 content. This has been confirmed in the case of slag's Al_2O_3 content. The situation is different when it comes to the Al content of metal, though. Al content has been found to be higher in acidic slag experiments, which is the reason why the first three trials' observations were inconsistent. When analyzed with EPMA, the results of a reconfirmation experiment where 0.3*Al stoichiometry was tested with both acidic and neutral slag show results that are similar to Factsage. The amount of Al in the metal was lower in the acidic slag experiment, but the amount of Al_2O_3 in the slag was still lower than in the neutral slag experiment. Contrarily, a reconfirmation experiment produced quite promising results and shows that as the $CaO:SiO_2$ ratio decreases, the Al content in metal decreases and the Al_2O_3 content in slag rises.

The effect of slag composition on the content of Ca and CaO in our outputs has proportional variation according to Factsage results. With a decline in the $CaO:SiO_2$ ratio, both the Ca content of metal and the CaO content of slag decrease. Our previous three trials, where Ca rich metal were seen in acidic slag experiments, did not support this. However, a reconfirmation experiment revealed that the Ca content in 0.3*Al+acidic slag was incredibly low; even lower than Factsage value, which supported the validity of this claim. The CaO content in slag was also found to be lower in acidic slag experiments than in neutral slag experiments in the first three trials, which is consistent with simulated values. In the previous three trials, the CaO concentration result was consistently obtained. It was further supported by a reconfirmation experiment, which determined that lowering $CaO:SiO_2$ causes a decrease in the amounts of Ca and CaO in metal and slag, respectively.

5.1.3 Mass Balance

5.1.3.1 Metal loss

Table 18: *Loss in total weight of input, loss in output metal and Al/Si ratio observed in different trials of different stoichiometry*

Slag Types	Stoichiometry	Trial	Loss in weight	Loss in metal	Si/Al ratio
Acidic (CaO:SiO_2=0.56)	0.3*Al	1	4.67	1.72	0.63
		2	1.46	1.85	0.62
		3	3.32	2.45	0.56
		Re. exp	1.16	2	0.60
	0.4*Al	1	2.07	0.62	0.74
		2	2.19	3.72	0.54
		3	3.6	4.24	0.50
	0.5*Al	1	0.61	1.43	0.72
		2	1.37	0.42	0.77
		3	1.9	3.19	0.62
Neutral (CaO:SiO_2=1.01)	0.3*Al	1	4.37	3.25	0.42
		2	3.28	2.68	0.49
		3	2.23	1.88	0.59
		Re. exp	0.38	1.59	0.63
	0.4*Al	1	2.55	2.28	0.63
		2	2.42	3.7	0.50
		3	3.75	2.97	0.57
	0.5*Al	1	2.06	3.02	0.64
		2	1.51	2.47	0.68
		3	4.05	3.53	0.60

Loss in mass has been calculated from the difference of total input feed and output. Similarly, loss in metal has been calculated from difference of expected Si metal from Factsage and actual Si metal from experiment.

Observation from Table 18 shows that loss in weight has been comparable in acidic slag experiments and neutral slag experiments. No specific trend has been observed on the basis on loss in mass with respect to different slag ratio. However, loss in metal has been observed higher in neutral slag experiments as compared to acidic slag experiments. Also, higher losses is observed in metal produced i the case of lower stoichiometry i.e 0.3*Al. Several factors are determinant in observation of metal loss in the product formed. One of the reason is heavy fuming during the heating process. Especially, during the holding time, when temperature reaches 1650°C, fumes start to appear in significant vision, through which SiO gas escapes and results in formation of output with less mass than input. Losses may also result from the formation of carbides when metal and carbon react. The slag contained silicon carbides as well as some aluminum carbides. With graphite crucibles, Hoseinpur and Safarian [26] investigated the interaction between Si and Si20wt%-Al alloys. They discovered that the surface of the crucible as well as its pores produced silicon carbides, aluminum carbides, and aluminum silicon carbides. It was also found that at 1800°C, SiC particles came loose from the walls and ended up in the melt. Metal are also lossened up while separating it from the slag present in product. Some trials had given powdered form slag, where one bulk oval silicon pieces was present with several small Si pieces getting dispersed along grinded slag. Large uncertainties are persistent as collection of entire small silicon pieces were inconvenient. Similarly, some trials where output product was a bulk mass, slag and metal were separated manually with hammer which led to loss of small amount in output product which can termed as human error. Another reason for loss in metal can be due to formation of metal droplets on several part of slag. This case was usually visible in experiments with neutral slags. Metal films seen on several location of slag deprived Si metal to transport into alloy and resulted in metal loss.

5.1.3.2 Elemental Balance in Acidic and Neutral slag experiments

The calculated Si, Al and Ca recovery to the metal and slag, together with corresponding values from reconfirmation trial and Factsage simulation has

been shown in Figure 49. For every trials of every stoichiometry, Si recovery are usually less than 100%. In the case of first three trials of acidic slag experiment, Si recovery was almost 72%. Remaining feed of Si was lost due to various losses discussed earlier. But the recovery was high and similar to Factsage calculations when same experiment (0.3*Al + acidic slag) was conducted during reconfirmation trial. Silicon recovery to metal and slag was 30% and 60% which is in accordance with Factsage values. Al seemed to be recovered less than required in every four trials. recovery to metal has been found negligible as expected while Al recovery to slag has been halted after 70%. Ca recovery in first three trials of acidic slag experiment seems to be higher than 100%. These has happened due to improper substitution of slag amount in mass balance calculation. Amount of mass of slag has been calculated by subtracting metal yield and losses in form of fumes from entire product. This makes amount of slag higher than its actual amount and thus results in high Ca recovery during mass balance.

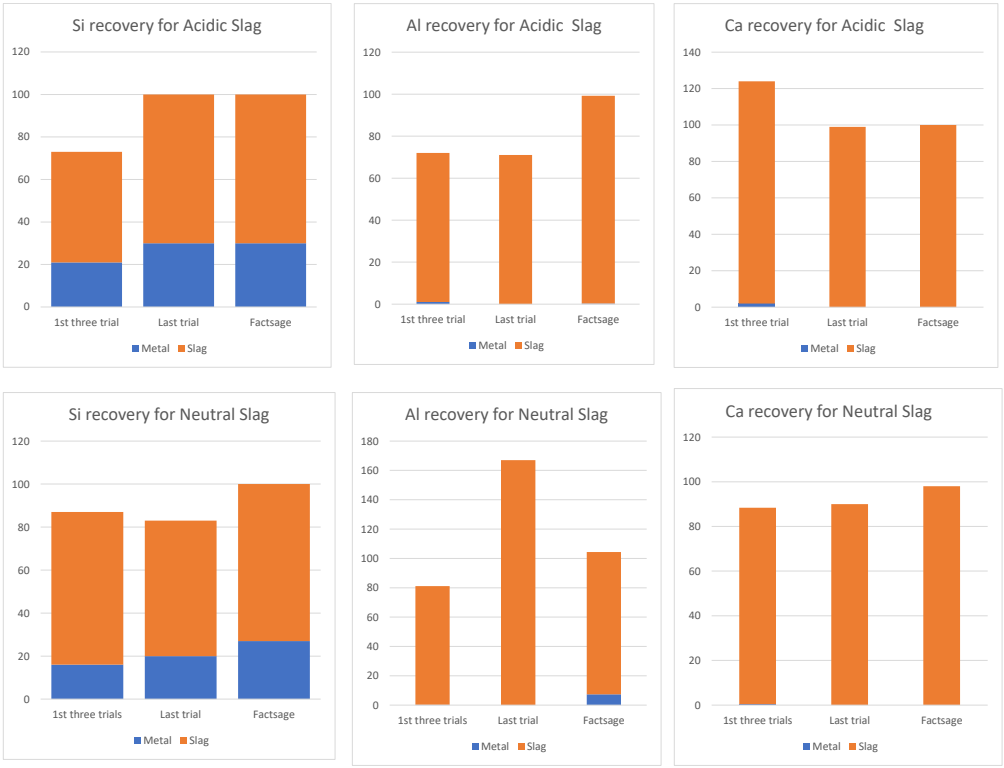

Figure 49: *recovery of Si, Al and Ca to slag and metal; Top three represents mass balance results from acidic slag experiments while bottom three represents mass balance results from neutral slag experiments*

In the case of neutral slag experiments, Si recovery to metal as well as to slag has been found less in first previous trials. Experiment done over reconfirmation trial also has less Si recovery as compared to expected simulated results. The reason is same as previously discussed in acidic slag experiments mass balance. According to Factsage small portion of Al gets recovered to metal which was not the case for all of our trials. Al barely got transported to metal whereas significant loss were observed in overall Al recovery representing some Al to have lost during experimental process. Ca recovery to metal and slag obtained from neutral slag experiments have almost similar values to simulated values. Though Ca has not be fully recovered, very few losses has been observed and recovery to metal is negligible as expected.

5.2 Experiment with pre-fused slag with CaF_2

One set of experiment was done with stoichiometric Al addition to pre-fused slag (neutral slag) containing CaF_2 at a temperature of 1650°C. Only one set of stoichiometric experiment was done during this study and the results has been compared with previous aluminothermic reduction experiments with stoichiometric Al conducted by author in specialization project.

Table 19: Si yield and loss in weight comparison between experiment using pre-fused slag and using pre-fused slag+CaF_2 slag

Slag	Reductant	Loss in mass	Si/Al ratio
rec	1*Al	5.82	0.86
rec+10%CaF_2	1*Al	2.26	0.85

When compared with experiment with stoichiometric Al and rec slag without CaF_2, loss in weight of input feed has been significantly less in experiments using CaF_2. Si yield from the product or Si/Al ratio is almost similar for both cases as stoichiometric reductant in same amount was used in both. In the case of physical structure, noticeable colour difference and more homogeneity can be observed when slag from this set of experiment is compared with previous stoichiometric aluminothermic reduction experiments.

Table 20: Comparison between metal and slag composition in product obtained from experiments without using CaF_2 and experiments using CaF_2

	Metal			Slag		
	Si	Al	Ca	SiO_2	Al_2O_3	CaO
Experiment without CaF_2	73.1	7.8	16.78	12.33	44.1	43.4
Experiment with CaF_2	76.91	6.04	15.20	11.33	41.31	46.63

Table 20 makes a brief comparison between experiments using stoichiometric Al with pre-fused slag and experiments using stoichiometric Al with pre-

fused slag containing 10% CaF_2. Significant alteration in metal and slag composition has not been seen but some positive feedback has been noticed due to increment of Si content by small amount. Si composition in Si has seen to be increased while the composition of Al and Ca in metal has increased in the experiment where CaF_2 is used along with rec. Similarly, in the case of slag, the results are quite similar to previous aluminothermic reduction experiments however SiO_2 and Al_2O_3 has been reduced by small margin.The result tabulated in Table 20 are obtained with EPMA, but analysis had been done under XRF too, which had almost similar result in contrast with EPMA. Only difference was in the concentration of CaO in slag which is shown little less in XRF analysis. XRF analysis of slag produced from this experiment reveals that 6.63 weight% of F is present in slag obtained. This can be the cause for less CaO content in slag in our current CaF_2 study as compared to previous experiments.

5.3 Al-Si Alloy preparation

The main objective of taking Al-Si alloy from melt spinner was to produce finer grain size and extend the solute solubility in the solution which is Al in our case. The analysis of phases studied under sample from pure Al, Al-Si alloy from muffle furnace and Al-Si melt spinner show somehow positive results in contrast to our main objective. When pure aluminium sample was analysed, only single phase is seen on pure Aluminium. Some dislocation were observed but it only consisted pure Al phase. SE image of Al-Si alloy made from muffle furnace had observation of small dark phases noticed to be gathered on some particular region of pure Al phase. It implies that Si is present in alloy but they are not distributed uniformly and are present in significant amount in some region where they are absent in most of the part of alloy. Image in Figure 50, represents vertical view of Al-Si ribbon sample (edges) obtained from melt spinner. Si distribution in alloy seems to be more homogeneous as compared to Al-Si alloy from muffle furnace. Clear image of Si distribution has not been obtained from SEM analysis of rapidly solidified Al-Si alloy, when Al-Si ribbon was observed horizontally. The phase analysis

from Al-Si alloy kept in vertical position in epoxy sample gives some insight depth in phase distribution. Three different phases are observed, where pure Al is represented by white phase, grey is represented by Si and dark grey by other contaminated metallic impurities.

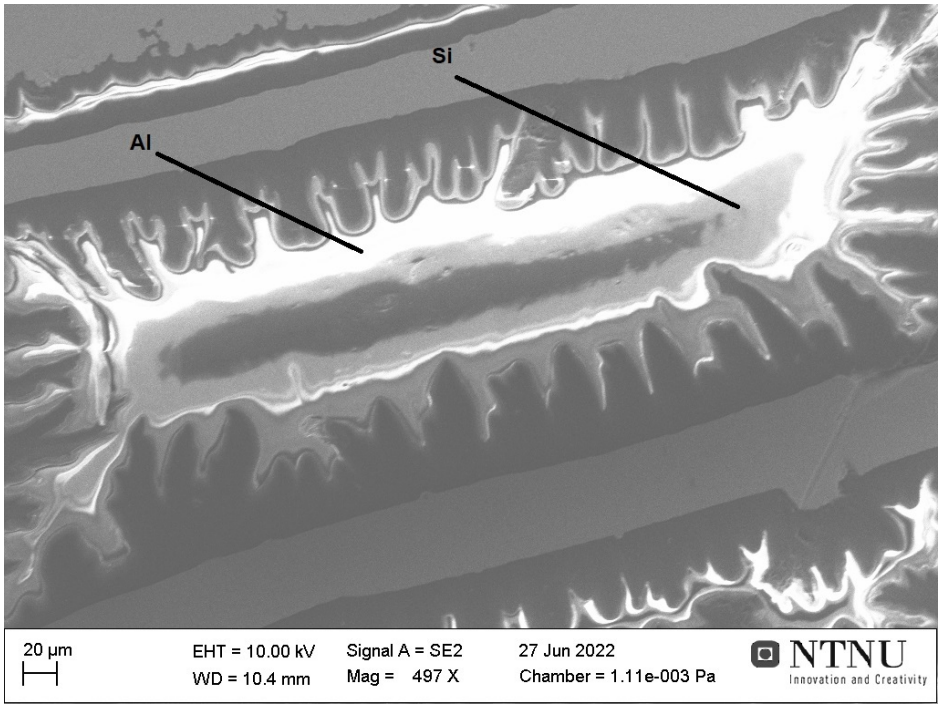

Figure 50: *SE image of Al-Si alloy after rapid solidification; Figure represents Al-Si alloy image when it was kept vertically on sample*

Mapping image of Al-Si alloy as represented in Figure 40 reveals that Si distribution is partially uniform in pure Al phase. Though several other phases, usually coming out from impurities has been observed in tiny amount, mostly from Mg and Fe, mapping image shows positive outcome. This has further backed by WDS analysis as illustrated in Table 17, where analysis of ten different points in Al-Si alloy gave average composition of Al and Si to be 80.23% and 19.46% respectively, which was our initial composition. Traces of Mg and Fe might have evolved in alloy either during heating process inside the crucible in muffle furnace or melting process inside melt spinner. Crucibles used in melt spinner had been used for other experiments before

and though it was thoroughly purified, some impurities might have entered into the system.

6 Conclusion

The major aim of this thesis study was to determine the possibility of silicon production with low calcium content. Study of the effect of calcium fluoride in aluminothermic reduction process and observation of micro-structure of Al-Si alloys from rapid solidification was major interest in this study. Results from under-stoichiometric studies using acidic and neutral slag provided inconsistent yet interesting observations but positive outcomes were observed in reconfirmation experiments. Results from study of CaF_2 also showed constructive results in obtaining pure silicon. Following points can be taken as concluding points for this thesis work:

6.1 Under-stoichiometric studies

1. Less amount of reductant gives higher purity silica in aluminothermic reduction reaction. Al and Ca content in metal decreases with decreasing reductant.

2. With decreasing amount of reductant, SiO_2 and CaO concentration in slag seem to be raised while Al_2O_3 content in slag is reduced.

3. Acidic slag gives results with high Si content in metal as compared to neutral slag. This case is reversed in the case of Al and Ca. This fact has not been justified by earlier three trials of acidic and neutral slag experiments but has been later confirmed with reconfirmation experiment and Factsage results.

6.2 Experiment using CaF_2

1. Experiment seemed to have less mass loss during heating process. Small amount of mass loss and high metal yield is observed from experiment using rec slag with 10% CaF_2.

2. Si content in metal has been increased with use of CaF_2 in rec slag. At the same time, Al and Ca content has been reduced which is favorable

effect.

6.3 Al-Si alloy

1. Rapid solidification of Al-Si alloys tend to result in ribbons with a finer grain structure and a quite homogeneous surface, but sufficient homogeneity could not be achieved due to various experimental, human, and material errors. Si dispersions in the Al phase were uniform in some locations, while still being uneven in others, according to SEM analysis and EPMA results. However, compared to Al-Si alloy from a muffle furnace, the rapid solidification technique produced more homogeneity. WDS analysis would have provided a detailed view of the contents of each phase, but phase observation was challenging because the discovered phases were too small for analysis.

7 Future Work

1. Experiments conducted over this under-stoichiometric study has been done at a control temperature between 1650 °C and 1670 °C. Research can be made over different temperature ranging between equilibrium conditions requirement can be done for better understanding.

2. Irregularities were seen on results of acidic slag experiments when compared with Factsage simulated values. Lack of proper slag mixing prior to aluminothermic reduction process can be one of its cause. So, study can be made by melting master slag first for homogeneity and conducting aluminothermic reduction of same master slag.

3. Metal loss in the form of carbides are significant in aluminothermic reduction experiments. Larger mass of reductant getting in contact with graphite crucibles were observed which hindered the reduction of SiO_2. Investigation can be made further into this subject for utilisation of reductant as completely as possible.

4. Mass balances done for acidic and neutral slag experiments has not included Carbon in the system due to uncertainty of its content in our output product. Though significant amount of C was present in REC slag used, XRF analysis could not trace content of C in most of the metals and slags produced. Mass balance including C in the system could have fetched more information about the deviation we got during the study.

5. WDS analysis of Al-Si alloy could have been done for better understanding of composition of different phases present in the output product. This could help to trace out the Si and Al composition lying over different phases and aid up on comparison with other Al-Si; concluding the results of rapid solidification process most efficiently.

References

[1] [Accessed 20. Nov 2021]. [Online]. Available: https://en.wikipedia.org/wiki/Ellingham_diagram.

[2] M. Takla, N. Kamfjord, H. Tveit, and S.Kjelstrup, "Energy and exergy analysis of the silicon production process," 2013.

[3] A. Schei, J. Tuset, and H. Tveit, "Production of high silicon alloys," Jan. 1998.

[4] J. A.Schei and H.Tveit, *Production of High Silicon Alloys*. Trondheim: Trondheim, Norway : Tapir, ©1998, 1998.

[5] I. Kero, S. Grådahl, and G. Tranell, " Airborne Emissions from Si/FeSi Production," JOM, vol. 69, no. 2, pp. 365–380, 2017.

[6] D.Elwell and G. Rao, " Electrolytic production of Silicon," *Reviews of Applied Electrochemistry*, vol. 18, no. 15–22, 1988.

[7] Z. Xing, J. Lu, and X. Ji, "A brief review of metallothermic reduction reactions for materials preparation," *Small Methods*, vol. 2, no. 12, p. 1 800 062, 2018. DOI: https://doi.org/10.1002/smtd.201800062.

[8] D. F. Habashi, "Metallothemic reactions - Past, Present and Future," Research and Reports on Metals, vol. 2, no. 1, pp. 1–16, 2018.

[9] M. Barati, S. Sarder, A. McLean, and R. Roy, "Recovery of silicon from silica fume," 2010.

[10] S. E. Sadique, "Production and Purification of Silicon by Magnesiothermic Reduction of Silica Fume," M.S. thesis, University of Toronto (Canada), Jan. 2010.

[11] K. Yasuda and T. H. Okabe, " Solar-grade silicon production by metallothermic reduction," JOM, vol. 62, no. 12, pp. 94–101, 2010.

[12] G. Tranell, *SisAl Pilot: Innovative pilot for Silicon production with low environmental impact using secondary Aluminium and silicon raw material*, 2019.

[13] H. Philipson, G. L. Solbakk, M. Wallin, K. E. Einarsrud, and G. Tranell, *Kinetics of silicon production by aluminothermic reduction of silica using aluminium and aluminium dross as reductants*, 2021.

[14] K. Tang, "Iso-content curves for the Equilibrium between SiO2-CaO-Al2O3 Salg and Si-AlCa Metal," 2020.

[15] L. ŘEHÁČKOVÁ, S. ROSYPALOVÁ, R. DUDEK, J. KUKUTSCHOVÁ, and J. DOBROVSKÁ, "Effect of CaO/SiO2 ratio on viscocity and structure of slag," 2015.

[16] [Accessed 15. March 2022]. [Online]. Available: https://encyclopedia2.thefreedictionary.com/Basicity/.

[17] F. D. Richardson, "Slags and refining processes. the constitution and thermodynamics of liquid slags," *Discussions of the Faraday Society*, vol. 4, pp. 244–257, 1948.

[18] S.-C. Park, H. Gaye, and H.-G. Lee, "Interfacial tension between molten iron and cao–sio2–mgo–al2o3–feo slag system," vol. 36:1, pp. 3–11, 2009. DOI: 10.1179/174328108X358622.

[19] F.Hernandez, J. Ramírez, and R.Mackay, "Al-si alloys automotive, aeronautical, and aerospace applications," 2017.

[20] [Accessed 15. March 2022]. [Online]. Available: https://www.phase-trans.msm.cam.ac.uk/abstracts/M7-8.html/.

[21] M. Javidani and D. Larouche, "Application of cast al–si alloys in internal combustion engine components," vol. 59:3, pp. 132–158, 2014. DOI: 10.1179/1743280413Y.0000000027.

[22] S. Nikanorov *et al.*, "Structural and mechanical properties of al-si alloys obtained by fast cooling of a levitated melt," vol. 390, pp. 63–69, 2005. DOI: 10.1016/j.msea.2004.07.037.

[23] E. J. Lavernia and T. S. Srivatsan, "The rapid solidification processing of materials: Science, principles, technology, advances, and applications," vol. 45, pp. 287–3259, 2010. DOI: 10.1007/s10853-009-3995-5.

[24] [Accessed 15. March 2022]. [Online]. Available: https://www.slideshare.net/legendsundar/rapid-solidification-technology.

[25] G. L. Solbakk, "The Effect of Varying CaO/SiO2 Ratios and Reductant Addition in Silicon Production by Aluminothermic Reduction of Silica Based Slags," M.S. thesis, NTNU, 2021.

[26] A. Hoseinpur and J. Safarian, "Mechanisms of graphite crucible degradation in contact with si–al melts at high temperatures and vacuum conditions," vol. 171, p. 108 993, 2020. DOI: 10.1016/j.vacuum.2019.108993.

A Appendix

A.1 XRF results of Si alloy from three trials of Acidic Slag Experiments

Table 21: *Table represents Si alloy composition from three different trials of Acidic Slag Experiments with under-stoichiometric aluminium*

Trial	Reductant stoichiometry	Si %	Fe %	Cu %	Mn %	Mg %	Cr %	Ni %	Ti %	V %	Al %	Ca %
Trial 1	0.3*Al	90.70	0.54	0.008	0.02	0.013	0.008	0.011	0.01	0.24	0.88	7.56
	0.4*Al	85.55	0.54		0.02	0.025	0.005		0.012	0.11	1.89	11.853
	0.5*Al	81.73	0.51		0.03	0.006	0.016		0.015	0.1	2.7	14.891
Trial 2	0.3*Al	89.34	0.5		<0.01	0.015	0.008		0.016	0.083	1.14	8.898
	0.4*Al	86.27	0.81		0.01		0.009		0.013	0.061	1.65	10.585
	0.5*Al	81.48	0.48		<0.01	0.006		0.002	0.011	0.039	2.8	14.734
Trial 3	0.3*Al	90.15	1.09	0.008	<0.01	0.032	0.017		0.012	0.033	0.87	7.785
	0.4*Al	86.06	0.52		0.02	0.007			0.025	0.027	1.89	11.428
	0.5*Al	82.73	0.55		0.02	0.007	0.021	0.009	0.015	0.035	2.57	14.042

A.2 XRF results of Si alloy from three trials of Neutral Slag Experiments

Table 22: *Table represents Si alloy composition from three different trials of Neutral Slag Experiments with under-stoichiometric aluminium*

Trial	Reductant stoichiometry	Si %	Fe %	Cu %	Mn %	Mg %	Cr %	Ni %	Ti %	V %	Al %	Ca %
Trial 1	0.3*Al	94.71	0.61		0.01	0.003	0.013		0.012	0.076	0.35	4.214
	0.4*Al	90.08	0.73		0.01	0.016			0.013	0.024	1.01	8.115
	0.5*Al	87.98	0.57		0.02	0.026			0.023	0.032	1.34	9.995
Trial 2	0.3*Al	94.60	0.74		0.03	0.003	0.008	0.002	0.013	0.057	0.39	4.141
	0.4*Al	91.70	0.77		0.02	0.008	0.007		0.024	0.021	0.77	6.558
	0.5*Al	87.97	0.6		0.02	0.019	0.006		0.009	0.038	1.34	9.663
Trial 3	0.3*Al	93.64	0.78		0.02		0.006		0.036	0.016	0.53	4.975
	0.4*Al	91.75	0.83		0.03	0.005	0.006		0.034	0.032	0.82	6.474
	0.5*Al	89.53	0.64		0.02	0.006		0.005	0.02	0.034	1.11	8.631

A.3 XRF results of slag from three trials of Acidic Slag Experiments

Table 23: *Table represents slag composition from three different trials of Acidic Slag Experiments with under-stoichiometric aluminium*

Trial	Reductant stoichiometry	Al2O3 %	C %	CaO %	Fe2O3 %	MgO %	O %	P2O5 %	SiO2 %	SO3 %	SrO %	WO3 %
Trial 1	0.3*Al	17.3		46.8	0.07	0.13		0.01	35.6	0.03	0.01	
	0.4*Al	16.4		48.1	0.02	0.18		0.01	35.2		0.02	
	0.5*Al	16.7		47.1	0.05	0.17		0.01	36	0.02	<0.01	
Trial 2	0.3*Al	28.7		44.6	0.02	0.12		0.02	26.5	0.03	0.01	
	0.4*Al	26.7	0.57	41.9	0.1	0.04	34.9	<0.01	30.6	0.02	<0.01	0.02
	0.5*Al	27.8		41.8	0.06	0.08		0.02	30.2	0.01	0.01	
Trial 3	0.3*Al	33.5		41.9	0.02	0.06			24.5		<0.01	0.03
	0.4*Al	34.8	0.58	41.4	0.05	0.04	34.1	<0.01	23.1	0.02	<0.01	0.02
	0.5*Al	32.4		40.9	0.05	0.08		0.01	26.6		<0.01	0.01

A.4 XRF results of slag from three trials of Neutral Slag Experiments

Table 24: *Table represents slag composition from three different trials of Neutral Slag Experiments with under-stoichiometric aluminium*

Trial	Reductant stoichiometry	Al2O3 %	C %	CaO %	Fe2O3 %	MgO %	O %	P2O5 %	SiO2 %	SO3 %	SrO %	WO3 %
Trial 1	0.3*Al	15.8		46.7	0.03	0.15		<0.01	37.3	0.01	0.01	
	0.4*Al	13.3		48.5	0.05	0.12			38		<0.01	
	0.5*Al	11.4		48.8	0.01	0.24		0.02	39.4	0.02	0.01	0.03
Trial 2	0.3*Al	14.2		46.6	0.08	0.18		<0.01	38.9	0.02	<0.01	
	0.4*Al	15.1	0.6	47.2	0.07	0.16	34.7	0.01	36.8	0.02		
	0.5*Al	15.8		47.8	0.02	0.03		0.01	36.3	0.01	<0.01	
Trial 3	0.3*Al	28		44.9	0.02	0.12		<0.01	27	0.02	0.01	0.02
	0.4*Al	23.7	0.166	46.3	0.01	0.18	34.6		29.6	0.03	0.01	0.04
	0.5*Al	22.2		45	0.02	0.04		0.01	32.7	0.02		

A.5 EPMA results for metals from reconfirmation experiment

Table 25: *Table represents Si alloy composition from reconfirmation experiments obtained with EPMA*

	Material	Point	Si	Al	Ca	V	Mg	Ti	Mn	Fe	O	Na	Cl
		1	98.859	0.086	0.104	0	0	0	0	0.199	0.668	0.029	0.055
	0.3*Al	2	98.849	0.103	0.114	0.08	0.007	0.012	0	0.196	0.545	0.003	0.092
	+	3	98.843	0.09	0.052	0.003	0	0.01	0	0.133	0.615	0.078	0.176
	Acidic	4	98.469	0.08	0.146	0	0	0.037	0	0.242	0.769	0.061	0.197
	Slag	5	98.714	0.079	0.13	0	0.014	0.074	0.036	0.299	0.536	0.032	0.086
		6	98.906	0.056	0.059	0	0.004	0.006	0.049	0.049	0.736	0.015	0.09
	0.3*Al	1	93.429	0.388	3.469	0.053	0.028	0	0.038	0.801	1.566	0.062	0.167
height	+	2	94.924	0.341	3.542	0	0.032	0.023	0	0.425	0.673	0.013	0.027
	Neutral	3	93.923	0.372	3.338	0	0.053	0.011	0.043	0.741	1.37	0.038	0.094
	Slag	4	93.215	0.311	2.237	0.066	0.023	0.044	0	0.856	3	0.04	0.207
	1*Al	1	75.842	6.391	15.107	0.013	0.15	0.001	0	0.384	1.865	0.069	0.155
	+	2	77.923	6.034	14.399	0.041	0.126	0.019	0	0.268	0.988	0.057	0.099
	REC	3	73.302	6.426	18.527	0.008	0.133	0.04	0	0.317	1.173	0.008	0.035
	Slag	4	76.815	6.347	15.342	0	0.134	0.029	0.023	0.291	0.922	0.071	0.027
	with	5	78.986	5.565	13.958	0	0.118	0	0.015	0.298	0.93	0.04	0.055
	CaF2	6	78.615	5.474	13.878	0.003	0.105	0.018	0.011	0.282	1.517	0.041	0.057

Table 26: *Table represents Slag alloy composition from reconfirmation experiments obtained with EPMA*

Material	Point	Al_2O_3	SiO_2	CaO	MgO	MnO	TiO_2	FeO	V_2O_3	CuO	NiO	SO_3
0.3*Al	1	16.076	46.864	36.586	0.308	0	0.058	0.042	0	0.065	0	0
+	2	16.167	46.704	36.551	0.277	0	0.101	0.072	0.026	0	0	0.102
Acidic Slag	3	15.826	47.739	36.092	0.291	0	0.051	0	0	0	0	0
0.3*Al	1	25.158	30.907	43.056	0.46	0	0.071	0.043	0.055	0.132	0.051	0.069
+	2	25.857	29.605	43.832	0.413	0.039	0.057	0.171	0	0	0.027	0
Neutral Slag	3	23.625	30.214	45.274	0.445	0.025	0.078	0.094	0	0.165	0	0.079
1*Al	1	41.15	11.571	46.572	0.403	0	0	0.153	0.039	0	0.097	0.016
+	2	41.64	10.693	47.029	0.351	0.061	0	0.176	0.047	0	0	0.003
REC	3	41.03	11.654	46.365	0.389	0.021	0	0.237	0.043	0.203	0	0.059
Slag	4	41.133	11.632	46.478	0.349	0	0	0.294	0.036	0	0	0.077
with	5	41.459	11.218	46.631	0.379	0	0.03	0	0.051	0.139	0	0.093
CaF2	6	41.468	11.198	46.705	0.342	0	0	0.005	0	0.154	0.025	0.102

A.6 BSE images of Si alloys from Acidic Slag Experiment

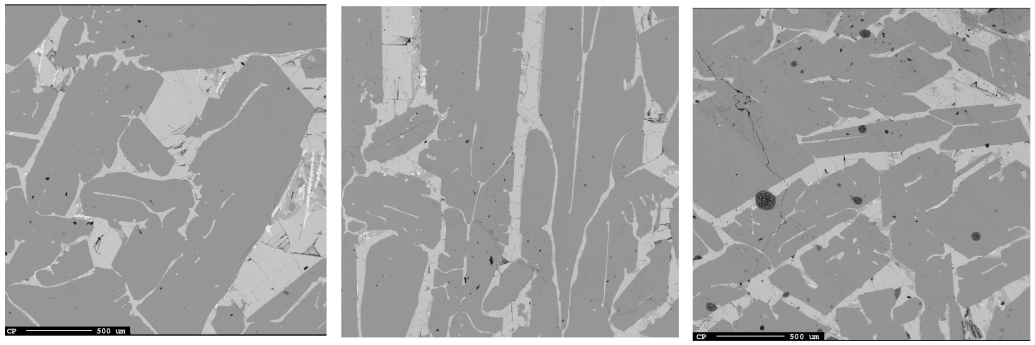

Figure 51: *BSE image of Si alloy obtained from three different stoichiometries during acidic slag experiment. Left: 0.3*Al, Middle: 0.4*Al. Center: 0.5*Al*

A.7 BSE images of Si alloys from Neutral Slag Experiment

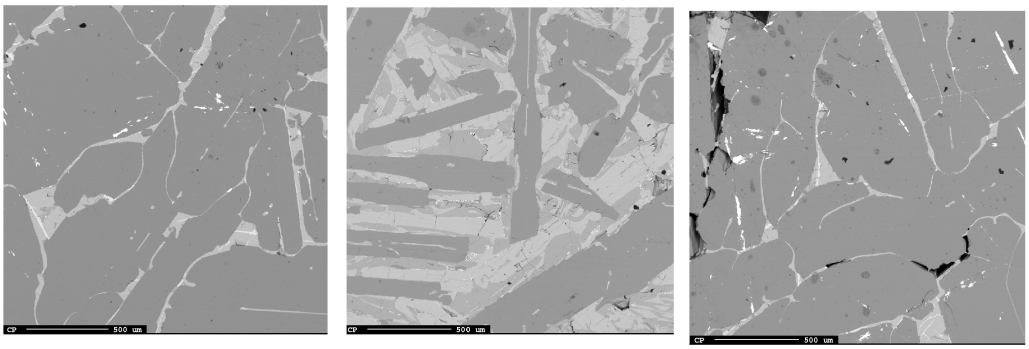

Figure 52: *BSE image of Si alloy obtained from three different stoichiometries during neutral slag experiment. Left: 0.3*Al, Middle: 0.4*Al. Center: 0.5*Al*

A.8 BSE images of slags from Acidic Slag Experiment

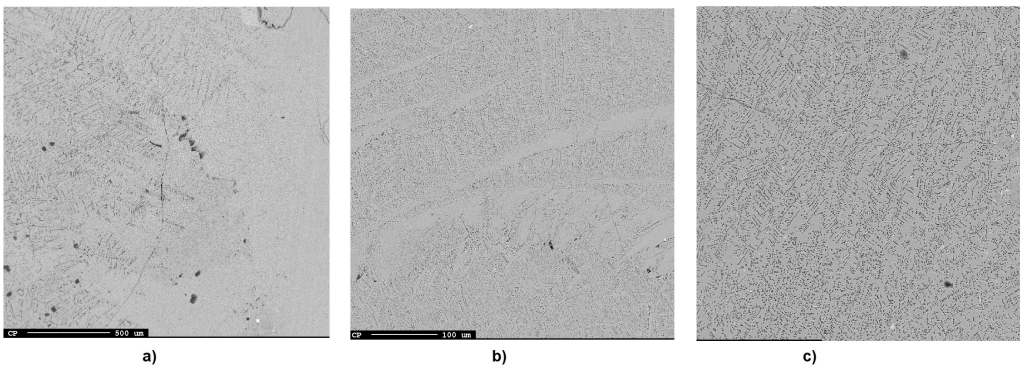

Figure 53: *BSE image of slags obtained from three different stoichiometries during acidic slag experiments. Left: 0.3*Al, Middle: 0.4*Al. Center: 0.5*Al*

A.9 BSE images of slags from Neutral Slag Experiment

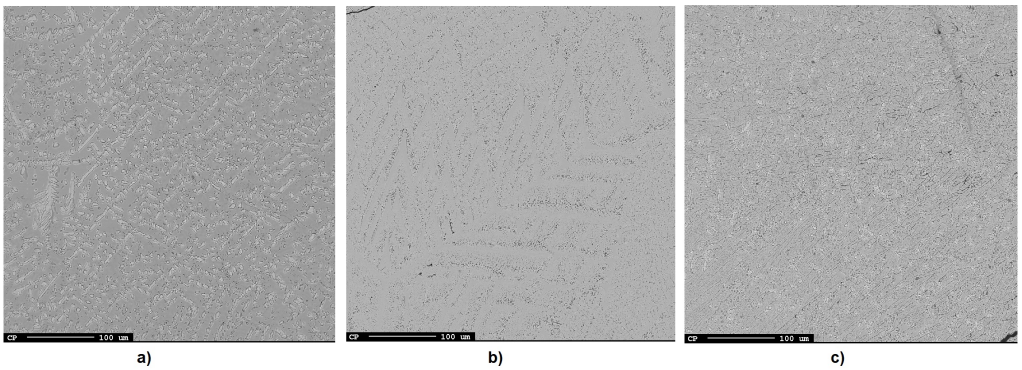

Figure 54: *BSE image of Si alloy obtained from three different stoichiometries during neutral slag experiment. Left: 0.3*Al, Middle: 0.4*Al. Center: 0.5*Al*

A.10 BSE images of Si alloys from experiment using CaF_2

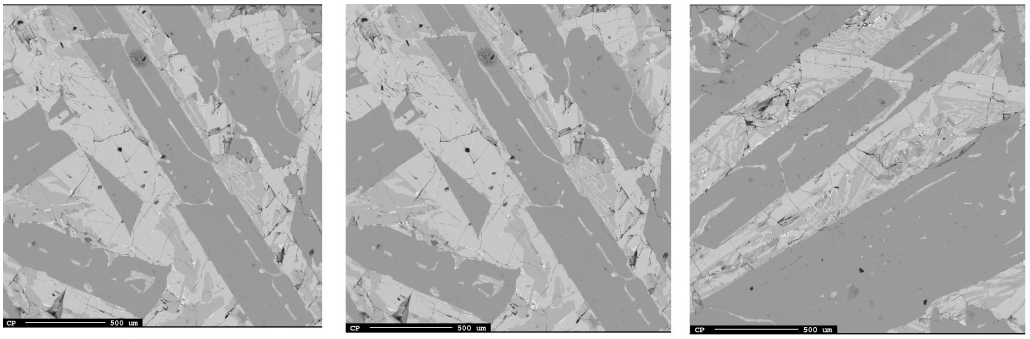

Figure 55: *BSE images of Si alloy obtained from experiment using REC slag with CaF_2 and stoichiometric aluminium*

A.11 BSE images of Slag from experiment using CaF_2

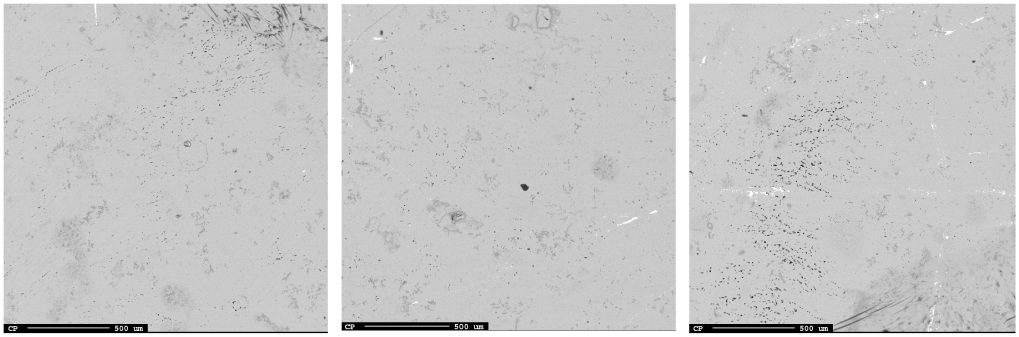

Figure 56: *BSE images of slag obtained from experiment using REC slag with CaF_2 and stoichiometric aluminium*

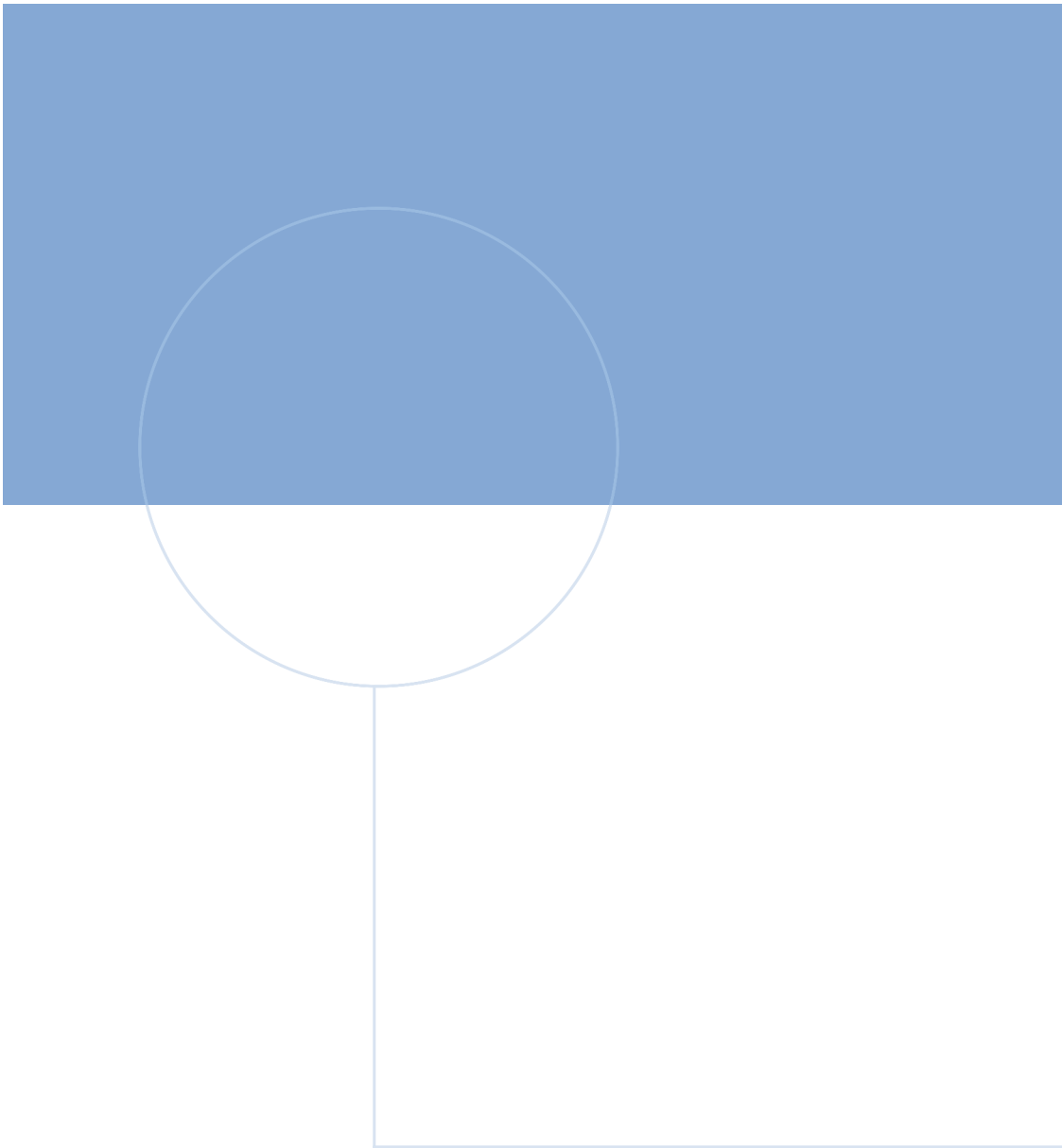

NTNU

Kunnskap for en bedre verden